

**DEVELOPMENT OF DETERIORATION MODELS FOR BRIDGE DECKS USING
SYSTEM RELIABILITY ANALYSIS**

Farzad Ghodoosipoor

A Ph.D. DISSERTATION

The Department

of

Building, Civil, and Environmental Engineering

Concordia University

Montréal, Québec, Canada

July 2013

CONCORDIA UNIVERSITY
SCHOOL OF GRADUATE STUDIES

This is to certify that the thesis prepared

By: **Farzad Ghodoosipoor**

Entitled: **DEVELOPMENT OF DETERIORATION MODELS FOR BRIDGE DECKS
USING SYSTEM RELIABILITY ANALYSIS**

and submitted in partial fulfillment of the requirements for the degree of

DOCTOR OF PHILOSOPHY (Civil Engineering)

Complies with the regulations of the University and meets the accepted standards with respect to originality and quality.

Signed by the final examining committee:

Chair

External Examiner

External to Program

Examiner

Examiner

Thesis Supervisor

Approved by

ABSTRACT

Generally, in the existing Bridge Management Systems (BMS) deterioration is modeled based on the visual inspections where the corresponding condition states are assigned to individual elements. In this case, the limited attention is given to the correlation between bridge elements from structural perspective. In this process, the impact of the history of deterioration on the reliability of a structure is disregarded which may lead to inappropriate conclusions. The Improved estimate of service life of a bridge deck may help decision makers enhance the intervention planning and optimize the bridge life cycle costs. A reliability-based deterioration model can potentially be an appropriate replacement for the existing procedures.

The objective of this thesis is to evaluate the system reliability of conventional bridges designed based on the existing codes. According to the methodology developed in this thesis, the predicted element-level structural conditions for different time intervals are applied in the non-linear Finite Element model of a bridge superstructure and the system reliability indices are estimated for different time intervals. The resulting degradation curve could be calibrated and updated based on the outcomes of the visual inspections. Also, the reliability of innovative bridges that use non-conventional materials or structural forms such as Steel-Free Deck System has been evaluated by applying the newly developed method. The available deterioration models for conventional superstructures are not applicable for the innovative bridge systems. Since there is no established deterioration model available for these innovative structures, it is difficult to predict the reliability of such bridges at different time intervals. The method developed

here adopts the reliability theory and establishes deterioration models for conventional and innovative bridges based on their failure mechanisms.

This method has been applied in simply-supported traditional reinforced-concrete bridge superstructures designed according to the Canadian Highway Bridge Design Code (CHBDC-S6), and in an innovative structure with a Steel-Free Deck System, namely the Crowchild Bridge, in Calgary, Canada, as case studies. As an example to show the application of such developed deterioration curve, the developed model has been adopted in an old superstructure in Montreal. The results obtained from the newly developed model and bridge engineering groups' estimations are found to be in accordance. Based on the reliability estimates, the conventional bridges designed based on the new code are found to be in a good condition during the initial stages of their service life, but their condition degrades faster once corrosion in steel reinforcements is initiated and spalling of concrete becomes evident. In case of the Steel-Free Deck, there is a low probability of failure at the end of the 75 years of its service life. It is found that the element-level assessment of a concrete deck is a conservative approach, since the interaction between the structural elements results in considerably higher reliability index and lower probability of failure. This thesis demonstrates how the proposed system reliability-based evaluation method can be adopted in determining the structural condition of a bridge which represents an important step forward in Bridge Management Systems. The system reliability deterioration model can be easily integrated to the existing Bridge Management Systems (BMS) by replacing the existing condition index by the reliability index or adding it to the assessing process as an additional parameter.

ACKNOWLEDGEMENT

This thesis is dedicated to my father, may his soul rest in peace, who passed away during the time I was writing my thesis. He valued education above all else. I regret he did not live long enough to attend my graduation, but I am glad to know he saw this process through to its completion. Thank you for giving me the opportunities to accomplish all that I have.

I wish to express my deepest gratitude to my supervisors Dr. Ashutosh Bagchi and Dr. Tarek Zayed, for their kind instructions, continuous guidance and encouragement through this study. I would also like to thank Mr. Adel R. Zaki from SNC-Lavalin Inc. for providing me all the information needed for this thesis. I also acknowledge the help provided by Mr. Rob Scott, the Structural Inspection & Maintenance Coordinator in the city of Calgary for providing relevant information about the Crowchild Bridge.

Many thanks to my colleagues Dr. Hossein Azimi, Dr. Arash Rahmatian, Mr. Hamed Roshanaei, and Mr. Tushith Islam for their support and valuable advice.

Especially, I would like to give my special thanks to my mother and sisters for their love and support.

Table of Content

Chapter1: Introduction	1
1.1 Introduction	1
1.2 Problem Statement.....	2
1.2.1 Conventional Steel-Reinforced Concrete Decks	3
1.2.2 Innovative bridge deck Systems	4
1.3 Research Scope and Objectives.....	5
1.4 Research Methodology	6
1.5 Thesis Overview	7
Chapter2: Literature Review and Data Collection	9
2.1 Routine Bridge Inspections	9
2.2 Accuracy and Reliability of Routine Inspections	10
2.3 Condition Rating Systems in Canada	11
2.3.1 Condition rating system in Ontario-MTO	13
2.3.2 Condition Rating System in Quebec	13
2.3.3 Live Load Capacity Factor –CHBDC	14
2.4 Reliability Analysis of Structures.....	14
2.4.1 Reliability index	16
2.4.2 Reliability Index Analysis Using Rackwitz-Fissler Procedure	17
2.4.3 Reliability Analysis Using Simulation	20
2.5 Load Models.....	21
2.5.1 The Dead Load	21
2.5.2 The Live Load Model.....	22
2.6 Modes of Failure for Steel- Reinforced Concrete Bridge Superstructure	25
2.7 Modes of Failure for Steel- Free Bridge Deck System	27
2.8 Deterioration Mechanisms of the Bridge Elements.....	31
2.8.1 The Steel Bridge MembersCorrosion.....	31
2.8.2 Service Life of reinforced Concrete Decks Exposed to Chloride Attack.....	32
2.9 The Deterioration Models.....	35
2.9.1 Pontis	37
2.9.2 The Bridge Management System in Japan J-BMS.....	38
2.9.3 Deterioration Model Based on Weibull Probability Distribution	39
2.9.4 The Reliability Based Multi-linear Deterioration Model	39
2.10 The Statistical variations of structural parameters... ..	40
Chapter3 Methodology	43
3.1 Introduction	43
3.2 Methodology of the System Reliability-Based Deterioration Model.....	44
3.3 Degradation Scenarios of Overpass Bridge Decks.....	48
3.4 Modeling Procedure, Non-linear Finite Element Analysis Method.....	49
3.5 Finite-Element Modeling of Bridge Decks	53
3.5.1 Conventional Steel-Reinforced Deck 53	
3.5.2 Innovative Steel-Free Deck.....	55
Chapter4 Reliability assessment of steel-free deck system bridges	57
4.1 Introduction	57
4.2 Capacity and Load Models.....	58

4.2.1 Reduction in ultimate capacity due to tandem loading	59
4.2.2 Fracture of Welded Connections	60
<i>i</i> Brittle Fracture of Welded Connections.....	60
<i>ii</i> Fatigue Criteria.....	62
4.3 Implementation of the Developed Model to the Case Study.....	63
4.3.1 Reliability Analysis of the Crowchild Bridge	64
4.4 Details of the FE Modeling of the Crowchild Bridge	69
Chapter5 Reliability assessment of Conventional Bridge Deck Systems	75
5.1 Introduction	75
5.2 System Reliability Model, System Resistance Model.....	76
5.3 Adoption of the Developed Model to the Case Study bridges	77
5.3.1 Finite Element Modeling of the conventional bridge deck systems	79
5.3.2 Estimating the Reliability Index for the Case Study Bridges.....	80
Chapter6 Reliability-Based Deterioration Models for Bridge Decks	82
6.1 Introduction	82
6.2 A Deterioration Model for Conventional Deck.....	84
6.2.1 Adoption of the Developed Model to a Case Study.....	92
6.3 Reliability Based Deterioration Model for the Steel-Free Deck System	98
6.3.1 Discussion on Innovative GFRP Bridge Decks	101
6.4 Comparison Between the Developed deterioration patterns	102
Chapter7 Conclusions and Recommendations	104
7.1 Summary and Conclusions	104
7.1.1 Summary	104
7.1.2 Conclusions	105
7.2 Research Contributions	107
7.3 Research Limitations	109
7.4 Potential Future Research.....	110
7.4.1 Current Research Enhancement	110
7.4.2 Future Research Extension.....	111
References	113
Appendix A: Design Procedure of Conventional Concrete Super structure	118

List of Tables

Table 2.1 Standard condition rating in the US.	12
Table 3.1 The collapse load obtained from the two software systems.....	53
Table 4.1 Impact test temperatures and charpy impact energy requirements for primary tension members.....	61
Table 4.2 Impact test temperatures and charpy impact energy requirements for the weld metal.....	61
Table 4.3 Static deflections obtained from static load test	71
Table 4.4 Natural frequencies obtained from field tests and FEM model.....	74
Table 5.1 Best fit distributions for the ultimate capacity and reliability index	81
Table 6.1 Best fit distributions for the ultimate capacity of the system (17.5m span).....	86
Table 6.2 Best fit distributions for the ultimate capacity of the system (12 m span).....	88

List of Figures

Fig. 1.1 Cross Section of a Steel-Free Deck slab	5
Fig. 2.1 PDFs of Load, Resistance and the Safety Margin.....	15
Fig. 2.2 Reliability Index, the Shortest Distance in the Space of Reduced Variables.....	16
Fig. 2.3 Iterative Technique to Calculate β based on Normal Approximation.....	19
Fig. 2.4 Probability Chart and Simulated Values of Limit State Function	21
Fig. 2.5 CDF of Moments for Simple Span.....	23
Fig. 2.6 Trilinear and Idealized Bilinear Moment-curvature Relation.....	27
Fig. 2.7 Deck Slab Crack Pattern & Rigid Body Rotation of Wedges.....	30
Fig. 2.8 Service Life of Corrosion-damaged Concrete Structures	35
Fig. 2.9 Multi-linear Reliability-based Deterioration Model	41
Fig. 3.1 The methodology to develop a reliability based deterioration model at the system level.....	47
Fig. 3.2 Reliability-based Assessment Using Simulation	48
Fig. 3.3 De-icing Salt Contamination Scenario for a Conventional Deck	49
Fig. 3.4 De-icing Salt Contamination Scenario for Steel-Free Deck System	50
Fig. 3.5 Reinforced Concrete Beam Used to Verify the modeling Procedure	51
Fig. 3.6 Plastic Hinge Properties for Section with Top and Bottom Rebars	52
Fig. 3.7 Condition of Plastic Hinges Just Before and After Collapse	52
Fig. 3.8 Finite Element Models for Conventional Steel-Reinforced Concrete Decks	54
Fig. 3.9 Cross Section and Developed FEM Model of Crowchild Trail Bridge	55
Fig. 4.1 Multiple Wheel Loads on the Deck	59
Fig. 4.2 Overall View of Crowchild Trail Bridge, Calgary, Alberta.....	63
Fig. 4.3 Simulation Technique to Find the Distribution for the Deck Capacity	65
Fig. 4.4 FE model of Steel Structure to Calculate Lateral Stiffness.....	68
Fig. 4.5 Best Fit Distribution for the Lateral Stiffness and the Capacity of the Steel- Free Deck	68
Fig. 4.6 Plotted Limit State Function Simulated Values and Reliability Index	69
Fig. 5.1 Geometry and Cross Section for the Case Study Bridge (17.5 m Span).....	78
Fig. 5.2 Geometry and Cross Section for the Case Study Bridge (12 m Span).....	79
Fig. 6.1 Deterioration Prediction Curves Based on Different Models	87
Fig. 6.2 Deterioration Prediction Curves Based on Reliability Indices	88
Fig. 6.3 Normalized Deterioration Prediction Curves.....	89
Fig. 6.4 The Best Fit Deterioration Curves for the Conventional Decks	91
Fig. 6.5 Deterioration Curves based on the estimated condition index for the 75 th year	91
Fig. 6.6 Plan View and Cross Section of the Monk Bridge	93
Fig. 6.7 Spall and Deterioration on the Deteriorated Concrete Beam.....	94
Fig. 6.8 Spall and Deterioration Under the Deteriorated Concrete Slab	95
Fig. 6.9 The Best Fit Deterioration Curves for the Old Bridge	96
Fig. 6.10 Best Fit Distributions for the Lateral Stiffness and the Capacity of the Steel-Free Deck.....	100
Fig. 6.11 Plotted Limit State Function Simulated Values and Reliability Indices.....	101
Fig. 6.12 System Deterioration Curves for a Conventional and Steel-Free Deck.....	103

Chapter 1: Introduction

1.1 Introduction

Civil infrastructure, including the public transportation systems are subjected to deteriorating conditions due to aging, fatigue, corrosion, inadequate maintenance and special loading patterns (increasing load spectra) all over the world; hence, they should be inspected and monitored regularly and rehabilitated whenever they fail to satisfy the appropriate performance levels. Inspection and condition assessment of a bridge is a fundamental and critical task in Bridge Management Systems; therefore, special care must be taken to accurately assess the bridge performance in order to make a proper repair or strengthening decision. Among all civil public transportation infrastructure systems, highway bridges play a vital role in the transportation networks. Most of Bridges in Canada were built between 1950 and 1975. Unfortunately, even the minimum required maintenance effort has not been made on many of these important public infrastructures. From about 60,000 bridges in Canada almost 30,000 have reinforced concrete decks in an intensive deteriorating condition. Over 14% of these bridge decks need urgent rehabilitation or replacement and 46% of them need to be considered as a rehabilitation case within the next 10 years (Bisby, 2006). The cost of repairing and replacing deteriorated bridges has been estimated to be approximately \$100 billion in the United States (McDaniel et al. 2010). The corrosion of steel reinforcement, due to the use of salt-based de-icing materials is the main cause of deck degradation.

In the existing Bridge Management Systems, deterioration is modeled based on the visual inspections where the corresponding condition states are assigned to individual elements. Therefore, a limited attention is given to the correlation between different

elements from structural point of view. These models are based on the assumption that the probability of an element being in a particular state at any time only depends on its condition state in the previous inspection period (Frangopol and Neves 2004). As a result of independence between future and past deteriorations, the impact of history of deterioration on the reliability of structure is disregarded and it may entail inappropriate conclusions. To overcome these limitations, researchers have proposed deterioration models based on structural safety in terms of continuous reliability profile (Thoft-Christensen 1998, Kong and Frangopol 2003). These models however could not be updated based on the results of visual inspections (Frangopol and Neves 2004).

One of the solutions for deck degradation prevention is to build a bridge deck that has no internal steel reinforcement. The Innovative bridges such as Steel-Free Deck Systems and bridge decks with Fiber Reinforced Polymer (FRP) provide corrosion-free replacements for conventional deck systems (Newhook 1997, Mufti *et al.* 2007). Reliability-based deterioration model can potentially prove to be an appropriate technique for monitoring and predicting the behaviour of such bridge decks during the bridge life cycle.

1.2 Problem Statement

Engineers, researchers and infrastructure managers often encounter some of the following problems regarding the prediction of the optimum time for major interventions in Bridge Management Systems.

1.2.1 Conventional Steel-Reinforced Concrete Decks

In order to improve the degradation models for conventional steel-reinforced concrete bridge decks, researchers have proposed various mathematical functions to model the deterioration prediction curves. Examples of these deterioration models include multi-linear function (Frangopol and Neves 2004), bi-quadratic convex curve (Myamoto *et al.* 2001), and Weibull cumulative probability distribution function (Grussing *et al.* 2006). The problem with predicting the deterioration pattern using these functions is that they represent the element-level deterioration, where the interaction between different elements in relation to the structural integrity is ignored. Moreover, these models have been obtained based on the expert judgment or historical evidences (Myamoto *et al.* 2001); consequently, they lack the specific functional and structural aspects of a structure. Therefore, there is a need for a rational criterion to verify the correctness of such models with the structural integrity perspective.

A Bridge Management System (BMS) applies the Bridge Condition Index (BCI) or the Bridge Health Index (BHI) based on the element level condition indices as determined from the visual inspection results. Instead of applying the BCI or the BHI to indicate the condition of a bridge, the system reliability-based condition indicator can be applied in the BMS to indicate the system level condition, or it can be added to the BMS as an additional assessing parameter. A System reliability-based deterioration prediction model contributes to predicting the time for potential major interventions in a more precise and rational approach.

1.2.2 *The Innovative Bridge-Deck Systems*

In the case of innovative corrosion-free structural systems, the cracking of concrete due to regular live loads or other natural phenomena has little influence on the failure modes. Consequently, current assessment techniques, consisting mainly of detecting cracks and steel corrosion, are not applicable for evaluating Steel-Free Deck and concrete bridge decks reinforced with Fibre Reinforced Polymer (FRP) bars. Since the available methods for predicting the structural condition of a bridge as developed for conventional bridges do not apply to this system, the development of a deterioration model for such a system would be of interest.

Steel-Free Deck is an innovative corrosion-free structural system. The composite action is provided through the shear connectors as illustrated in Figure 1.1. When a heavy truck wheel load is sustained between the two girders, as a result of high tensile stresses at the bottom of the slab, cracks appear in these zones. The top flanges of the supporting girders tend to move away from the point of the load application. This outward displacement is prevented by the steel straps welded to the top flange of the adjacent girders. Compressive membrane forces then are developed within the concrete deck slab as the reaction to tensile force in the steel straps. These forces enable the slab to withstand the heavy loads through the arching action as shown in Figure 1.1.

Considering the above mentioned problems, a rational technique should be implemented in Bridge Management Systems in order to evaluate the structural performance and avoid subjective diagnosis while assessing the performance of novel systems. In addition, considering the corrosion mechanisms, a rational deterioration and

performance prediction model is of essence which would make the engineers predict the life span and the time of maintenance more objectively.

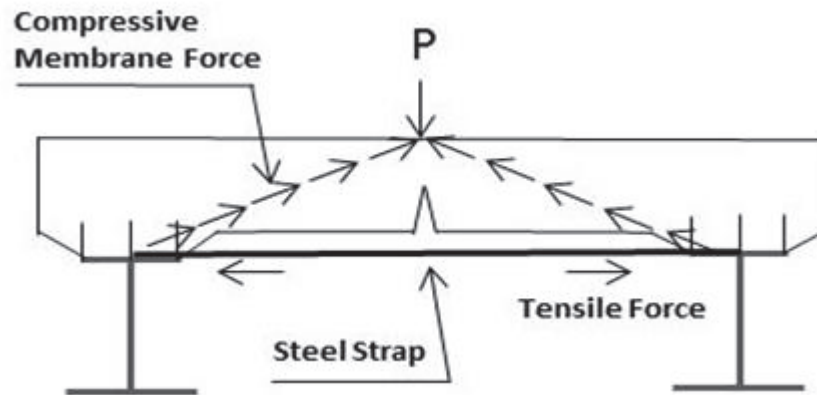


Figure 1.1 Cross Section of a Steel-Free Deck slab (adapted from Newhook 1997)

1.3 Research Scope and Objectives

The objective of the present research is to evaluate the system reliability of bridges at different time intervals applying a rational and numerical technique where the uncertainty of structural parameters, correlation between structural elements, load redistribution, and redundancy of the structure are considered. This thesis demonstrates the effectiveness of developing the degradation profile for the whole structure. The purpose of a reliability-based evaluation is to account for the uncertainties associated with loads and the resistance of the system using the probability of failure P_F , and the reliability index β as the safety criteria. The reliability index can be used as a benchmark to indicate the system performance. By estimating the reliability index for different time intervals, it is possible to find the best fit deterioration function for a particular bridge structure. In this thesis the reliability theory is adopted to establish a deterioration model based on the failure

mechanisms of bridges. In order to accomplish this objective, the following sub-objectives are considered:

1. Identify the main parameters affecting the resistance of conventional and innovative bridge decks and study the variation of such parameters
2. Develop a system reliability assessment method for evaluating the performance of conventional and innovative system bridges e.g., steel-free deck system bridges
3. Develop a deterioration model for bridges based on a system reliability-based method
4. Compare the deterioration patterns of conventional and innovative decks and comment on such structural systems performance over the bridge life cycle

The newly developed models have a key contribution in diminishing the consequences of subjective rating procedures, and providing rational techniques to evaluate the innovative systems. They would have the flexibility to include the information obtained from routine inspection of a bridge and update the deterioration models as well. The methodology of obtaining these objectives is described in detail in this thesis.

1.4 Research Methodology

The methodology to achieve a reliability-based deterioration model at the system level developed here consists of the following phases. Firstly, the structural specifications and the variation of the structural parameters are collected based on the available data in the literature and are incorporated into a structural analysis model. Next, the distribution of the system resistance is obtained by implementing random set of values for different parameters in such model. The reliability index at the system level for different time

intervals is calculated based on the estimated distribution of the system resistance and the probabilistic load variation model obtained from the literature. As structural condition deteriorates, the reliability index similarly decreases over time. Finally, the system level deterioration curve can be drawn which in turn contributes to the decision making process on an appropriate time for a major intervention. The details of this methodology are explained in the Chapter 3.

1.5 Thesis Overview

This thesis contains seven chapters: the first introduces the thesis by presenting the problem statements, the research objectives and a brief reference to the methodology. The second reveals the literature review including : i) the current condition assessment methods for bridges and problems regarding those techniques; ii) explanation of reliability analysis of structures and the corresponding methods; iii) presentation of the load models adopted in estimating the reliability of bridges; iv) description of the modes of failure for Steel- Reinforced Concrete and Steel-Free Bridge Decks; v) overview of the deterioration mechanisms of various bridge elements; vi) presentation of the Existing deterioration models for bridge elements; and vii) explanation of statistical variations of structural parameters.

Chapter three presents the details of the methodology where the System Reliability-based deterioration model is developed. The degradation scenarios of the overpass bridge decks under study in the current research are illustrated in this chapter as well. The Finite Element techniques applied in modeling the bridge decks are explained here. This is followed by an explanation of the procedure that validates the non-linear Finite Element analysis method. Chapters four and five describe the Reliability

assessment of Steel-Free Deck and conventional Steel-Reinforced concrete bridge decks, respectively. Chapter six presents the procedure through which the deterioration model for bridge decks applying system reliability analysis is developed. In this chapter a comparison is made between the developed deterioration patterns for conventional and innovative structural systems. The conclusions and future recommendations end the seventh chapter.

Chapter 2: Literature Review and Data Collection

2.1 Routine Bridge Inspections

After the collapse of the 2,235' long Point Pleasant Bridge, located between Virginia and Ohio over the Ohio river, and its horrifying consequences on December 1967, the need for a periodic bridge inspection program became essential in the United States. The congress asked for a national bridge inspection program. As a result, according to the National Bridge Inspection Standard (NBIS), every public bridge over 6.1 m long should be inspected at regular time intervals no longer than 2 years (Rens *et al.* 2005). Since then, routine inspections are regularly performed to analyze the physical and functional condition of the existing bridges (AASHTO 2004).

Since the deck is the structural element of a bridge which is exposed to traffic and de-icing chemicals, deck assessment could be the main concern in an inspection program. Reinforced concrete decks could be replaced after 15-20 years, while the other bridge components could endure for more than 50 years (Morcous and Lounis 2005). Some researchers suggest that condition of the whole bridge could be detected through deck inspection only (Glagola 1992). However, the other bridge components could face deterioration and need to be inspected in longer time intervals. The principal information used in each maintenance program and Bridge Management System is obtained through the visual inspection data collection during the routine bridge inspections. Based on this information, the condition ratings are assigned to the structural elements in order to assess the structural performance and predict the deterioration rate. According to the inspection reports, the need for any urgent action, maintenance, or replacement of the superstructure could be detected.

The existing Bridge Management Systems (BMS) such as PONTIS, BRIDGIT, and MTQ rating system mainly rely on subjective assessments based on Visual inspection results collected during routine inspections (Gattulli 2005). With reference to the engineer's proposal, Non-destructive Evaluation Techniques (NDT) may be adopted as a tool for condition assessment of a bridge. Different NDT methods may be used to gather supplementary information on the bridge condition. In this manner the engineers are able to assess the bridge condition more rationally. The condition ratings describe the general condition of the bridge. In general, condition ratings are assigned to deck, superstructure, and substructure, that describe the severity of deterioration and the extent to which it is distributed in the structural component (Phares *et al.* 2004).

2.2 Accuracy and Reliability of Routine Inspections

As already mentioned, the existing Bridge Management Systems mainly rely on subjective assessments based on visual inspection results collected during routine inspections. The recent catastrophic events like Laval De la Concorde Overpass collapse in 2006, Canada, and the I-35W Mississippi River bridge collapse in 2007 (Dubey 2008), are the results of subjective evaluation of bridges; therefore, the reliability of structural inspections has become a big concern among engineers during the past decades. To investigate the accuracy and reliability of routine bridge inspections, a study was implemented by the Federal Highway Administration Non-destructive Evaluation Validation Center under FHWA supervision in the US (Phares *et al.* 2004). A group of 49 state inspectors from 25 states were invited to inspect the two in-service and five decommissioned bridges located in northern Virginia and south-central Pennsylvania. In summer 2001, the inspectors were asked to implement routine inspections, and provide

exact condition ratings based on the procedures and inspection data sheets they used in their respective state. The results showed that 68% of the condition ratings vary within one rating point of the average and 95% vary within two points. (Rens *et al.* 2005, Phares *et. al* 2004). The standard condition rating system applied in this study is presented in Table 2.1. This significant variability shows how subjective the condition ratings used in the Bridge management systems are, and how the low reliability of such systems could entail catastrophic disasters in the future.

In general, the condition index with a 0 to 100 range can be categorized into the following five groups for all Bridge Management Systems: 0-19, 20-39, 40-59, 60-79, and 80-100 which represent dangerous, slightly dangerous, moderate, fairly safe and safe levels respectively. Dangerous condition is the state where the bridge should be removed from the service, the deck or any other intensely deteriorated component should be demolished and replaced with a new system. Slightly dangerous condition is a sign of the need for immediate repair (Miyamoto 2001).

2.3 Condition Rating Systems in Canada

In Canada, each province has its own provisions, and there is no federal specification for the bridge inventory (Hammad *et al.* 2007). Unlike the US, for each province in Canada there is specific condition rating system. Some of the Bridge Management Systems as Quebec BMS (QBMS), and Nova Scotia BMS (NSBMS) are found to be very similar to the Ontario BMS (OBMS) which is a typical representative of Bridge Management Systems in Canada (Xue *et al.* 2008).

Table 2.1 Standard Condition Rating in the US (adapted from Phares *et al.* 2004)

Condition Index	Condition	Explanation
N	NOT APPLICABLE	-
9	EXCELLENT CONDITION	-
8	VERY GOOD CONDITION	no problem noted
7	GOOD CONDITION	some minor problems
6	SATISFACTORY CONDITION	structural elements show minor deterioration
5	FAIR CONDITION	all primary structural elements are sound but may have minor section loss, cracking, spalling, or scour
4	POOR CONDITION	advanced section loss, deterioration, spalling, or scour
3	SERIOUS CONDITION	loss of section, deterioration, spalling or scour have seriously affected primary structural component. Local failures are possible. Fatigue cracks in steel or shear cracks in concrete may present.
2	CRITICAL CONDITION	advanced deterioration of primary structural elements. Fatigue cracks in steel or shear cracks in concrete may be present or scour may have removed substructure support. Unless closely monitored it may be necessary to close the bridge until corrective action is taken.
1	“IMMINENT” FAILURE CONDITION	major deterioration or section loss present in critical structural components, or obvious vertical or horizontal movement affecting structural stability. Bridge is closed to traffic but corrective action may put bridge back in light service.
0	FAILED CONDITION	out of service, beyond corrective action

2.3.1 Condition Rating System in Ontario-MTO

In Ontario based on detailed visual inspections, and in some cases on Non-Destructive Tests (NDT), the following four condition states exist per element type: excellent, good, fair and poor (OSIM 2008). The Bridge Condition Index (BCI) generated from the Bridge Health Index (BHI) used in the United States (Johnson and Shepard 1999) is used by the MTO to assess the bridge conditions based on the remaining economic value of the bridges (Hammad et al. 2007). The BCI is a weighted average of the condition state distribution for different elements of a bridge structure. The weighting factor is considered to be the element replacement cost. Therefore, elements with higher replacement cost have a higher weighting factor in the BCI (Ellis et al. 2008).

$$BCI = (\text{Current Replacement Value} / \text{Total Replacement Value}) * 100 \quad (2.1)$$

$$\text{Current Replacement Value} = \Sigma (\text{Quantity} * \text{Weight Factor} * \text{Unit replacement Cost}) \quad (2.2)$$

2.3.2 Condition rating system in Quebec – MTQ

The Bridge Management System in Quebec (QBMS) is based on the same technical background of the system in Ontario (OBMS). The bridge structure is to be inspected at a three-year interval. For each inspection, there is a list of elements to be inspected. Based on the condition of each Element, a list of maintenance needs is identified (Hammad *et al.* 2007). In the system used by MTQ, The bridge structure is evaluated by structure condition index “Indice d'état d'une structure” (IES in French) which has a value between 0 and 100, where 100 represents the best condition or a newly constructed bridge (Morcoux 2006). IES is based on the same concept as the BCI in the Ontario system (OBMS).

2.3.3 Live Load Capacity Factor–CHBDC-S6

For ultimate limit states, chapter 14 of the Canadian Highway Bridge Design Code (CHBDC-S6) provides a deterministic approach to evaluate the live load capacity of the bridge namely the live load capacity factor (F). This Factor is calculated as follows for structural components:

$$F = \frac{UR_r - \sum \alpha_D D - \sum \alpha_A A}{\alpha_L L(1+I)} \quad (2.3)$$

where, U is the resistance adjustment factor, D represents the dead load, L is the live load based on the code specifications, A corresponds the force effects due to the additional loads, and α is the load factor for each corresponding load. The CHBDC-S6 presents different thresholds for the live load capacity factor, where the usage of a bridge may be restricted to a certain magnitude of the load.

2.4 Reliability Analysis of Structures

Though the deterministic analysis of the structure is considered as a useful approach, due to the human error in construction, and variability in material strength, the randomness and probability of failure as a rational measure of the bridge performance in the analysis of structures are of necessity. Both the resistance and load effect are random variables. The failure of a structural system could be described by the limit state function as follows:

$$g(R, Q) = R - Q \quad (2.4)$$

In the above equation, R represents the resistance or capacity of the system, and Q is the load effect or demand (Nowak and Collins 2000). The limit state, $g(R, Q) = R - Q = 0$ represents the boundary between desired and undesired structural performance. Now, if

$g > 0$ the structure is safe, and if $g < 0$ there exists a lack of safety. The probability of failure, P_f , can be expressed in terms of the limit state function. R and Q are continuous random variables where both correspond to different probability density functions (PDF). The probability of failure is defined by the shaded area in Figure 2.1.

$$P_f = P(R - Q < 0) = P(g < 0) \quad (2.5)$$

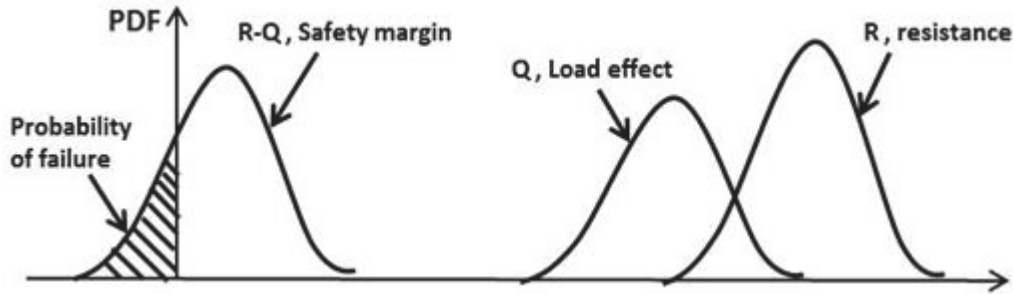


Figure 2.1 PDFs of Load, Resistance and the Safety Margin (adapted from Nowak and Collins 2000)

Converting all the random variables to their standard forms, the resistance R and load Q could be defined in terms of the reduced variables: where, μ , represents the mean value, and σ is the standard deviation. The limit state function can be defined in terms of the reduced variables. The existing reliability models for bridge structures is mainly associated with the Ultimate Limit States (ULS), mostly related to the bending capacity, shear capacity and stability. The serviceability limit states (SLS) may be involved when the target is users' comfort (Nowak 2004). The focus of this thesis is on the Ultimate Limit States.

$$R = \mu_R + Z_R \sigma_R \quad (2.6)$$

$$Q = \mu_Q + Z_Q \sigma_Q \quad (2.7)$$

$$g(Z_R, Z_Q) = (\mu_R - \mu_Q) + Z_R\sigma_R - Z_Q\sigma_Q \quad (2.8)$$

2.4.1 Reliability Index

Instead of estimating the probability of failure, P_F , the calculation of which seems complicated, calculating the reliability index seems less cumbersome. This index is defined as a function of the probability of failure, $\beta = -\Phi^{-1}(P_F)$, where Φ^{-1} is the inverse standard normal distribution function. When system resistance R and load Q follow normal distributions, the reliability index is defined as the shortest distance from the origin of the reduced variables to the line $g(Z_R, Z_Q) = 0$ (Figure 2.2). The shortest distance represents the least level of safety or the maximum probability of failure. According to the geometry presented in Figure 2.2, the reliability index β could be calculated through the following equation:

$$\beta = \frac{\mu_R - \mu_Q}{\sqrt{\sigma_R^2 + \sigma_Q^2}} \quad (2.9)$$

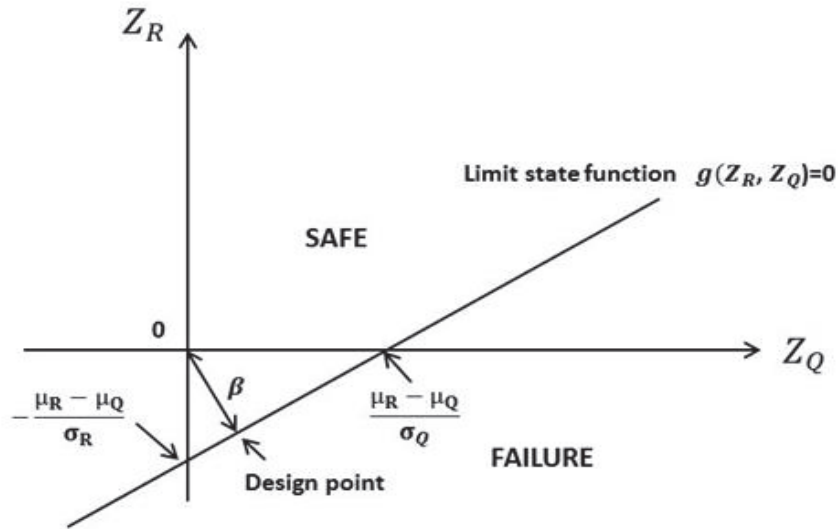


Figure 2.2 Reliability Index, the Shortest Distance in the Space of Reduced Variables (adapted from Nowak and Collins 2000)

Equation (2.9) is justified when both R and Q are independent and follow normal distributions; therefore, the coordinates of the design point with the maximum probability of failure (i.e. the minimum reliability) could be calculated as follows:

$$Z_R = -\frac{\beta \times \sigma_R}{\sqrt{\sigma_R^2 + \sigma_Q^2}} \quad (2.10)$$

$$Z_Q = \frac{\beta \times \sigma_Q}{\sqrt{\sigma_R^2 + \sigma_Q^2}} \quad (2.11)$$

Converting the reduced variables, Z_R and Z_Q , to R and Q random variables:

$$R = \mu_R - \frac{\beta \times \sigma_R^2}{\sqrt{\sigma_R^2 + \sigma_Q^2}} \quad (2.12)$$

$$Q = \mu_Q + \frac{\beta \times \sigma_Q^2}{\sqrt{\sigma_R^2 + \sigma_Q^2}} \quad (2.13)$$

2.4.2 Reliability Analysis Using Rackwitz-Fiessler procedure

The Rackwitz-Fiessler procedure is an iterative method based on normal approximation of non-normal distributions (equivalent normal distribution) for system resistance R and load Q at the design point (Nowak and Collins 2000). As mentioned before, the design point (X^*) is defined as the point of the maximum probability of failure on the limit state function, $g=R-Q=0$. Since this design point is not always defined a priori, an iteration technique may be used to estimate the reliability index.

If at a certain design point (X^*), the cumulative distribution function (CDF) of the non-normal function is $F_X(X^*)$ and the corresponding probability density function (PDF) is $f_X(X^*)$, an equivalent normal CDF and PDF with equivalent normal mean of (μ_X^e) , and

standard deviation of (σ_X^e) could be calculated as follows: where Φ is the CDF of the standard normal distribution and ϕ is the PDF of the standard normal distribution.

$$F_X(X^*) = \Phi\left(\frac{X^* - \mu_X^e}{\sigma_X^e}\right) \quad (2.14)$$

$$f_X(X^*) = \frac{d}{dX} \Phi\left(\frac{X^* - \mu_X^e}{\sigma_X^e}\right) = \frac{1}{\sigma_X^e} \phi\left(\frac{X^* - \mu_X^e}{\sigma_X^e}\right) \quad (2.15)$$

$$\mu_X^e = X^* - \sigma_X^e [\Phi^{-1}(F_X(X^*))] \quad (2.16)$$

$$\sigma_X^e = \frac{1}{f_X(X^*)} \phi\left(\frac{X^* - \mu_X^e}{\sigma_X^e}\right) = \frac{1}{f_X(X^*)} \phi[\Phi^{-1}(F_X(X^*))] \quad (2.17)$$

Replacing the corresponding equivalent mean and standard deviation values for resistance R and load Q into Equation (2.9), the reliability index of the system could be calculated through Equation (2.18), and the new design point can be calculated using Equations (2.19) and (2.20). Iterations will be continued until R^* and Q^* stabilize and do not deviate significantly from the last iteration. The reliability index then could be estimated by applying Equation (2.18) for the last iteration (Nowak and Collins 2000).

$$\beta = \frac{\mu_R^e - \mu_Q^e}{\sqrt{\sigma_R^{e2} + \sigma_Q^{e2}}} \quad (2.18)$$

$$R^* = \mu_R^e - \frac{\sigma_R^{e2} \cdot \beta}{\sqrt{\sigma_R^{e2} + \sigma_Q^{e2}}} \quad (2.19)$$

$$Q^* = \mu_Q^e + \frac{\sigma_Q^{e2} \cdot \beta}{\sqrt{\sigma_R^{e2} + \sigma_Q^{e2}}} \quad (2.20)$$

The iterative procedure to estimate the reliability index is illustrated in Figure 2.3 in the form of a flowchart, where μ is the mean and σ is the standard deviation of any distribution.

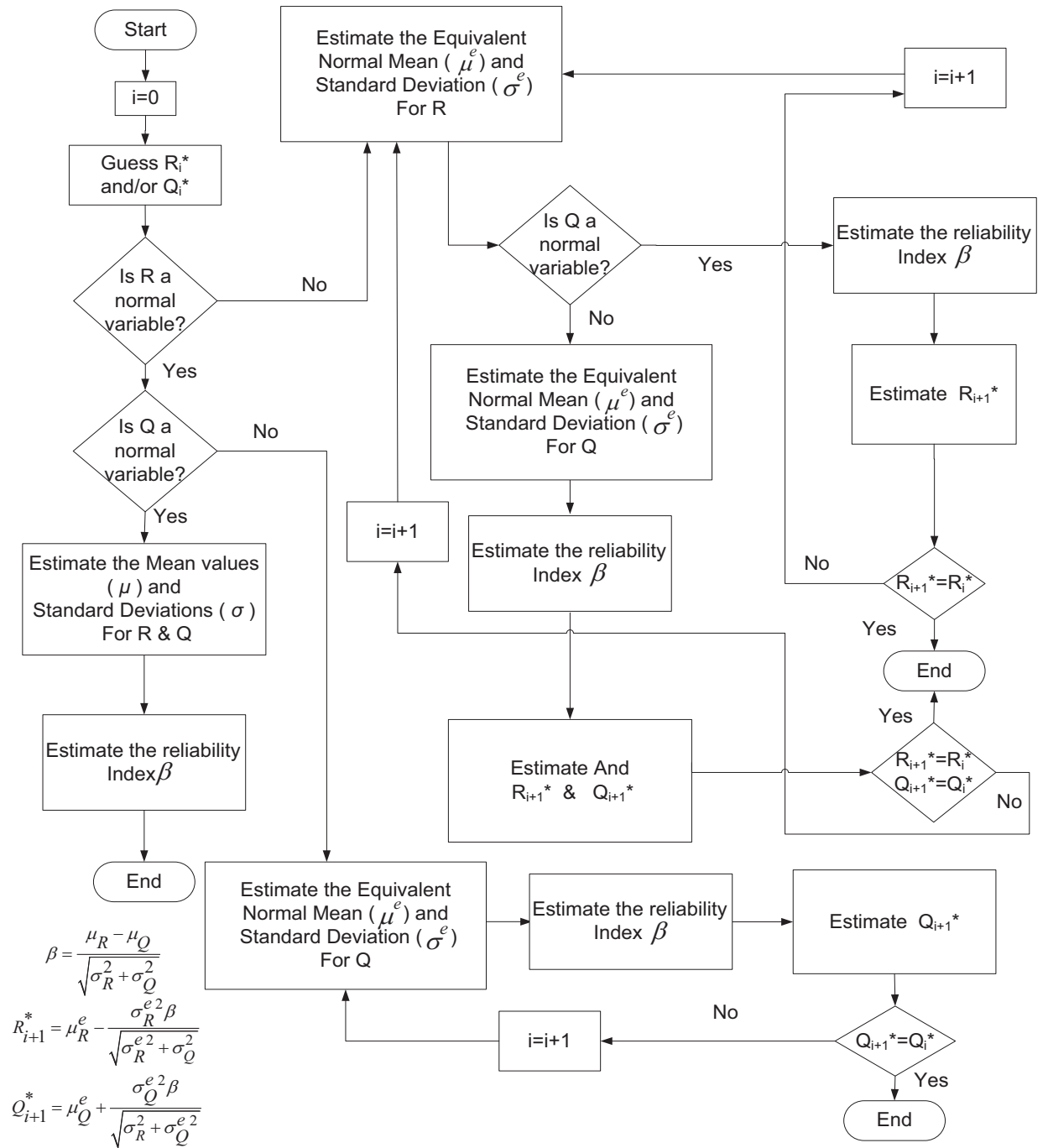


Figure 2.3 Iterative Technique to Calculate β based on Normal Approximation of Non-normal Distributions

Here, Φ is the CDF and ϕ is the PDF of the standard normal distribution. For instance, the equivalent normal parameters for a lognormal random variable can be expressed as follows (Nowak and Collins 2000).

$$\sigma_X^e = X^* \sigma_{\ln X} \quad (2.21)$$

$$\mu_X^e = X^* [1 - \ln(X^*) + \mu_{\ln X}] \quad (2.22)$$

$$\sigma_{\ln X}^2 = \ln \left[1 + \frac{\sigma_X^2}{\mu_X^2} \right] \quad (2.23)$$

$$\mu_{\ln X} = \ln(\mu_X) \quad (2.24)$$

2.4.3 Reliability Analysis Using Simulation

For complicated limit state functions, Monte-Carlo simulation may be the only feasible procedure to estimate the reliability index β and the probability of failure (Nowak and Collins 2000). By applying random values generated from the statistical data and the best fit probability density functions of deferent parameters, the simulated random values of the capacity (R) are obtained. Therefore, by applying the generated random load values (Q), one is able to simulate values of the limit state function $R-Q$. The next step is to plot the simulated values of limit state function on the normal probability chart. The probability of failure [$g(R, Q) < 0$] and the reliability index $\beta = -\Phi^{-1}(P_F)$ could be estimated from the probability chart. The reliability index could be estimated by the inverse of the standard normal distribution function $Z = -\beta = \Phi^{-1}(P_F)$ at the location where the plotted curve intersects a vertical axis passing through the origin (ie, when $g=0$). In case the plotted curve does not intersect the vertical axis, extrapolation of the curve is recommended in order to find β (Nowak and Collins 2000) as illustrated in Figure 2.4.

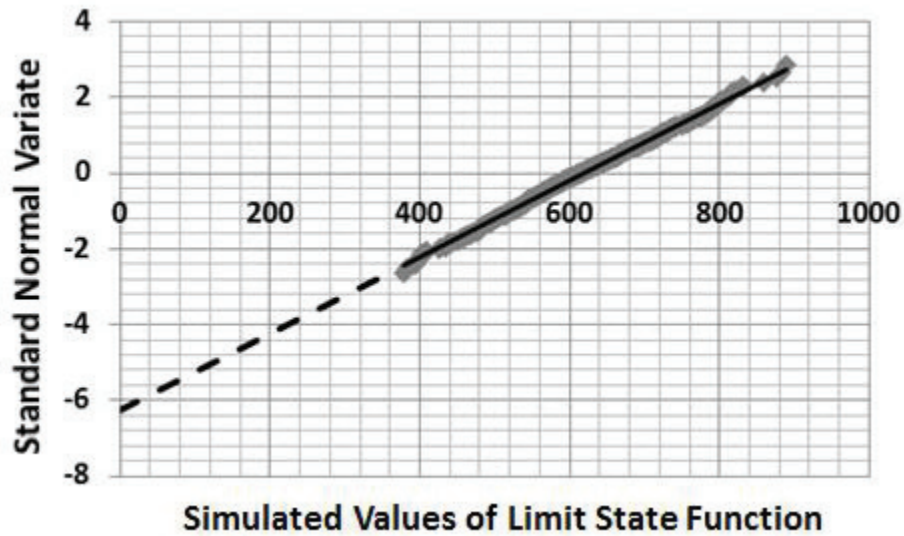


Figure 2.4 Probability Chart and Simulated Values of Limit State Function

2.5 Load Models

The regular load combination for highway bridges is the simultaneous presence of the dead, live and dynamic loads. The load combinations including wind, earthquake and collision forces require particular approach which is not in the realm of this thesis.

2.5.1 The Dead load

The following two dead load components are considered here: the *DL1* and *DL2*. The *DL1* is the weight of cast in place concrete obtained based on the available statistical data (Czarnecki and Nowak 2007), the bias factor (mean/nominal) $\lambda=1.05$ and the coefficient of variation $COV=0.10$. The *DL2* is the weight of the bituminous wearing surface obtained based on the mean thickness of 100 mm with the variation coefficient of $COV=0.25$. The nominal values for specific weight of concrete and wearing surface are

assumed to be 24 KN/m³ and 23.5 KN/m³ respectively. The dead load is treated as a normally distributed variable.

2.5.2 The Live load Model

In assessment of conventional Steel-Reinforced Concrete Bridge Deck System, the live load model (Czarnecki and Nowak 2007, Nowak 1993 and 1999) developed for the calibration of AASHTO LRFD (2004) is applied to calculate the reliability index. The nominal gross weight of the design truck is 325 KN. The design truck includes 3 axles where the nominal weights carried by axles are 35 KN, 145 KN and 145 KN (Similar to standard HS20 truck presented in AASHTO). The truck survey performed by the Ontario Ministry of Transportation, in 1975, (Nowak 1999) covers almost 10000 heavily loaded trucks. The bending moments and shear forces were calculated for a wide range of simple and continuous spans for each truck. The bending moments and shear forces are defined in terms of standard HS20 truck or lane loading (Nowak 1993 and 1999). As an example, the CDF for a simple span bending moment is plotted for one truck effect on normal probability chart as shown in Figure 2.5. In order to estimate the mean maximum truck moments and shears in 75 years of bridge life span, extrapolation is implemented on CDF's. It is assumed that almost 10000 surveyed trucks represent about two weeks of traffic; therefore, the number of trucks in 75 years would be 2000 times greater or N=20 million trucks. The probability of failure caused by such a heavily loaded truck passing the bridge is $\frac{1}{N} = 5 \cdot 10^{-8}$, which corresponds the Inverse Standard Normal Distribution Function $Z = -5.33$. The cumulative probability of passing such a heavily loaded truck and smaller vehicles passing the bridge is estimated to be $\frac{N-1}{N} = 0.999$ which corresponds to $Z = \Phi^{-1}(0.999) = 5.33$ on the normal probability chart. All the CDF's

were extrapolated to this value in order to estimate the maximum values in $T=75$ years. As a result, the mean maximum moments and shears estimated for different periods of time could be read from the graphs. For example, for a 120 feet span and $T=75$ years, the mean maximum moment is found to be 2.08 times the HS20 moment.

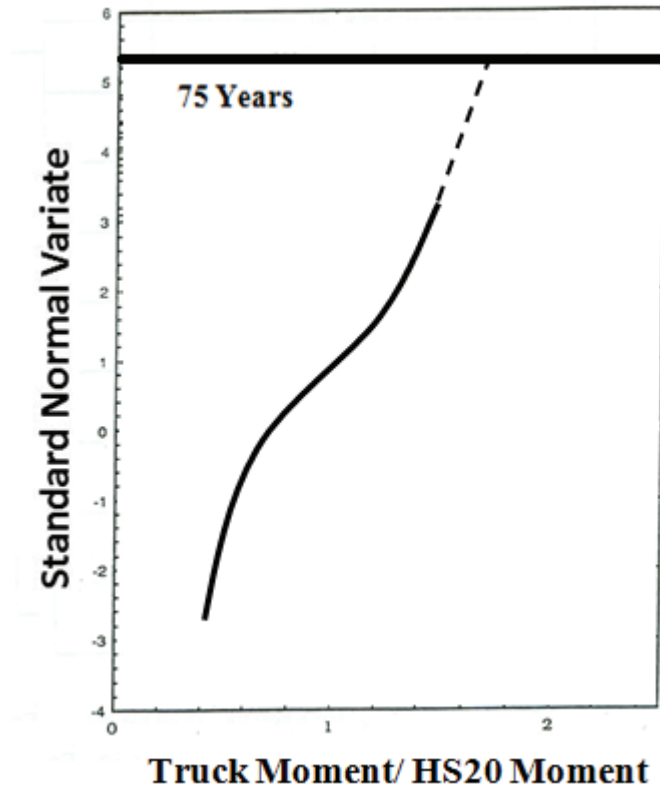


Figure 2.5. CDF of Moments for Simple Span (adapted from Nowak 1999)

As the result of simulations reveals (Czarnecki and Nowak 2007), for the two lane loaded bridge, the ratio of the mean maximum 75-year moment (weight) to that of the design truck varies from 1.2 for a 10 m span to 1.0 for a 50 m span with the coefficient of variation of $COV=0.11$ for all spans. In a case study reported in this thesis (to be discussed later), for a 17.5 m span, the bias factor is estimated to be 1.1625 with a corresponding mean maximum 75-year gross truck weight of 377.8 KN. It is assumed

that the Gross Vehicle Weight GVW is a random variable, but the axle spacing and the truck weight percentage per axle remains constant (Czarnecki and Nowak 2007). The centre-lines of the wheels of two adjacent trucks are placed 1.2 m apart. According to the statistical data, the transverse position of the truck within the roadway (kerb distance) follows a lognormal distribution. For a standard lane width of 3.63 m, the mean value for the kerb distance would be 0.91m with the variation coefficient of 0.33 (Czarnecki and Nowak 2007).

According to NCHRP Report #368 (Nowak 1999) in order to consider the maximum 75-year combination of live load “ L ” and the dynamic load “ I ”, it is assumed that the live load is a product of the static live load “ L ” (as the above mentioned) and the live load analysis factor “ P ” with the mean value of 1.0 and coefficient of variation 0.12. The variation coefficient of “ LP ” is calculated as the square root of the sum of squares of “ L ” and “ P ” variation coefficients. The mean maximum 75 year $LP+I$ would be the mean value of ‘ L ’ times the mean value of “ P ” and $(1+I)$, where “ I ” is the mean dynamic load taken as 0.1 with a variation coefficient of 0.8 for two trucks travelling side-by-side (Czarnecki and Nowak 2007). The standard deviation of maximum 75 year $LP+I$ is calculated as the square root of the sum of the squares of such parameter for “ LP ” and “ I ”. It is here assumed that the total live load is a normally distributed random variable (Nowak 1999). The details of the above calculations could be found in Nowak 1999.

In the Steel-Free Deck system assessment, the live load should be modeled as axle (wheel) load. According to the weigh-in-motion (WIM) measurements conducted on 13 bridges in highways in Michigan (Nowak et al. 1994a, 1994b) and based on the calibrating procedure in the 1994 AASHTO LRFD Code as explained before, the best fit

distribution for the axle weight data has been found to be lognormal with a mean value of 195.72 kN (44 Kips) and the coefficient of variation COV=0.25 (Nowak and Eamon 2008). The transverse dimension of the contact area is assumed to be 190 mm for each tire with a 120mm gap between tires for the dual tire wheel considered here. To simplify the calculations, the gap between two tires is ignored. The wheel contact area is assumed to be of a rectangular shape with the dimensions of 250 mm \times 500 mm. In the capacity calculation of Steel-Free Decks (to be discussed later), the contact area needs to be converted to an equivalent circularly loaded area having the same perimeter length as that of a rectangular contact area. In this case, the estimated diameter of an equivalent circular area becomes 477.5 mm (Newhook 1997). The dynamic load factor (impact factor) applied to estimate the actual wheel load is 1.4 in Canadian codes (Thorburn and Mufti 2001).

2.6 Modes of Failure for Steel- Reinforced Concrete Bridge Superstructure

Czarnecki and Nowak (2007) assumed that the bridge failure occurs when the non-linear deflection in any of the main members of the bridge reaches 0.0075 of the span length. In order to define the ultimate limit state for the structural elements, in addition to control the deflection of each member, the flexural and shear failures are also considered in this thesis. In a reinforced concrete structure, if the plastic rotation (rotation of the plastic hinge) of a given section exceeds a certain value, θ_p , that section is considered as failed in the flexural mode. In this case, θ_p is defined as a function of the curvature of that section at the start of yielding φ_y , the maximum curvature of the section in the ultimate state φ_u , and the length of the plastic hinge l_p . The simplest form of the plastic hinge

length of a concrete section (Park and Paulay 1975) used in this thesis is presented by Equation (2.26), where H is the section depth.

$$\theta_P = (\varphi_u - \varphi_y)l_P \quad (2.25)$$

$$l_P = 0.5H \quad (2.26)$$

The idealized trilinear Moment-Curvature relation (line OABCD) of a concrete section is illustrated in Figure 2.6. The initial uncracked stiffness EI_g and the cracked stiffness EI_{cr} are the slopes of the lines OA and OC, respectively. Here a bilinear representation of the Moment-Curvature relation is obtained from the trilinear curve where both the diagrams represent an equal amount of the absorbed energy. The effective stiffness of the cross section EI_{eff} is represented by the slope of line OB. The first cracking point “A” represents the state where the tensile stress in the outermost edge of the section reaches $0.4\sqrt{f'_c}$, the cracking strength for normal density concrete (CHBDC-S6). The first yielding point “C” appears when the tension steel first yields (Park and Paulay 1975). The ultimate state point “D” is defined as the point where the concrete reaches the ultimate strain 0.0035 in compression or the strain level in the tension steel exceeds the ultimate strain of 10% (CHBDC-S6).

While conducting the simulations in the this thesis, the observations indicate that for a newly constructed bridge girder, the ultimate state is governed by the crushing of concrete in compression; however, for a severely corroded girder at the end of service life of a bridge, the collapse is normally governed by the failure of the reinforcing steel in tension. It is important to note that the mechanical properties of steel reinforcement remains unchanged over time, while the effective cross-sectional area of the reinforcement is reduced due to corrosion. To consider the shear failure, shear hinges are

introduced in the main girders of the bridge superstructure. Due to the brittle shear failure of concrete, no ductility is assigned to the shear hinges. This entails an immediate shear failure of the section when the force reaches the shear strength of the member estimated in accordance with CHBDC-S6.

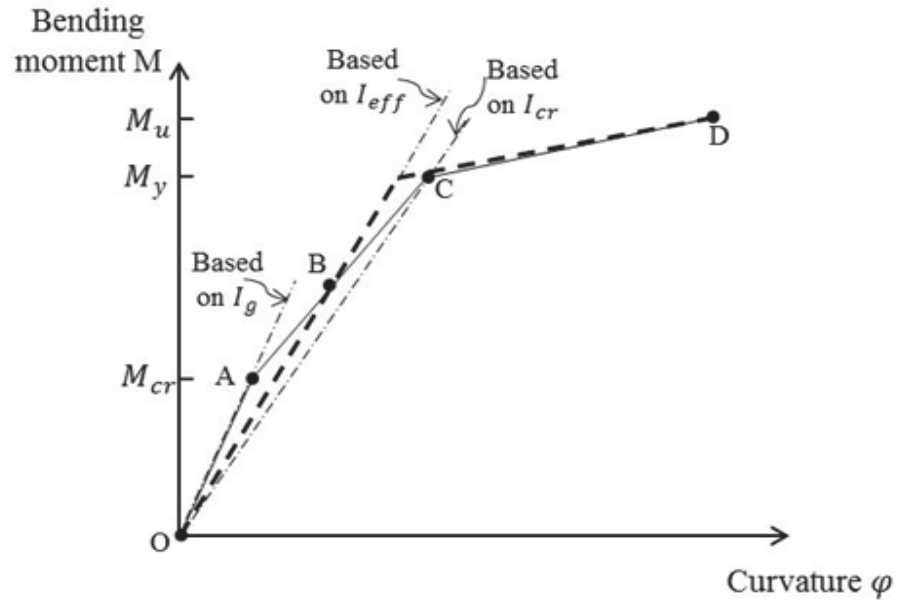


Figure 2.6 Trilinear and Idealized Bilinear Moment-curvature Relation

2.7 Modes of Failure for Steel- Free Bridge Deck System

As already mentioned, the corrosion of steel reinforcement is the main cause of deck degradation due to the application of salt-based de-icing substances. One of the suggested solutions is to build a bridge deck with no internal steel reinforcement. Steel-Free concrete bridge deck system is a relatively new approach in bridge design and construction. Innovative bridges such as Steel-Free Deck System and bridge decks with Fiber Reinforced Polymer (FRP) provide corrosion-free replacements for conventional deck systems. By monitoring several in-service structures, Mufti *et al.* (2007) found that

the non-corrosive Glass-Fiber-Reinforced-Polymer (GFRP) reinforcement in concrete did not experience any damage during 5-8 years of exposure. Also, since no internal steel reinforcement is used in the Steel-Free Deck, a similar behaviour is expected for such system as reported by other researchers (VanZwol *et al.* 2008). By changing the structural behaviour from a flexural to an arching action, the Steel-Free Decks provide a robust and corrosion-free structural performance.

There exist quite a few Steel-Free Deck bridges in Canada and the United States (Bakht and Mufti 1998, Dunn *et al.* 2005). Concrete cracking due to regular live loads or other natural phenomena has little influence on the failure modes of such systems. The Steel-Free Deck System is a relatively new approach in bridge design and construction. Not using internal steel reinforcement in a concrete bridge deck is an appropriate technique to prevent a high deterioration rate of a deck due to the use of de-icing salt. The longitudinal girders are restrained against lateral movement by connecting them with external steel straps underneath the concrete deck. Due to the external restraint, the deck and the strap system work as an arch (Figure 2.7). Under heavy truck wheel loads, radial cracks can appear at the bottom surface of a deck. They gradually migrate to the top surface. On the deck surface, circular cracks with a diameter equal to the clear spacing between steel girders are formed. If the wheel load is very heavy, the inclined shear cracks will reach the bottom of the slab and form wedges that act as rigid bodies rotating about a centre of rotation (CR) as shown in Figure 2.7. The intersection of the wedges and the loaded area is a conical shell with a very high compressive stress. This conical area is also referred to as the punch cone area. The outside boundaries of the slab affected

by the wheel load are defined as the circle where the diameter is the centre line of adjacent girders, C ; therefore, the outer radius of the wedge is $C/2$ and the inner radius is $B/2$. The estimated diameter of an equivalent circular loaded area is explained in the Section 2.5.2. The depth of the wedge is the full depth of the slab in place of the hunches just above the steel girders in capacity calculations. The angle between the radial cracks forming the outside boundaries of the wedge is defined by $\Delta\phi$ (Figure 2.7). When a wedge rotates with an angle ψ , the corresponding lateral displacement Δ_L is restrained by the force $K\Delta_L$, where K is the stiffness of the straps in units of force/displacement per unit length of the circumference. The force acting on a single wedge component, as shown in Figure 2.7, is an oblique compressive force T . The lateral restraining force F_w is mainly developed by steel straps and the top flange of the supporting steel girders (Newhook 1997), the vertical support reaction $\frac{P\Delta\phi}{2\pi}$, and a circumferential force R , developed as the wedge rotates within the angle ψ . The formulation for calculating the capacity of the system is briefly described in this section in reference to Figure 2.7, and the detailed formulation can be found in Newhook (1997). In the formulation described below, y represents the distance of center of rotation C.R to the top surface of the deck which could be calculated by a trial and error procedure. An increase in the wheel load can result in one of the following three modes of failure for the system.

- yielding of steel strap beneath the concrete deck, $\epsilon_y = \frac{f_y}{E}$
- crushing of concrete in punch cone areas, when the circumferential strain at the top surface of the slab $\epsilon_{ct} = 0.002$

- Fracture of welded connections between steel straps and top flange of supporting girders

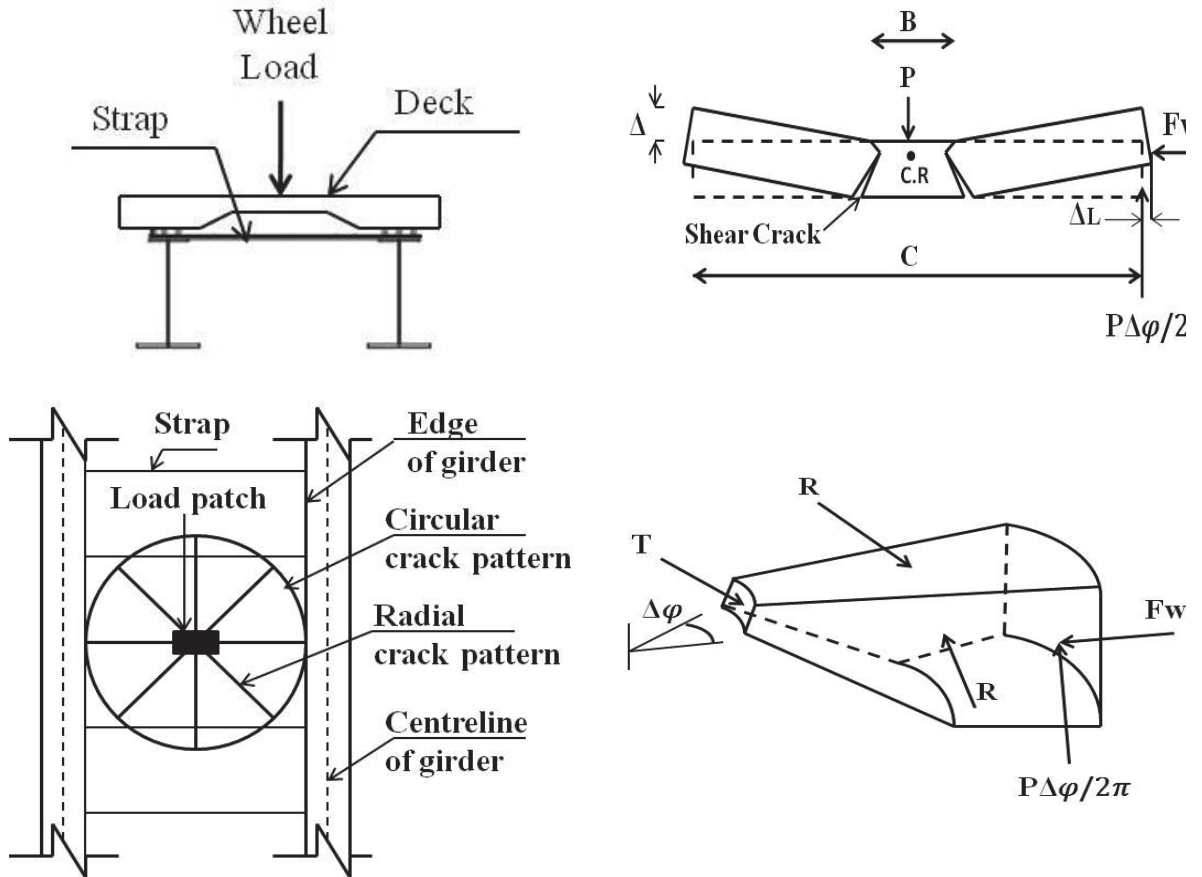


Figure 2.7 Deck Slab Crack Pattern & Rigid Body Rotation of Wedges, (adapted from Newhook 1997)

$$\Delta = \frac{C}{2} \psi \quad (2.27)$$

$$F_w = K\psi(d - y) \frac{C}{2} \Delta \phi \quad (2.28)$$

$$R = \left[\frac{B}{2y} + 1 \right] \frac{y^2}{2} \left[\ln \frac{\frac{C}{2}}{\frac{B}{2} + 1} \right] \sigma_{ct} \quad (2.29)$$

$$P = 2\pi \tan(\alpha - \psi) W \quad (2.30)$$

$$W = K \frac{C}{2} \psi (d - y) - R \quad (2.31)$$

$$\alpha = \tan^{-1} \left[\frac{\frac{R}{W} \left(d - \frac{y}{3} - \frac{C_2}{2} \right) + \left(d - \beta_1 \frac{y}{2} - \frac{C_2}{2} - \psi \left(\frac{C}{2} - \frac{B}{2} \right) \right)}{\frac{C}{2} - \frac{B}{2} + \psi \left(d - \beta_1 \frac{y}{2} - \frac{C_2}{2} \right)} \right] + \psi \quad (2.32)$$

$$C_1 = \frac{P}{0.85\pi B \sin(\alpha - \psi) \sigma_3} \quad (2.33)$$

$$y = \frac{C_1 \cos(\alpha - \psi)}{\beta_1} \quad (2.34)$$

2.8 Deterioration Mechanisms of the Bridge Elements

2.8.1 The Bridge Steel Members Corrosion

The loss due to corrosion in a steel member can be described as the function $C = At^B$ where C is the average corrosion penetration in μm , t is the number of years, A and B are the corrosion parameters, summarized in Kayser and Nowak (1989). If de-icing salt is used frequently on the deck, the environmental condition may be assumed to be similar to harsh marine environment. As an example, for such a deteriorating environment and in case of weathering steel, $A=40.2$ and $B=0.56$. It is observed that corrosion mostly effects the top surface of the bottom flange and $\frac{1}{4}$ of the web height of the supporting steel girders due to deck leakage and traffic spray accumulation (Kayser and Nowak 1989). The corrosion rate is higher in the first few years after initiation and it lowers gradually afterwards. Since no protective coating is used in case of weathering steel, it is assumed here that the corrosion process begins right after the construction. However, in case of

Carbon steel, the time for paint and coating removal should be considered in the calculations.

2.8.2 Service Life of Steel-reinforced Concrete Decks Exposed to Chloride Attack

The corrosion of steel reinforcement is the main cause of deck degradation due to the application of salt-based de-icing substances. Corrosion induced damage of any reinforced concrete bridge deck exposed to chlorides could be divided into different phases mainly: early-age cracking of concrete, corrosion initiation of steel reinforcement, cracking of the concrete cover, and delamination or spalling (Cusson *et al.* 2011). The following five parameters mainly affect the prediction of service life of a steel reinforced concrete deck: (i) the surface chloride content of concrete, C_s ; (ii) effective chloride diffusion coefficient of concrete representing the concrete permeability, D_c ; (iii) chloride threshold of the reinforcement, C_{th} ; (iv) corrosion rate of steel reinforcement, λ ; and (v) the concrete cover of steel reinforcement. These parameters are highly variable (in space and over time), uncertain (in measuring and estimating), and not easy to monitor. Therefore, the deterioration prediction models need to be updated and calibrated based on the results of visual inspections and/or instrumental observations (e.g., Non-Destructive Evaluation (NDE) and Structural Health Monitoring (SHM), etc.), if available. In this thesis, the relevant field data are selected from the literature for those locations with similar environmental situation as in Canada where considerable amount of deicing salt is used during the long and cold winter periods. It is essential to mention that these data are used to draw a primary deterioration curve which should be updated based on the results of periodic inspections and/or monitoring during the life span of a bridge. The following

parameters are identified to have a major influence on the predicted service life of a steel reinforced concrete deck:

- (a) The maximum value of surface chloride content of concrete C_s suggested by Weyers (1998) is 8.8 kg/m^3 for the New York state. This value is considered as the C_s to build up a primary deterioration curve for a cold region. Higher values for this parameter have been found in barrier walls after 10 years of exposure at the Vachon Bridge in Laval, QC, as reported in Cusson *et al.* (2011). In this case, C_s might be underestimated. On the other hand, the values reported by Weyers (1998) are for bare concrete bridge decks that are not protected by a waterproofing membrane. In Canada, however, most bridge decks are designed with a waterproofing membrane. In the latter case, C_s may be overestimated. It is therefore important to recognize the high uncertainty of this parameter alone, which can also vary over time
- (b) The effective chloride diffusion constant, D_c corresponding to the above level of C_s is assumed to be $84 \text{ mm}^2/\text{year}$ as suggested in Weyers (1998). The chloride diffusion coefficient is taken as a single (mean) value for the calculations conducted in this thesis. This parameter, however, can be quite different depending on the concrete used, and therefore, has an influence on the time it takes for the chlorides to reach the reinforcement. Such coefficient should be based on the permeability of concrete or on its water-cement ratio. For simplicity, most models assume it is constant, but it can vary over time
- (c) Chloride threshold of the reinforcements, C_{th} is the critical chloride concentration which causes dissolution of the protective passive film around the steel reinforcement. The most used value for this parameter is 0.71 kg/m^3

(Weyers 1998). The chloride threshold of steel bars is taken as a single value for the calculations in this thesis. This parameter, however, can be different depending on steel type and cement quantity used in the concrete, and therefore has an influence on the time it takes for chlorides to reach the threshold value.

- (d) The current density corresponding to corrosion i_{corr} is a governing parameter. Stewart and Rosowsky (1998) suggested a uniformly distributed random variable for the current density with the mean value of $i_{corr} = 1.5 \mu\text{A}/\text{cm}^2$. Assuming that corrosion of steel reinforcement leads to a uniform reduction in the bar diameter, the corrosion rate could be stated as $\lambda \approx 0.0116 i_{corr}$ (mm/year)

In order to predict the onset of corrosion, the Crank's solution of Fick's second law of diffusion (Cusson *et al.* 2011) is applied in this thesis. According to the Fick's second law the chloride content $C(x,t)$ after time t and at depth x from the concrete surface can be estimated as:

$$C(x, t) = C_S \left[1 - \text{erf}\left(\frac{x}{2\sqrt{tD_c}}\right) \right] \quad (2.35)$$

There is a rapid reduction in chloride diffusion coefficient in the first 5 years of exposure to deicing substances, but it tends to be constant afterwards (Vu and stewart 2000). The error function (*erf*) is twice the cumulative distribution of the normal distribution with a mean of zero and variance of 0.5. When the chloride concentration reaches its critical threshold (C_{th}), the protective passive film around the reinforcement will be dissolved; therefore, the steel reinforcement corrosion process will begin. Replacing the threshold value in Equation (2.35), the time to steel rebar corrosion initiation could be estimated.

The model proposed by Liu and Weyers (1998) is adopted to estimate the time to longitudinal cracking of concrete. According to this model when the rust is produced around the corroded steel bar, gradually it reaches a critical amount which fills the total interconnected pores around the steel and concrete interface and this can generate the critical tensile stress to produce cracks on the concrete surface. It is assumed here that the spall and delamination of concrete cover occur when the crack width reaches the limit of 1 mm, while the predictive model suggested by Vu *et al.* (2005) is adopted here to calculate the time to spall. The estimated time to spall is sensitive to the diameter of steel rebars.

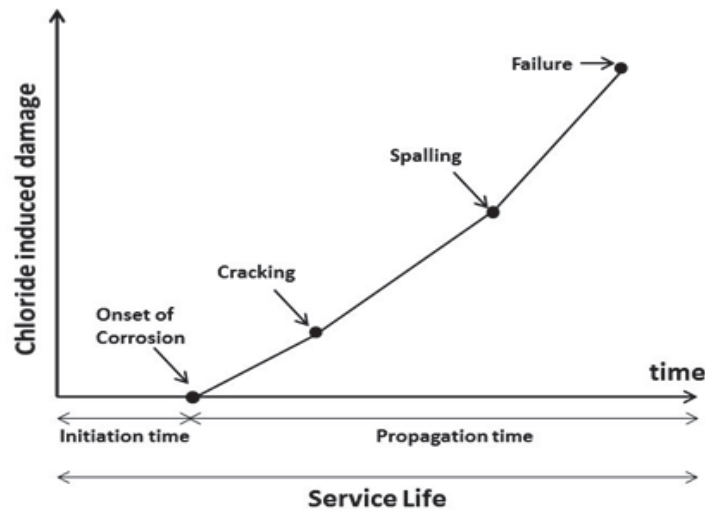


Figure 2.8 Service Life of Corrosion-damaged Concrete Structures (Adapted from Morcous and Lounis 2005)

2.9 The Deterioration Models

The service life of a structural system or the corresponding components depends on the environmental factors and the level of maintenance. Deterioration models are the valuable tools which help engineers to estimate the service life of the structures. As

already mentioned, the Bridge Condition Index (BCI), and reliability index (β) could be used as symptoms indicating the structural health; therefore, by calculating the structural health indices during the life span of the system, one would be able to determine or predict the condition of the whole system or its components at any time interval. The BCI is expressed in the scale of 0 to 100, where 100 defines a defect free condition. Based on the results of visual inspections, the present deterioration can be characterized, and by applying the predicted function of deterioration the remaining life of the bridge could be predicted. The BCI and the reliability index (β) could be reasonably assumed to be similar since they are related as follows (Grussing *et al.* 2006):

- BCI and β are maximum at the beginning of the service life
- BCI and β deteriorate unless corrective action is implemented
- As structural condition deteriorates, BCI and β decrease in a similar manner

In the current Bridge Management Systems, the deterioration curves for the bridge members are normally drawn as a convex graph where the vertical axes represents the structure condition index which in turn represents the health condition and load carrying capacity of the system, and the horizontal axes defines the bridge age. Various deterioration prediction models for bridge elements are developed earlier based on the guidelines of different Bridge Management Systems. Researchers have proposed different mathematical functions in order to model deterioration prediction curves; examples of which include: multi-linear function (Frangopol and Neves 2004), biquadratic convex curve (Myamoto *et al.* 2001), and Weibull cumulative probability distribution function (Grussing *et al.* 2006). The problem with predicting the deterioration pattern by applying these functions is that they represent the element-level deterioration, hence the interaction

between different elements in relation to the structural integrity is ignored. It is worth mentioning that these models are obtained based on the expert judgments or historical evidences (Myamoto *et al.* 2001). Consequently, they may not consider the specific functional and structural aspects of a structure. Therefore, there is a need for a rational criterion to verify the correctness of such models from the structural integrity perspective. A Bridge Management System (BMS) applies the Bridge Condition Index (BCI) or the Bridge Health Index (BHI) derived based on the element level condition indices as determined from the visual inspection results. Instead of using the BCI or the BHI to indicate the condition of a bridge, the system reliability-based condition indicator can be applied in the BMS to indicate the system level condition, or it can be added to the BMS as an addition parameter. A System reliability based deterioration prediction model would assist the decision makers to predict the time for potential major interventions in a more precise and rational manner. Some of the deterioration models related to the major current Bridge Management Systems are briefly described below.

2.9.1 PONTIS

The Markovian deterioration model applying the discrete condition states assessed by visual inspection is being adopted in many Bridge Management Systems including PONTIS (Golabi and Shephard 1997, Thompson *et al.* 1998, Frangopol and Neves 2004). There are some drawbacks and limitations with this method (Frangopol *et al.* 2001); the future condition depends only on the current condition, not on the deterioration history, and the condition deterioration is assumed to be a single step function. Considering the independency between the future and the past deterioration histories, and also considering previous maintenance actions, the Markovian deterioration model may result in incorrect

decision making. Transition Markovian matrix could be provided based on a great amount of data and subjective assumptions. This method is not adopted in this thesis because of the above mentioned drawbacks.

2.9.2 The Bridge Management System in Japan, J-BMS

Developing a program called Concrete Bridge Rating Expert System, based on the knowledge and experience acquired from experts and experimental data collected, the J-BMS proposes a biquadratic function for the convex deterioration curve representing the load carrying capacity (Miyamoto 2001).

$$I = b_L - a_L t^4 \quad (2.36)$$

where, b_L is the initial condition index, a_L is a experimental constant the value of which is determined experimentally , and t is the age of the bridge. Considering the initial condition index just after opening the bridge to traffic as $CI=100$, the initial condition index is always $b_L = 100$. The proposed BMS predicts the deterioration processes for existing bridge individual elements. The system suggests that the deterioration functions be modified and updated based on the data obtained from inspections. Estimating the structural condition index based on each inspection, engineers are able to define a_L , b_L and establish the preliminary deterioration curve for every bridge member. The great advantage of this model is the convex deterioration that the curve could be defined based on only one time inspection data. The calibration of the curve after each inspection or monitoring cycle is important (Miyamoto et al.2001).

2.9.3 Deterioration Model Based on Weibull Probability Distribution

The Weibull cumulative probability distribution method is adopted to model the deterioration curve for each component section (Grussing *et al.* 2006). The Weibull statistical distribution represents the probability of a component failure in time. The mathematical form of the convex deterioration curve model for bridge component is given by the following equation:

$$C(t) = a \cdot e^{-\left(\frac{t}{\gamma}\right)^\alpha} \quad (2.37)$$

where, $C(t)$ stands for the condition index as a function of time (t) in years, (a) is the initial condition index, (γ) represents the service life adjustment factor, and (α) is the accelerated deterioration factor. Reasonable assumptions should be made to compute parameters a , α and γ . Considering the initial condition index just after opening the bridge to traffic as $CI=100$, the initial condition index is always $a=100$. If the condition index equals a terminal value at the end of service life, by implementing only one set of inspection data, one is able to draw the condition life cycle curve. It is also essential to calibrate the expected condition with the actual observed condition as time goes on and degradation increases. The validation of this model to be adopted in civil infrastructure systems is highly recommended.

2.9.4 The Reliability Based Multi-linear Deterioration Model

Frangopol and Neves (2004) proposed a multi-linear deterioration model for structural elements which is represented as bi-linear functions under no maintenance (Figure 2.9). In their model the deterioration rate is assumed to be constant. Therefore, this model is

not able to capture the variable deterioration rates for steel structures and reinforced concrete structural systems.

2.10 The Statistical variations of structural parameters

For the purpose of generating the random values for the parameters governing the capacity of a bridge, the Oracle Crystal Ball software (2008) has been used here. By applying the random values of the governing variables, the simulated random values of the deck capacity R would be estimated for different time intervals. The statistical data on these parameters, as obtained from the literature, are described as follows:

According to Mirza and MacGregor (1979a), when the nominal value of the yield strength of the reinforcing steel $F_y=400$ MPa, with reference to the nominal area of the steel bars, the best fit distribution of this parameter is reported to follow a beta distribution with Alpha=3.02, Beta=7.95, Minimum= 54 Ksi (373.3 Mpa), and Maximum=102 Ksi (703.26 Mpa). They have also mentioned that modulus of elasticity of reinforcing steel E_s can be considered to be normally distributed with the mean value of 201,000 MPa and a variation coefficient of 3.3%.

With a bias factor (ratio of mean to nominal value) of 1.123 and a coefficient of variation $COV = 0.06504$ for the high strength concrete used in bridge construction (Tabshand Aswad 1997), the compressive strength of concrete is assumed here to follow a normal distribution. Considering the variation of the specific weight of cast in place concrete γ_c as explained in the dead load model (Section 2.5.1), the modulus of elasticity for concrete E_c is calculated as follows (CHBDC-S6).

$$E_c = (3000 \times \sqrt{f'_c} + 6900) \times \left(\frac{\gamma_c}{2300}\right)^{1.5} \quad (2.38)$$

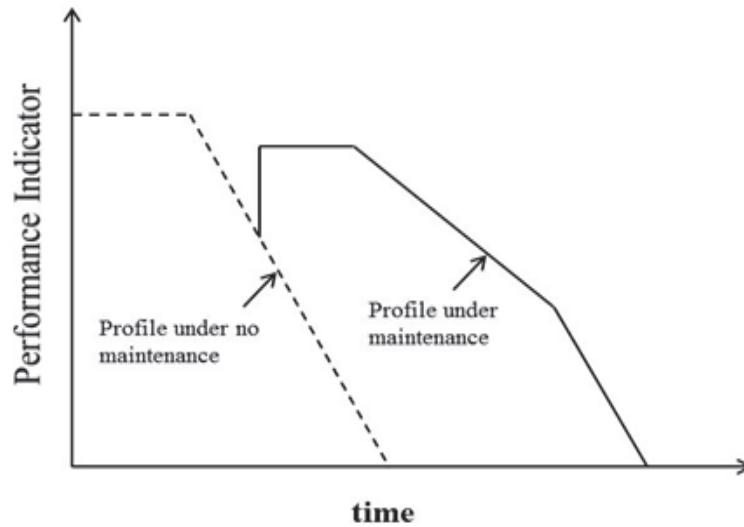


Figure. 2.9 Multi-linear Reliability-based Deterioration Model (adapted from Frangopole and Neves 2004)

Mirza and Macgregor (1979b) suggested that the dimensions of reinforced concrete members can be assumed as normally distributed. For slab thickness, in case of cast in-situ concrete, the recommended mean deviation from the nominal value is +0.79 mm with the standard deviation of 11.9 mm. For the thickness of beam web, mean deviation from nominal value is suggested as +2.38 mm with the corresponding standard deviation of 4.76 mm. In case of the overall depth of a beam, the mean deviation from the nominal dimension is suggested as -3.175 mm with the standard deviation as 6.35 mm. Concrete cover is found to have a significant effect on rebar corrosion and resulting spall and delamination of a concrete member. For the top reinforcement of a concrete slab, a considerable mean deviation from nominal and standard deviation of +19.84 mm (to the center of bars) are proposed based on the statistical data by Mirza and Macgregor (1979b). The cover for top reinforcement of cast in place slab is noticeably higher than the nominal value which might be due to construction workforces walking on the bars during the construction. For the bottom reinforcements in a slab, the mean deviation from

the nominal value is +8.73 mm with a standard deviation of 10.31 mm. In case of a concrete beam, the data shows that the cover may be assumed to have a normal distribution.

For hot-rolled steel beams and straps, the thickness of the member components has a very low coefficient of variation and can be considered as a deterministic value. But due to the variations caused by human errors in fabrication, the width of the members may follow a lognormal distribution with a bias factor of $\lambda_F = 1.0$ and a coefficient of variation $COV = 0.05$ (Nowak and Collins 2000). The yield strength of structural steel F_y may follow a lognormal distribution with a mean value of $1.1 F_y$ and a coefficient of variation $COV = 0.1$ (Bennett and Najem 1987).

Chapter 3: Methodology

3.1 Introduction

The deterioration curves could be defined based on visual inspections and evaluations, while the need for more objective techniques to predict the system performance is highly demanded. Structural analysis using Finite Element modelling is a powerful tool which may be used in the performance prediction models in order to assess the system reliability more objectively. After reviewing different deterioration models, it becomes evident that there are some specific shortcomings with each model. Therefore, a rational performance prediction model based on a structural analysis and reliability calculation is required. The attempt is made in this thesis to implement the rational techniques into performance assessment and prediction model for bridges with conventional and/or innovative structural system where a more objective model to predict and follow the deterioration process of bridge infrastructures is proposed.

The objective of the present research is to evaluate the system reliability of bridges at different time intervals by adopting a rational method and numerical technique where the uncertainty of structural parameters, correlation between structural elements, load redistribution, and redundancy of the structure are considered. This thesis demonstrates the effect of the degradation profile developed for the whole structure. The purpose of a reliability-based evaluation is to account for the uncertainties associated with the loads and the resistance of the system using the probability of failure P_F , and the reliability index β as the safety criteria. The reliability index can be used as a benchmark through which the performance of a system is indicated. Estimating the reliability index for different time intervals, one is able to find the best fit deterioration function for a

particular bridge structure. The reliability theory is adopted in this thesis to establish a deterioration model based on the failure mechanisms of bridges. In case of conventional steel-reinforced bridge deck system, as case study examples, this developed method has been applied in simply supported concrete bridge superstructures designed according to the Canadian Highway Bridge Design Code (CHBDC-S6). The Non-linear Finite Element models of bridges have been developed and the system reliability index has been determined for different time intervals. Finally, the degradation profile of the bridge superstructure has been established and updated.

In case of the innovative systems that use non-conventional materials or structural forms, due to lack of established deterioration model it is difficult to predict the reliability of such systems at different time intervals. The newly developed method here is applied to an innovative structure with a Steel-Free Deck System, namely the Crowchild Bridge, in Calgary, Canada, as a case study. The cracking of concrete caused by regular live loads or other natural phenomena does not have an important influence on the failure modes of the system; consequently, the current assessment techniques applied in bridge management systems are not applicable in this system. A Finite Element model of the bridge has been developed and calibrated through the experimental results that yield static deflection, vibration characteristics, load distribution, and crack patterns. The system reliability has been determined for different time intervals by adopting the proposed method.

3.2 Methodology of the System Reliability-based Deterioration Model

The methodology in developing a reliability-based deterioration model at system level is demonstrated in the flow-chart, Figure 3.1. The structural specifications and the

variation of the structural parameters obtained from the literature review (Section 2.10) are incorporated into a Finite Element model. The distribution of the system resistance is achieved by implementing the random set of values for different parameters in the structural analysis model (Box No. 4, Figure 3.1). Based on the estimated distribution of the system resistance (Box No. 5, Figure 3.1), the probabilistic load variation model obtained from the literature (Section 2.5, Box No. 6, Figure 3.1), the distribution of the Limit State Function can be estimated through simulation. The reliability index β at the system level for different time intervals is calculated through the procedure described earlier (Section 2.4). The β is used as a tool for measuring the probability of a structural system that would meet the performance requirements for each time interval. As the structural condition deteriorates, the reliability index similarly decreases over time. The system level deterioration curve can be drawn as is illustrated in Box No.10, Figure 3.1. The developed deterioration curve could be updated applying the defects observed during the visual inspections and/or monitoring into structural analysis and FE model over time.

By comparing the estimated reliability index and the target index representing an acceptable safety level, the decision makers are able to predict the appropriate time for major interventions. Reliability-based degradation profile can be applied to evaluate the condition of conventional and innovative bridge systems. Since the available methods for predicting the structural condition of innovative systems that use non-conventional materials or structural forms do not apply, the reliability-based deterioration model may be a suitable evaluation technique for a given length of service life. A Bridge Management System (BMS) uses the Bridge Condition Index or the Bridge Health Index derived from the element level condition indices as determined by the visual inspection

results. Instead of using the Bridge Condition Index or the Bridge Health Index to indicate the condition of a bridge, the system reliability-based condition indicator can be applied in the BMS to indicate the system level condition, or it can be added to the BMS as an additional parameter. A System reliability based deterioration prediction model helps decision makers to predict the time for potential major interventions in a more precise and rational manner.

Where the best fit distribution for the limit state function is normal (as is found for the Steel-Free Deck), the cumulative distribution function plotted on the normal probability chart would be a straight line. By using Monte-Carlo simulation and the normal probability paper, one is able to read the reliability index β and the probability of failure P_F easily on the paper. As mentioned in the Section 2.4.3, in case the plotted curve does not intersect the vertical axis, extrapolation of the curve is recommended to find β . This methodology procedure is presented in Figure 3.2.

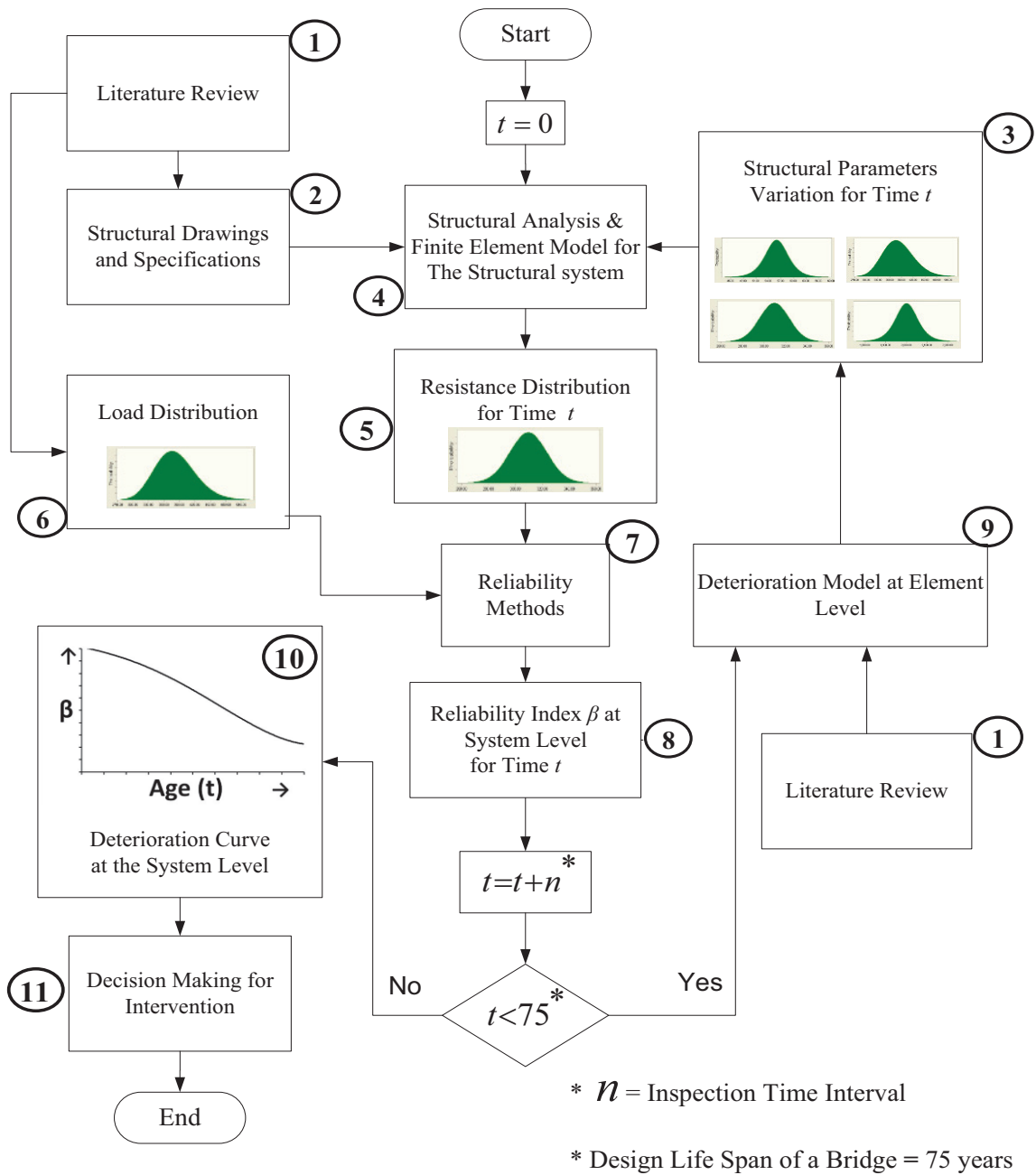


Figure 3.1 The Methodology to Develop a Reliability Based Deterioration Model at the System Level.

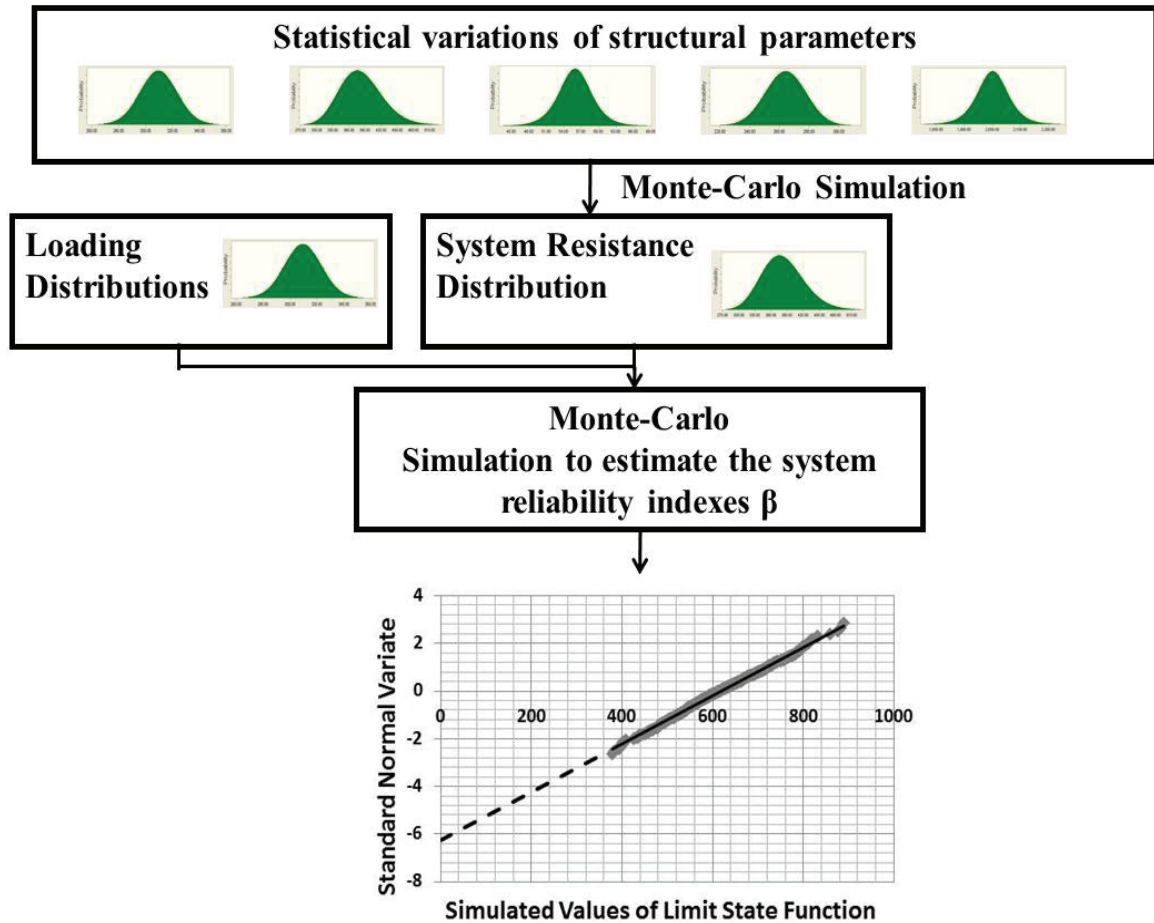


Figure 3.2 Reliability-based Assessment Using Simulation

3.3 Degradation Scenarios of Overpass Bridge Decks

Assuming that during the life span of an overpass bridge the drains are well maintained, in case of conventional steel-reinforced bridge decks, the only scenario considered in this thesis is when de-icing salt reaches the top surface of the beam through the permeable wearing surface and becomes airborne due to traffic beneath the bridge. As a conservative assumption, it is assumed here that de-icing salt contaminates all the soffits of the beam and the slab as shown in Figure 3.3. Corrosion of steel reinforcement leads to reduction of the bar diameter which results in the degradation of the capacity of a

structural element. Spall or delamination is the cause of decreased capacity caused by concrete compression zone reduced by the depth of spalled cover. Spalling of the top or bottom cover also leads to reduction of shear capacity due to the decreased depth of the cross section by one or both covers (Vu and Stewart 2000). Here, it is assumed that when delamination takes place, the spalled debris are still connected to the structure and have not fallen down; consequently, the spalled zone does not contribute to the capacity of the bridge, but it is still considered as a part of the dead load. For the end of life span (50th to 75th year), the spalled areas were excluded from dead load calculations.

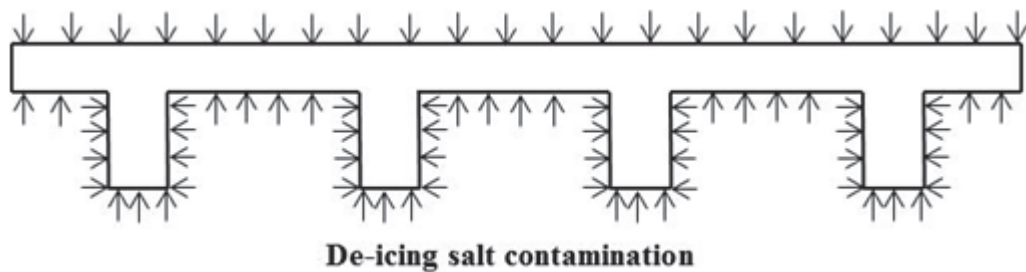


Figure 3.3 De-icing Salt Contamination Scenario for Conventional Steel-reinforced Deck

In case of innovative Steel-Free Deck, It is observed that in general corrosion has an effect on the top surface of the bottom flange and $\frac{1}{4}$ of the web height of the supporting steel girders (Section 2.8.1). The corrosion of the top surface of the steel straps is attributed to deck leakage in this thesis.

3.4 Modeling Procedure, Non-linear Finite Element Analysis Method

In order to evaluate the capacity of a steel-reinforced element in a non-linear state, not only the deflection should be limited to a certain value (i.e. the 0.0075 of the span

length), but the rotation (curvature) of plastic hinges should be controlled so it would not reach a collapse level (Figure 2.6).

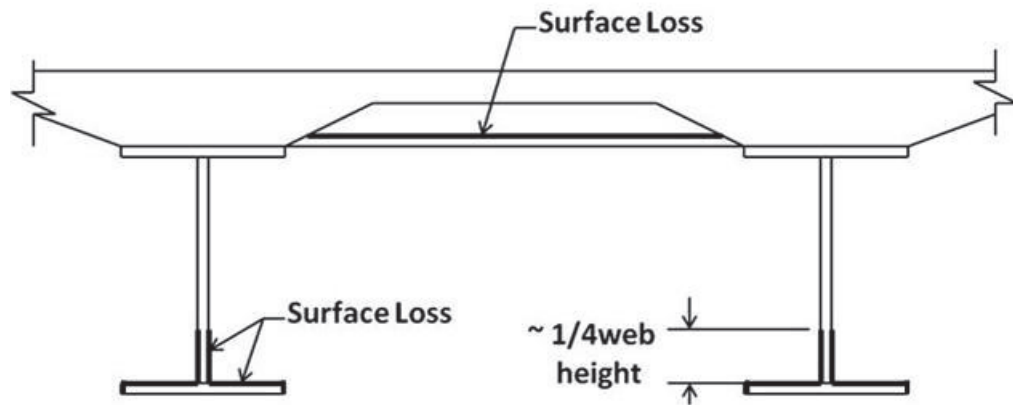


Figure 3.4 De-icing Salt Contamination Scenario for Steel-Free Deck System

In order to verify the results obtained from SAP2000 (2003), a reinforced concrete beam with the length of 10 m (Figure 3.5) has been modeled in two different non-linear analysis programs, SAP2000 and DRAIN-2DX where the latter is one of the best known nonlinear static and dynamic analysis program (Prakash et al. 1993). These two-dimensional (2D) models are able to capture the non-linear behaviour at the element level. The purpose of this verification is to make sure that the nonlinear behaviour of the plastic hinges in a beam is modeled correctly. While a hinge may be oriented in space in any manner, for a beam it is always oriented along its axes. As the behaviour of a hinge is always defined in 2D in the local coordinates, for capturing the hinge behaviour in bending of a beam about the major axis, a 2D model of the beam is sufficient. Once the element level model is validated, the 3D model of the bridge employing such element level models of hinges in individual girders is expected to work well. A vertical pushover analysis (monotonically increasing vertical loads) has been implemented on the beam by applying two symmetrical concentrated point loads (similar to the truck loads on a bridge

deck) with a certain distance ($1/3$ of span) from each edge of the single span simply supported beams. The moment-curvature diagram for the sample beam as shown in Figure 2.6 has been established and implemented in SAP2000 and DRAIN-2DX separately.

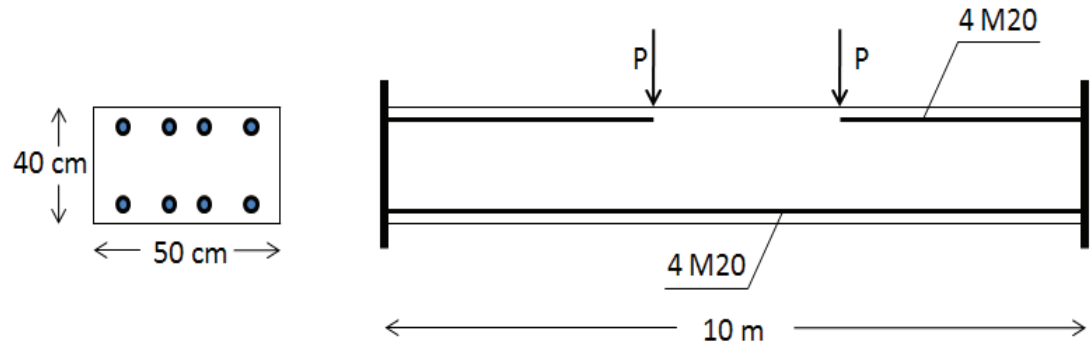


Figure 3.5 Reinforced Concrete Beam Used to Verify the modeling Procedure

The properties of plastic hinges in both positive and negative moment directions are calculated according to the procedure explained in Section 2.6, and presented in Figure 3.6 for the section with top and bottom rebars. The length of a plastic hinge is 50% of the section height as discussed in Section 2.6. The obtained results from both softwares are presented in Table 3.1. The ultimate load and corresponding rotations of plastic hinges obtained from two software systems are in agreement (less than 3% difference). When the two point loads reach the magnitude of 77 KN, the plastic hinges at the two ends of the section reach their maximum capacity (limit of rotation). In this case the flexural mode of failure is reached before the element reaches the 0.0075 of the span length.

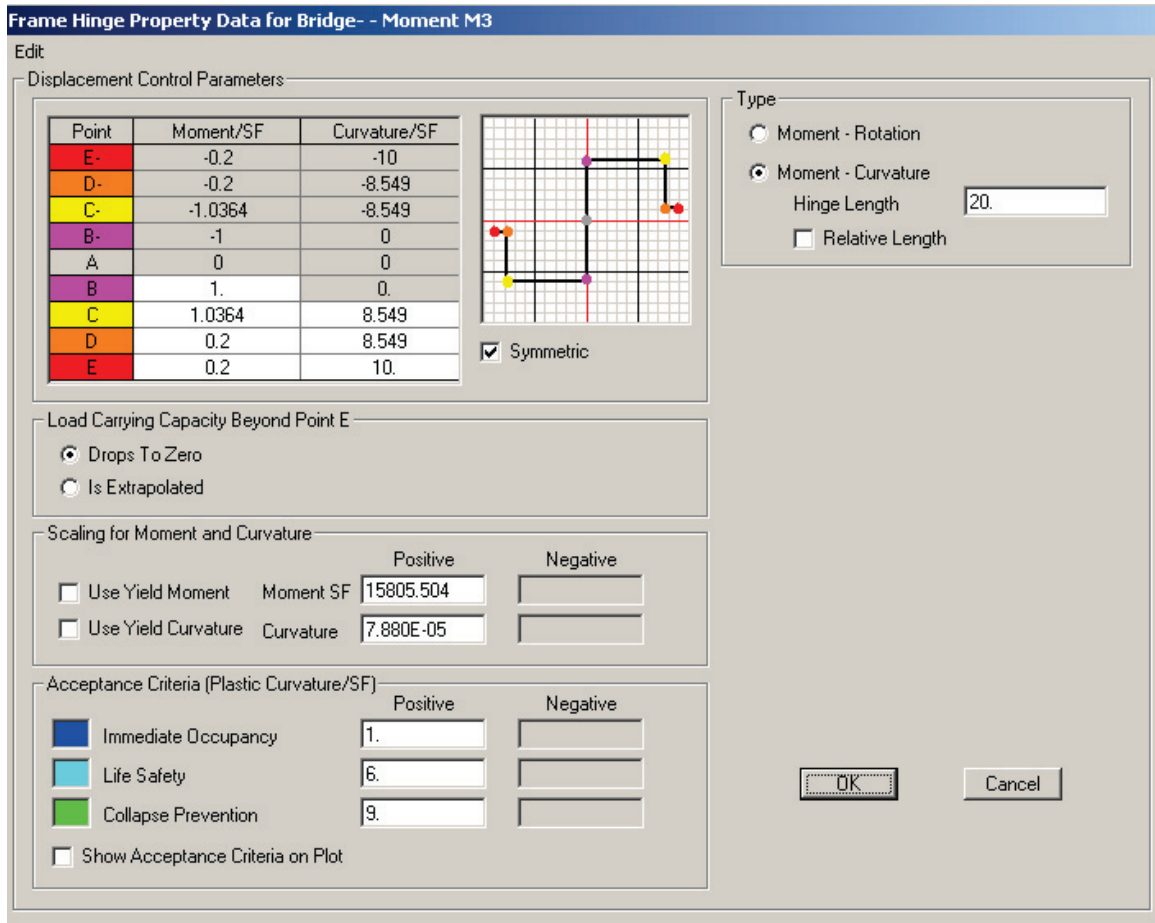


Figure 3.6 Plastic Hinge Properties for the Section with Top and Bottom Rebars

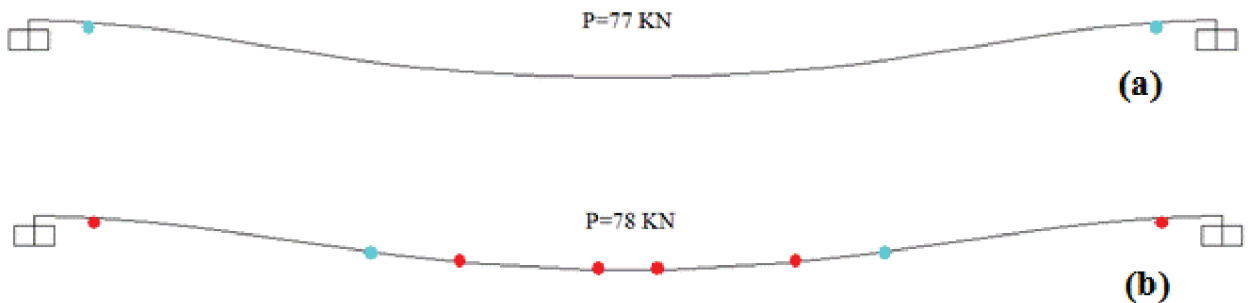


Figure 3.7 Condition of Plastic Hinges Just (a) Before and (b) After Collapse (Blue hinges indicate yielding, and red hinges indicate the ultimate stage).

Table 3.1 The collapse load obtained from the two software systems

Software	Load (KN)	Moment (KN.cm)	Max. Plastic Rotation (rad)	Max. Deflection(cm)
SAP2000	77	1619200	0.0129	6.89
Drain-2DX	77	1590000	0.0133	6.99
difference %	-	1%	3%	1%

3.5 Finite-Element Modeling of Bridge Decks

3.5.1 Conventional Steel-reinforced Deck

In case of conventional steel-reinforced concrete decks, two 3D models have been developed through SAP2000. Model 1 (Figure 3.8a) employs shell elements, and Model 2 (Figure 3.8b) is built based on the grillage analogy (Stallings and Yoo 1992) as a planar grid of longitudinal (main T-section beams parallel to the roadway) and transverse members (perpendicular to the roadway). The former model is considered to be more accurate, while the latter is more efficient. Effort has been made to correlate both the models with each other. The advantage of adopting the grillage model with frame elements, Model 2, is that the plastic hinge properties could be assigned to this kind of element. In Model 1, a plastic hinge cannot be defined since the plasticity is distributed over the shell elements and governed by the 3D yield criteria. In Model 2, one is able to calculate the hinge properties (Figure 2.6) and assign them as the user-defined hinge properties in the program for each plastic hinge. In order to consider the cracking effect in Model 1, the stiffness of the shell elements is reduced to 40% of the original stiffness

(CSA, A23.3-04). To calibrate Model 2 based on the results of Model 1, the stiffness of longitudinal members in Model 2 is reduced in the same manner, while the stiffness of each weightless transverse element is adjusted in a manner that both the models show the same deflection for different transverse positions of the two side-by-side design trucks (Figure 3.8b) as proposed by Czarnecki and Nowak (2007). To estimate the reliability index of the bridge superstructure, the calibrated model, Model 2, has been adopted based on the grillage analogy for the rest of simulations since it needs less time for computation and is more simplified while dealing with less number of parameters as compared to the shell-based model. However, the simplified model is closely correlated with the full model (shell-based) in order to capture the effect of all the details and damages in the bridge superstructure. The magnitudes of truck loads shown in Figure 3.8b are increased incrementally to reach the ultimate system capacity for simulation purposes.

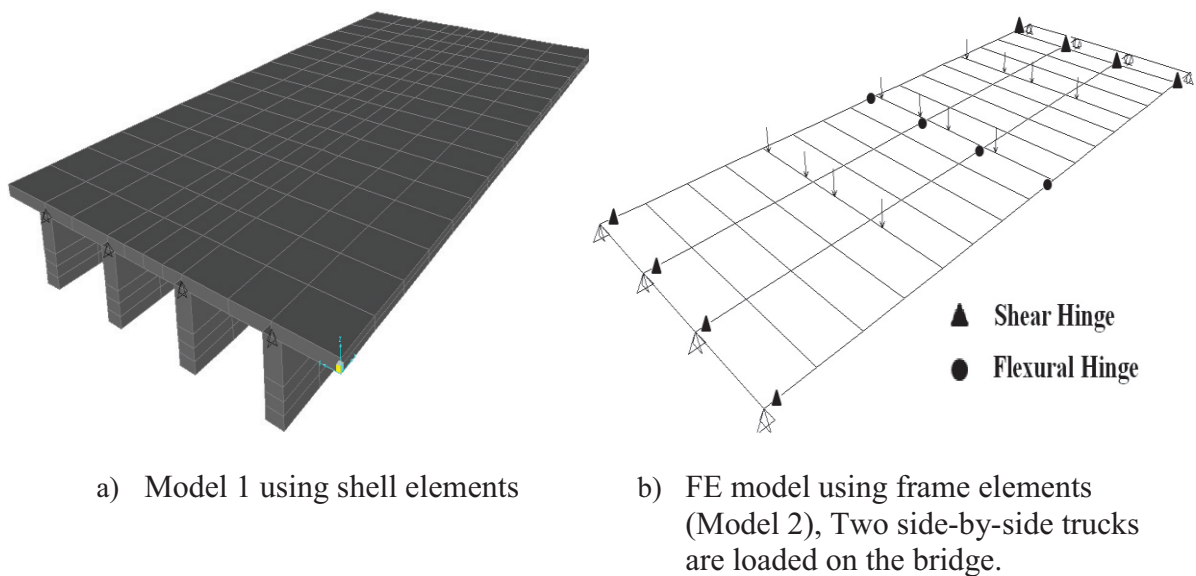


Figure 3.8 Finite Element Models for Conventional Steel-Reinforced Concrete Decks

3.5.2 Innovative Steel Free Deck

To investigate the behaviour and response of the Steel-Free Deck System for different time periods, the SAP2000 is applied. A three dimensional Finite Element model of the bridge (Figure 3.9) has been developed by applying frame elements for the Piers, diaphragms and steel straps, as well as shell elements for the steel girders, the concrete deck and the side barriers. To consider the composite action, steel girder elements are connected to the deck elements using body joint constraints so that the connected joints move together as a rigid body. Bridge bearings are modeled here by using link elements between the top of the piers and the bottom flanges of the steel girders.

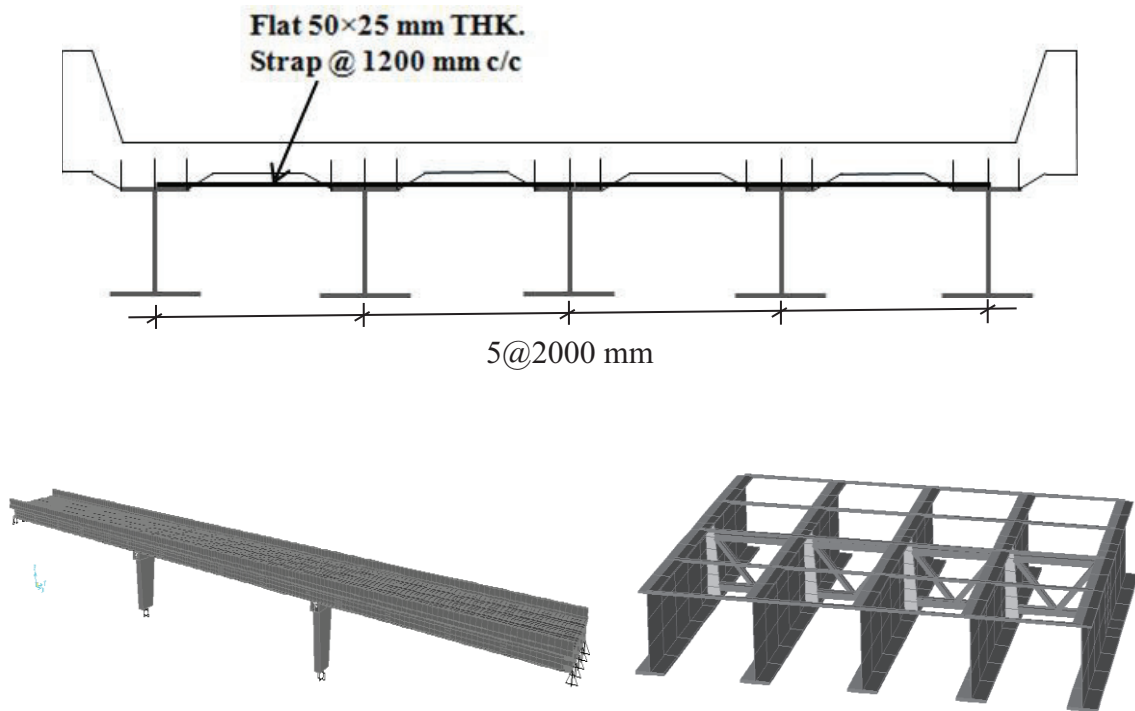


Figure 3.9 Cross Section (adapted from Van Zwol *et al.* 2008), and Developed FEM Model of Crowchild Trail Bridge

Link properties are defined as using very strong springs under compression, but weak springs under shear and they have longitudinal orientation (North-South of the bridge). According to drawings of the Crowchild bridge, the case study bridge, the pier supports at their base are fixed. At the southern abutment, pin supports are assumed ; while, at the northern abutment, roller supports are considered together with the link elements to model the bridge bearings. The FE model has been calibrated according to the field testing results for static deflections, vibration characteristics (natural frequencies of the first four mode shapes), load distribution, and crack patterns reported by other researchers (VanZwol *et al.* 2008). More details and result will be discussed in chapter 4.

Chapter 4: Reliability assessment of steel-free deck system bridges

4.1 Introduction

As mentioned earlier, the cracking of concrete due to regular live loads or other natural phenomena has little influence on the failure modes of innovative corrosion-free systems. Consequently, current assessment techniques, consisting mainly of detecting cracks and steel reinforcement corrosion, are not applicable for evaluating the Steel-Free Deck system. Since the available methods for predicting the structural condition of a bridge are developed for conventional bridges and are not applicable in the innovative systems, the development of a deterioration model for such a system would be of interest.

One of the objectives of the present research is to evaluate the reliability of bridges that use non-conventional materials or structural forms, particularly Steel-Free Deck System. The reliability theory is adopted in this thesis to establish a deterioration model based on the failure mechanisms of the bridges. The failure modes for Steel-Free Decks are mainly concrete crushing, the yielding of the restrain straps, and the fracture of welded connections.

As a case study sample, the Crowchild Bridge, an innovative structure with a Steel-Free Deck System located in Calgary is the subject here. It should be noted that almost all existing Steel-Free Deck bridges have very similar structural systems (Bakht and Mufti 1998). Therefore, the Crowchild Bridge could be considered as a representative of such a system. The superstructure of the Crowchild bridge was reconstructed in 1997 and it has been instrumented and monitored regularly ever since. The results of the visual inspections and ambient vibration tests are reported between 1997 and 2004 (VanZwol *et al.* 2008). The results reveal variations in the natural

frequency of the bridge over the years and the crack mapping at the deck underside is reported by the inspectors. In this thesis, a detailed Finite Element model using SAP2000 software has been developed and correlated with the measured vibration characteristics and inspection data. Such changes may be related to environmental effect (e.g. temperature) or changes in support conditions. In the Finite Element simulation, the properties of the elastic bearings and stiffness of the structural elements have been changed in order to reflect various scenarios including jamming of bearings. Using Mont Carlo simulation technique, the reliability index β and probability of failure of the system have been determined for different time intervals.

4.2 Capacity and Load Models

In the model proposed by Newhook (1997) as discussed in Section 2.7, to simulate the vehicle tire print (loaded area), the rectangular geometry proposed in Section 2.5.2, has been converted to an equivalent circular area of equivalent perimeter. In this case, the estimated diameter of an equivalent circular area is 477.5 mm (Newhook 1997). The dynamic load factor (impact factor) used to estimate the actual wheel load is 1.4 in Canadian codes (Thorburn and Mufti 2001, CHBDC-S6). In this thesis, the formulation for computing the capacity of such systems as discussed in Section 2.7 has been implemented in Microsoft excel software. The results have been validated by the outcomes of the software developed by Newhook (1997). An increase in the wheel load can result in one of the following three modes of failure for the system:

- yielding of steel strap beneath the concrete deck, $\epsilon_y = \frac{f_y}{E}$

- crushing of concrete in punch cone areas, when the circumferential strain at the top surface of the slab $\varepsilon_{ct} = 0.002$
- Fracture of welded connections between steel straps and top flange of supporting girders

4.2.1 Reduction in ultimate capacity due to tandem loading

The reduction in the ultimate punching load caused by tandem loading is represented by the ultimate punching load ratio $\frac{P'_u}{2P_u}$, where P'_u and P_u are the ultimate punching loads due to the tandem loading and single load, respectively (Newhook 1997).

$$P'_u = P_u \left(1 + \frac{S_w}{S_g} \right) \leq 2P_u \quad (4.1)$$

where, S_g is the distance between the adjacent steel girders which is 2000 mm for the Crowchild Bridge, and S_w is the distance between adjacent loads (Figure 4.1). Here, the axle spacing is considered to be 600 mm, and the capacity of a Steel-Free Deck calculated for a single load needs to be decreased by 35% to account for tandem loading (Newhook 1997).

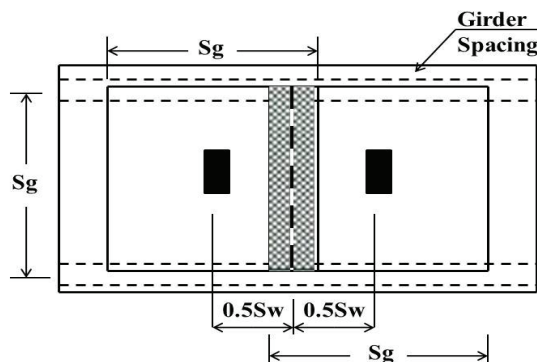


Figure 4.1 Multiple Wheel Loads on the Deck (adapted from Newhook 1997)

4.2.2 Fracture of Welded Connections

i: Brittle Fracture of Welded Connections

Brittle fracture of welded connections is found to be a serious problem; its history goes back to the World War II when a great number of welded connections in ships and tankers failed during the cold winters (Dieter 1986). Normally, ductile steels may become brittle under certain condition and climates. Steel properties like tensile strength are normally measured based on slow strain rate experiments, however, high rate of loading may entail different steel properties such as tendency for brittle fracture. In bridges, because of dynamic and impact loads as high rate loadings, a great deal of attention should be directed to brittle fracture of steel material and welded connections. The standard Charpy Impact Test (Dieter 1986) is widely used to select materials resisting the brittle fracture by the means of transition temperature curves. If a material has sufficient notch toughness subjected to severe conditions as well as low temperature and high rate loads, the structural member and connections can be designed using the standard strength evaluation methods without considering the fracture or stress concentration effects of cracks or flaws (Dieter 1986). Transition temperature curve is the main tool to determine the temperature above which the brittle fracture does not occur at elastic stress levels.

Ductility transition temperature is a commonly applied criterion corresponding to a low magnitude of energy absorbed C_v during the Charpy test. As a result of many tests conducted on steel ship plates during the World War II, a transition temperature corresponding $C_v = 20\text{J}$ was established as an acceptable criterion for low-strength steel. This value is still being used for evaluating the toughness of ordinary low-strength structural steel (see Table 4.1). For higher strength steel, the value of C_v exceeds 20J.

This value should be verified by experiments. According to the Table 4.1, for high strength CAN/CSA-G40.21-350AT steel that is used in the Crowchild bridge construction, the energy level C_v corresponding the ductility transition temperature is 27 J. As a rule, the weld metal should always have better tensile and fracture properties as compared to those of the base metal. By comparing Tables 4.1 and 4.2 it is revealed that the weld metal should be able to absorb the same level of energy, C_v , in lower temperatures.

Table 4.1 Impact test temperatures and Charpy impact energy requirements for primary tension members (adapted from CHBDC-S6)

CSA G40.21 grade	Minimum average energy, J	Test temperature, T_t , °C For minimum service temperature, T_s , °C		
		$T_s \geq -30$	$-30 \geq T_s \geq -60$	$T_s < -60$
Commonly used steels				
260 WT	20	0	-20	-30
300WT	20	0	-20	-30
350WT and AT	27	0	-20	-30
400WT and AT	27	0	-20	-30

Table 4.2 Impact test temperatures and Charpy impact energy requirements for the weld metal (adapted from CHBDC-S6)

Base metal CSA G40.21 grade	Minimum average Energy, J	Test temperature, T_t , °C For minimum service temperature, T_s , °C	
		$T_s \geq -30$	$T_s < -60$
260 WT	20	-30	-40
300 WT	20	-30	-40
350 WT and AT	27	-30	-40
400 WT and AT	27	-30	-40
480 WT and AT	27	-45	-45
700 QT	40	-45	-45

The transition temperature at which the fracture initiates with no prior plastic deformation, and becomes 100% brittle, is recognized as Nil Ductility Transition

Temperature (NDTT). This criterion is well-known among engineers who use it for selecting materials that can withstand brittle fracture. To select a proper material for different usage and climates, the chemical composition of the steel should be seriously considered since it contributes to the changes in the transition temperature in great manner. The carbon content has a reverse effect on the brittle fracture strength. A maximum temperature decrease of approximately 50 degrees in transition temperature is possible by increasing the MN/C (MN represents manganese content and C is the carbon content) to the maximum limit of 7/1 (Dieter 1986).

For the Crowchild bridge in Calgary, Alberta with a minimum - 45 degrees reported temperature, special care should be taken to select appropriate materials to avoid brittle fracture of welded connections. The CAN/CSA-G40.21-350AT weathering steel with maximum 0.2% Carbon, and maximum 1.35% Manganese content seems to be a proper material for bridge construction in this area. According to the bridge drawings and specifications, E48018-1 is used as the weld metal, this electrode is a perfect match with 350AT steel (CSA-W59). Based on the assumption that the base and weld metal products have undergone proper quality controls, the related tests conducted are in conformity with Tables 4.1 and 4.2 specifications, and the qualified welding procedures were followed, the probability of brittle fracture in the welded connections is found to be negligible for this bridge.

ii: Fatigue Criteria

To design the welded strap connections in steel-free deck bridges, the stress in the weld is limited to 48 MPa. This confirms the CHBDC-S6 requirements for class W connection detail with over 2 million cycles of load reversals. The fatigue criterion is found to

govern the weld design in comparison to the yield strength of the straps in steel-free deck bridges (Newhook 1997). Since the steel straps and supporting steel girders are fabricated using the same material with the same thermal coefficient, and due to lack of sudden temperature variation, as exists for special structures as heating tanks or airplanes, the thermal fatigue may not be considered in designing the welded strap connections. To sum up, the probability of fracture in the welded connections of the Crowchild bridge is estimated to be negligible, and this fracture may not be a likely mode of failure for this bridge.

4.3 Implementation of the Developed Model to the Case Study

The innovative superstructure of the Crowchild Trail bridge, was constructed in 1997. It is one of the few Steel-Free Deck bridges in North America and is the first continuous span Steel-Free Deck in the world. The bridge carries a traffic load of thousands of vehicles on a daily basis (Vanzwol *et al.* 2008). According to the specifications the concrete compressive strength of the Crowchild Trail Bridge is 50 MPa.



Figure 4.2 Overall View of Crowchild Trail Bridge, Calgary, Alberta (VanZowl *et al.* 2008)

According to the design drawings, three continuous spans of 29.83 m, 32.818 m, and 30.23 m length were installed over two piers from north to south. Five continuous steel plate girders, 2000 mm apart, support the 185 mm thick deck. Steel straps of 50 mm × 25 mm are installed below the concrete deck and welded to the top flange of steel girders in the transverse (lateral) direction in order to resist the tensile force in the same direction (Figure 3.9). The height of the haunches between the deck and the top of the steel girders is 80 mm. The Crowchild Bridge is instrumented and subjected to ambient vibration tests in different time intervals. In addition, a crack map of the deck underside was documented by inspectors in 1997, 1998 and 2004 (VanZwol *et al.* 2008).

4.3.1 Reliability Analysis of the Crowchild Bridge

Implementing the methodology explained in Figures 3.1 and 3.2, the two main distribution functions required to estimate the reliability of the structure are the Load and the Capacity. For the live load model as mentioned in Section 2.5.2, the best fit distribution for the axle weight data is a lognormal distribution with a mean value of 195.72 kN (44 Kips). The coefficient of variation (COV) is 0.25 (Nowak and Eamon 2008), and the estimated diameter of an equivalent circular area is 477.5mm (Newhook 1997).

In order to capture the best fit distribution to the capacity of such system, the first step is to consider the variations of structural parameters which must be incorporated into a Monte-Carlo simulation system. As already mentioned, a model of the capacity of such system has been formulated and validated using the formulation implemented in Microsoft excel. Using the generated random values for each of the structural parameters, a set of values for the capacity of the bridge deck has been calculated for the first year

after the bridge was opened to traffic. These values have been reduced by 35%, considering the tandem loading on the deck according to the recommendations provided in Newhook (1997).

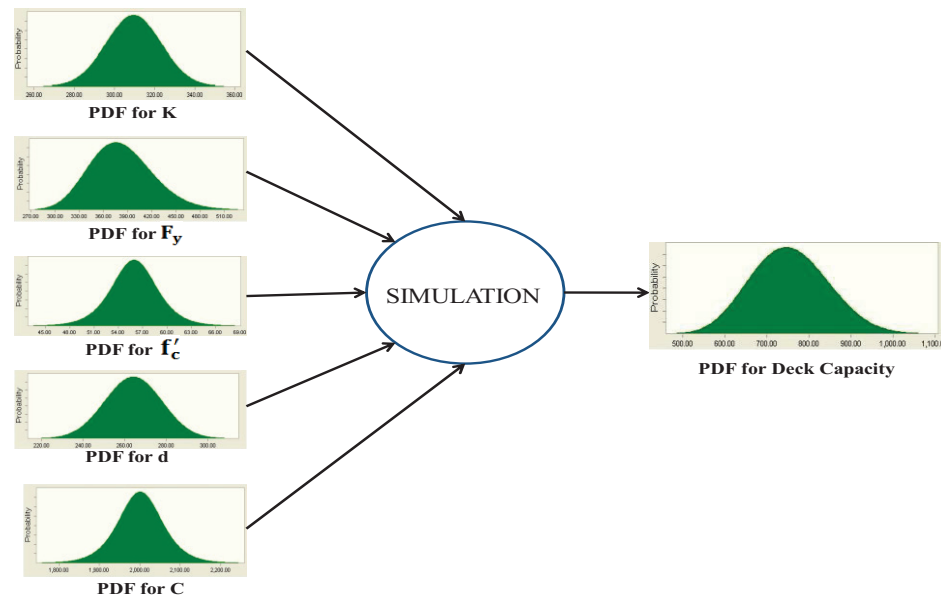


Figure 4.3 Simulation Technique to Find the Distribution for the Deck Capacity

The statistical data for each parameter used in estimating the capacity of a Steel-Free Deck System (Newhook 1997) are collected and discussed in the following. By using the random values generated from the statistical data, the simulated random values of the deck capacity R are generated. For hot-rolled steel beams and straps, the thickness of the member components have very low coefficients of variation and can be considered as deterministic values. Due to the variations caused by human error in fabrication, the width of a member follows a lognormal distribution with a bias factor of $\lambda_F = 1.0$ and a coefficient of variation of $COV = 0.05$ (Nowak and Collins 2000). Some approximations are proposed by researchers to estimate the lateral stiffness of the system (Newhook1997). However, the most accurate and reliable method may be Finite Element modelling of the system. By implementing the random values for the width of the

supporting girder flanges and steel straps in the FE model of the steel structure, it is possible to estimate the best-fit distribution for the lateral stiffness of the system for a newly constructed and corroded structure at different time intervals. As mentioned in Section 2.10 the yield strength of structural steel F_y follows a lognormal distribution where the Oracle Crystal Ball software is used to generate 500 random values for this parameter. According to the drawings, the design nominal yield strength of structural steel in the Crowchild Bridge is $F_y = 350$ MPa . The compressive strength of concrete is assumed to follow a normal distribution as explained in Section 2.10 where the nominal design concrete strength used in the Crowchild Bridge deck is 50 MPa according to the drawings. Mirza and Macgregor (1979) suggested a normally distributed slab thickness for cast in-situ concrete. In this thesis a COV= 0.05 is assumed for generating the random values for slab thickness. The diameter of the circle defining the outside boundaries of the cracked slab (Figure 2.7) is determined by the distance between the centre-line of the adjacent girders (Newhook 1997). For this parameter, because of probable construction errors, a reasonable assumption of a normal distribution with a COV= 0.03 is applied in generating the random values. A nominal mean value of 2000 mm is used according to the drawings.

The stiffness corresponding to the lateral resistance of the system depends on the cross-sectional area, the spacing of the steel straps and the geometry and spacing of supporting steel girders. By adopting the FE model, in addition to the stiffness of the steel straps, the effect of the supporting steel girders, adjacent straps, and diaphragms becomes evident. The FE model of the Crowchild bridge is adopted to estimate the lateral stiffness of the steel structure. To find the value of the lateral stiffness, a unit load of 1000KN/m

along the unit length of the bridge is applied in two opposite directions, to both ends of a single steel strap connecting a pair of supporting girders (Figure 4.4). The stiffness (K) is calculated as the unit load divided by half of the total elongation of the steel strap (Δ_L , Figure 2.7) in the units of force per displacement per unit length. By adopting the FE model, the lateral stiffness of the system has been estimated for the first and 75th year of the corroded structure. Since the northern span of the Crowchild Bridge is the only span with no FRP or steel reinforcement in the deck, it is assumed to be the critical span regarding failure, and the location of the minimum lateral stiffness has been found through trial and error using the FE model. A set of 500 random values for the widths of the top and bottom flanges of the steel girders and for the width of the steel straps have been generated for the simulation process. These random values have been implemented in to the FE model in order to calculate the corresponding values of the lateral stiffness of the steel structure.

The best fit distribution to lateral stiffness for the first year after opening to traffic has been estimated to be a Beta distribution ($\alpha=100$, $\beta = 100$, Minimum 114.46 and Maximum 504.66) in the units of N/mm/mm (Figure 4.5). Using the generated random values for each of the selected structural parameters, a set of values for the capacity of the bridge deck has been calculated by simulation. These values have been reduced by 35% considering the tandem loading on the deck. An impact factor of 1.4 is applied to take the dynamic load effect into account (CHBDC-S6, Thorburn and Mufti 2001). The results indicate that the best fit distributions for a 500 set of data calculated for the system capacity is a Beta distribution with $\alpha=10$, $\beta=15.04$, Minimum 373.33 KN and Maximum 1327.24 KN).

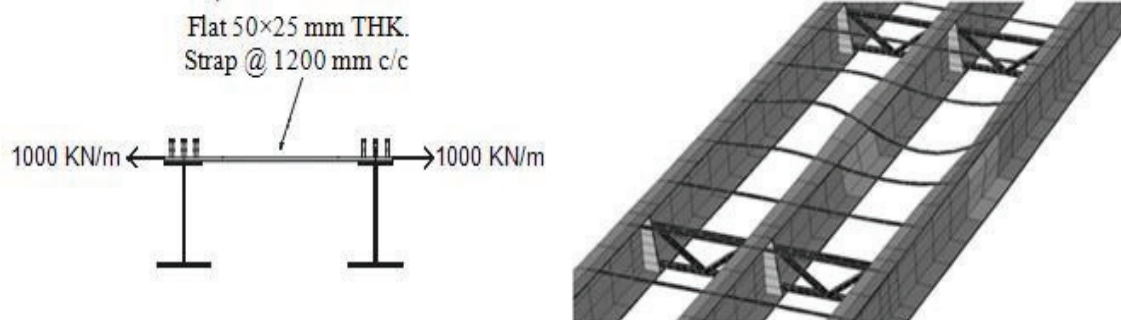
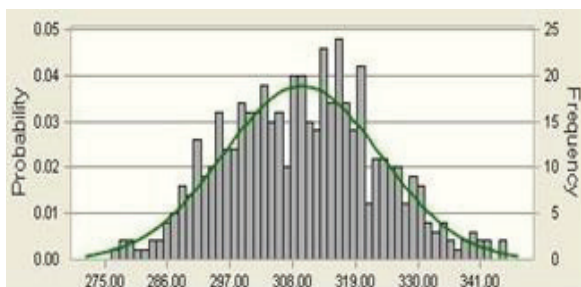
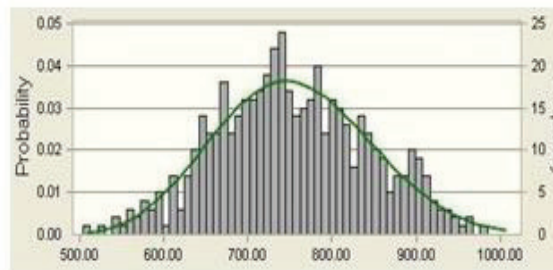


Figure 4.4 FE model of steel structure to calculate lateral stiffness (Steel strap and supporting girders are deformed due to lateral loading)



Lateral stiffness model for the first year

Beta distribution ($\alpha=100$, $\beta = 100$, Minimum 114.46 N/mm/mm and Maximum 504.66 N/mm/mm)



Deck capacity model for the first year

Beta distribution ($\alpha =10.$, $\beta =15.04$, Minimum 373.33 KN and Maximum 1327.24 KN)

Figure 4.5 Best Fit Distributions for the Lateral Stiffness and the Capacity of the Steel-Free Deck

For generating the random values for half of the axle weight (dual tires) (Q), the Oracle Crystal Ball software is used where 500 random values for the load and eventually for the Limit State Function $g=(R-Q)$ have been estimated. Random values of the Limit State Function are plotted on a normal probability chart. The Limit State Function is found to be normally distributed since the cumulative probability plot is almost a straight line. Simulations are continued until the calculated reliability index β stabilizes with no

significant change in successive iterations. The results of simulations indicate that the reliability index could be obtained based on 500 values for the capacity and load for the system with confidence. The best line to fit the curve is plotted using a spreadsheet tool (i.e., Microsoft Excel) and is extrapolated to intersect the vertical axis passing through the origin $g(R,Q)=0$, as shown in Figure 4.6. For the first year, the reliability index is 6.27. Compared to the element level reliability index, $\beta = 3.5$, used in calibrating the LRFD bridge code in USA (Nowak 1995), there is a low probability of failure for Steel-Free Deck system.

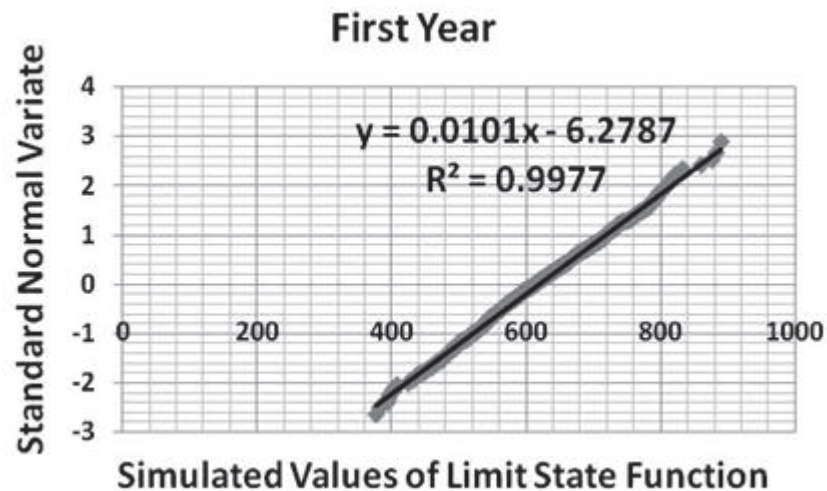


Figure 4.6 Plotted Limit State Function Simulated Values and Reliability Index

4.4 Details of the FE Modeling of the Crowchild Bridge

To investigate the behaviour and response of the structural system of the Crowchild Bridge for different time periods, SAP2000, a well-known software system, has been used to develop the bridge FE model. This model attempts to capture all the structural details according to the drawings and specifications. A three dimensional Finite Element

model of the bridge (Figure 3.9) has been developed by using frame elements for the Piers, diaphragms and steel straps, as well as shell elements for the steel girders, the concrete deck and the side barriers. Over two piers, three continuous spans of 29.83 m, 32.818m, and 30.23m length are installed from north to south respectively. Five continuous steel plate girders, 2000 mm apart, support the 185 mm thick steel-free concrete deck. Steel straps of 50mm x 25mm are welded to the top flange of the steel girders in the transverse direction. According to the drawings concrete strength is $f'_c = 50$ MPa, and the structural steel type is corrosion resistant (Weathering) steel CAN/CSA-G40.21-350AT. To consider the composite action in the FE model, the steel girder elements are connected to the deck elements using body joint constraints so that the connected joints move together as a rigid body. Bridge bearings are modeled using link elements between the top of the piers and the bottom flanges of the steel girders. Link properties are defined as using very strong springs under compression, while weak springs are under shear; in the longitudinal direction (North-South of the bridge). According to drawings, the pier supports at their base are fixed. At the southern abutment, pin supports are assigned while for the northern abutment, roller supports are considered together with link elements for modeling the bridge bearings.

The FE model has been calibrated according to the experimental results obtained from the static deflections, vibration characteristics (natural frequencies of the first four mode shapes), load distribution, and crack patterns reported by other researchers (VanZwol *et al.* 2008). The higher modes of frequencies from field testing may not be reliable and are not considered here since they may not be sufficiently excited during the

ambient vibration tests. The girder deflections from the static load testing and the FE model are also found to be very close for all the supporting girders as shown in Table 4.3.

Table 4.3 Static deflections obtained from static load test (VanZowl *et al.* 2008) and FEM mode

Girder No.	Static test (mm)	FEM result (mm)	difference %
1	12.3	12.4	0.8
2	10.1	9.8	2.9
3	6.3	6.14	2.5
4	3.05	3.01	1.3
5	0.4	0.387	3

In order to correlate the natural frequencies obtained from the numerical model and the results from the ambient vibration test in 1997, just before opening the bridge to traffic, the stiffness of the bearings in longitudinal direction and the stiffness of the deck components have been adjusted iteratively. Some modifications have been made regarding in the element properties, such as the variation in the deck thickness, which may occur due to construction errors. The spring stiffness of the link elements in the longitudinal direction of the bridge is also adjusted to update the FE model. The parameters given above have been adjusted to compensate for the features that could not be modelled precisely, such as the concrete cracking, the complex boundary conditions, the loosening/stiffening of the bolt connections etc. (Bagchi 2005).


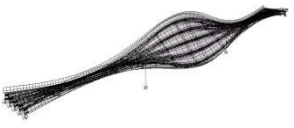
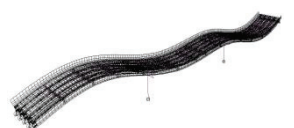
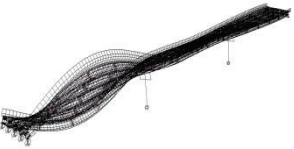
In addition to conducting the ambient vibration tests, the crack map of the deck underside is documented by inspectors in 1997, 1998 and 2004 (VanZwol *et al.* 2008). The Physical properties such as stiffness and boundary conditions in the FE model have

been modified in order to determine the sensitivity of the natural frequencies and assess the likely causes of variation in vibration characteristics and natural frequencies of the bridge. Just after construction of the bridge deck in 1997, the concrete was assumed to have been uncracked. In order to model the Steel-free deck cracking in 1999 and 2004, the stiffness of concrete elements was modified by SAP2000 by adjusting the deck stiffness (Shell elements) in the longitudinal and transverse direction. The piers and side barriers are assumed to be cracked and the stiffness of these elements is reduced over time. For simulating the bridge condition in 1999, the deck stiffness along longitudinal direction is assumed to be 70% of uncracked stiffness (the base model in 1997) for north and middle span, and 80% for the southern span. Along the transverse direction, a 20% reduction is assumed for the whole deck stiffness. Side barriers are assumed to have lost 50% of their stiffness due to the cracks which have appeared after several freeze/thaw cycles. The cracks in the piers are simulated by reducing the moment of inertia of the corresponding frame elements by 30%. For simulating the condition in 2004, a 10% reduction of deck stiffness in both directions has been assumed as compared to 1999.

In correlating the FEM model to field tests by trial and error, the longitudinal stiffness of the bearings are observed to have significant contribution in controlling the natural frequencies of the structure. Between 1997 and 1999, the frequency values have decreased which is a natural consequence of cracks in concrete elements and a marginal loosening of bearings. Surprisingly, the natural frequencies of the mode shapes have increased between 1999 and 2004. The FE model is adopted here to investigate the likely reasons for this occurrence by adjusting the stiffness of the springs representing the bearing element. It is possible that after seven cold winter periods, the bridge bearings

may have deteriorated and their degrees of freedom have been affected. It should also be noted that the natural frequencies are sensitive to the temperature as well. The field tests were conducted in similar weather conditions so that the temperature effect can be minimized. The natural frequencies obtained from field tests and the FEM model are shown in the Table 4.4.

Table 4.4 Natural frequencies obtained from field tests (VanZowl *et al.* 2008) and FEM model

Mode shape No.	Natural frequency		Natural frequency		difference	
	Field test (HZ)		FEM model (HZ)		%	
First mode (vertical) 	1997	2.78	1997	2.84	1997	2.2
	1999	2.6	1999	2.67	1999	2.6
	2004	2.8	2004	2.87	2004	2.5
Second mode (Torsional) 	1997	3.13	1997	3.21	1997	2.5
	1999	2.9	1999	2.98	1999	2.8
	2004	3.16	2004	3.067	2004	2.9
Third mode (Vertical) 	1997	3.76	1997	3.75	1997	0.2
	1999	3.62	1999	3.52	1999	2.7
	2004	3.78	2004	3.68	2004	2.6
Fourth mode (Torsional) 	1997	4.05	1997	3.94	1997	2.7
	1999	3.85	1999	3.74	1999	2.7
	2004	4.19	2004	4.07	2004	2.8

Chapter 5: Reliability assessment of Conventional Bridge Deck Systems

5.1 Introduction

As already mentioned, in the existing bridge management systems, the structural behavior is assessed based on the results of visual inspections where the corresponding condition states are assigned to individual elements; therefore, limited attention is given to the correlation between bridge elements from a structural perspective. A reliability-based assessment model is potentially an appropriate replacement method for the existing procedures. The objective of this chapter is to evaluate the system reliability of conventional (i.e. steel reinforced) slab-on-girder bridges designed based on the existing codes. The developed method adopts the reliability theory and evaluates the structural safety for such bridges based on their failure mechanisms. This method has been applied to a pair of simply supported concrete bridge superstructures designed according to the Canadian Highway Bridge Design Code (CHBDC-S6). Based on the reliability estimates, the bridges are in a good condition during the initial stages of their service life.

Evaluating the system reliability of bridges by adopting a rational and numerical technique, uncertainty of structural parameters, correlation between structural elements, load redistribution, and redundancy of the structure can be considered. The purpose of a reliability-based evaluation is to account for the uncertainties associated with loads and the resistance of the system using probability of failure P_F , and the reliability index β as the safety criteria. The developed method explained in Figure 3.1 has been applied to simply supported concrete bridge superstructures designed according to the Canadian Highway Bridge Design Code (CHBDC-S6). Non-linear Finite Element models of the bridges have been developed and the system reliability indices have been determined.

5.2 System Reliability Model, Steel-Reinforced Concrete Bridge System Resistance model

Czarnecki and Nowak (2007) reported that by taking in to account the interaction between structural elements, load redistribution, redundancy and ductility of the structure, the load carrying capacity of the whole structural system becomes considerably greater than that of estimated based on the capacities of the individual components. In the above study, the ultimate limit state for the structural resistance was only considered in terms of the deflection of the main girders due to live load (0.0075 of the span length). The results of this thesis indicate that for a conventional reinforced concrete bridge superstructure, the probable governing mode of failure might be the flexural collapse of the structural elements as opposed to deflection control. While conducting the simulations here, it was observed that for a newly constructed bridge girder, the ultimate state was being governed by the crushing of concrete in compression. On the contrary, for a severely corroded girder at the end of service life of a bridge, the collapse is normally governed by the failure of the reinforcing steel under tension.

To calculate the system reliability of conventional Steel-Reinforced Concrete Deck System, two main distribution functions are required, capacity and load (Figure 3.1). Load distribution is considered as explained in Section 2.5, including the Dead load, Live load and Dynamic load effect. It is assumed that Gross Vehicle Load (GVW) is a random variable, but the axle spacing and percentage of the truck weight per axle remains constant (Czarnecki and Nowak 2007). The bridge resistance is defined in terms of gross vehicle weight GVW of two side-by-side trucks which leads to the failure. Here, the failure of the system is defined as when any plastic hinge reaches its ultimate capacity or any main girder deflects 0.0075 of the span length in a vertical pushover analysis

(monotonically increasing vertical loads). The considered axle configuration of each truck is same as the design truck, as per AASHTO. Two trucks are placed in the longitudinal direction to generate the maximum bending moment. The centre-lines of the wheels of the adjacent trucks are placed 1.2 m apart. According to the statistical data, the transverse position of the truck within the roadway (kerb distance) follows a lognormal distribution. For a standard lane width of 3.63 m, the mean value for the kerb distance would be 0.91m with the coefficient of variation of 0.33 (Czarnecki and Nowak, 2007). The resistance of the system R_{system} is considered to be the expected value of the GVWs estimated for different transverse positions. The main structural parameters affecting the resistance of such system are the yield strength of the reinforcing steel F_y , The modulus of elasticity of reinforcing steel E_s , the compressive strength of concrete f'_c , the modulus of elasticity for concrete E_c , and the dimensions of the reinforced concrete members. For the purpose of the reliability calculation, the uncertainty in the governing parameters as mentioned above should be considered and the random values for each of them should be generated. The statistical variations of structural parameters are discussed in the Section 2.10.

5.3 Adoption of the Developed Model to the Case Study bridges

The developed method explained in Figure 3.1 was applied to the simply supported concrete bridge superstructures designed according to the simplified method and CL-625 loading of Canadian Highway Bridge Design Code (CHBDC-S6). The AASHTO HL-93 design load and Canadian CL-625 load are quite different in terms of wheel spacing and axle loads, but they yield approximately the same design moments and shear (Wacker, and Groenier 2010). A set of two bridges with similar configuration but different spans (a

17.5 m span and a 12 m span) have been designed according to the CHBD-S6 Code. The geometry of the bridges with 17.5 and 12 m span (Centre-to-Centre of bearings) together with the cross section of the T-section main beams are illustrated in Figures 5.1 and 5.2, respectively. Four simply supported rectangular concrete beams (Roller support for one side and hinge support for the other), which are 2.3 m apart support the 0.2 m thick concrete slab. In order to meet the requirements of the code and for simplicity, the nominal concrete cover is assumed to be 60 mm on all surfaces. Four concrete diaphragms are designed and installed in the transverse direction at two ends and quarters of the span on each side.

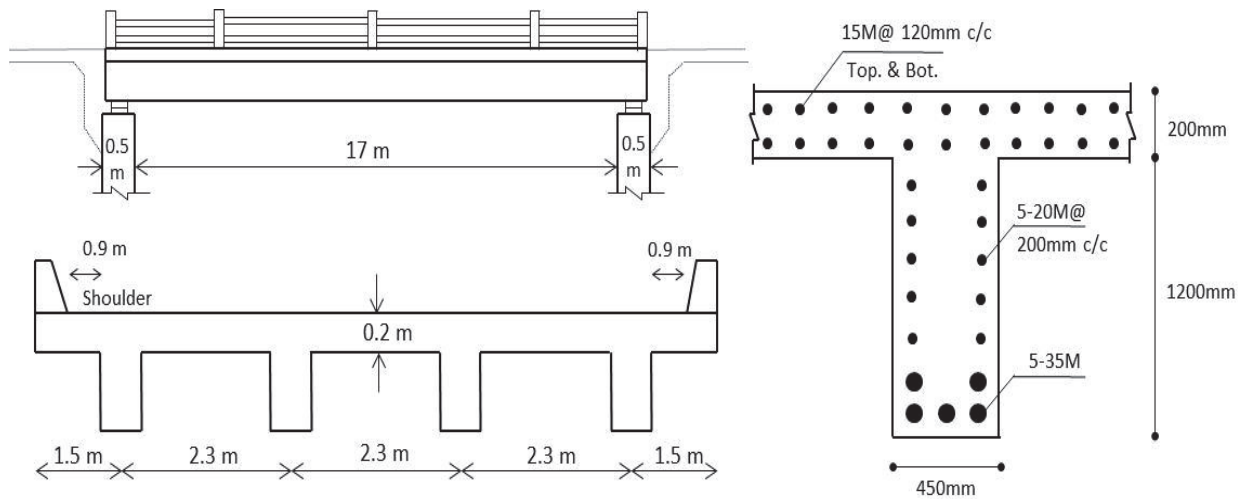


Fig 5.1 Geometry and Cross Section for the Case Study Bridge with 17.5 m span

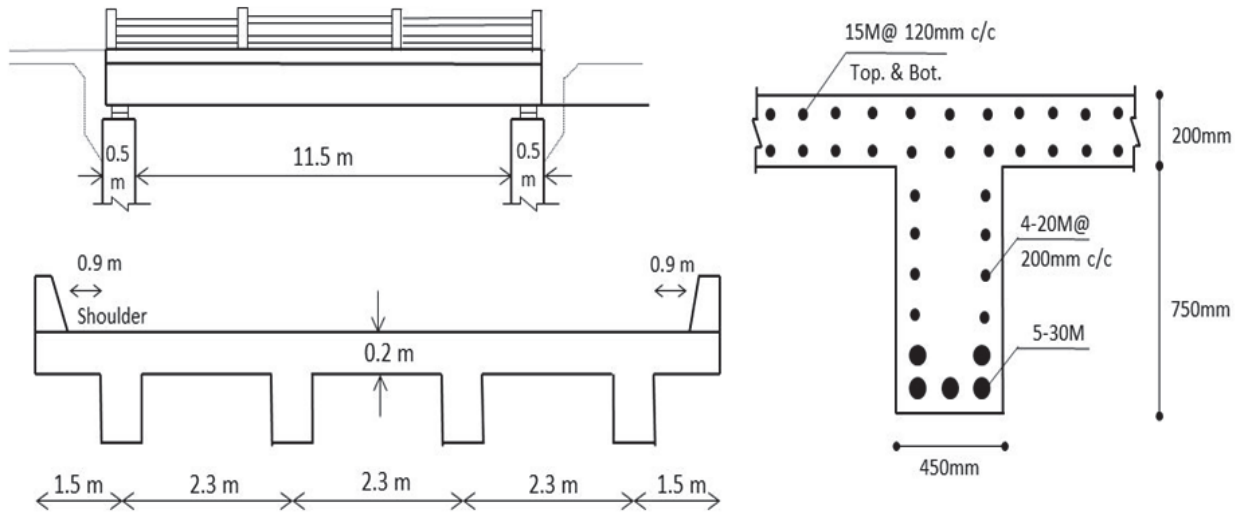


Fig 5.2 Geometry and Cross Section for the Case Study Bridge with 12 m span

5.3.1 Finite Element Modeling of the conventional bridge deck systems

As explained in Section 3.5.1, by using SAP2000, non-linear Finite Element models of the bridges have been developed and the system reliability index has been determined for different time intervals. For each of the designed bridges shown in Figs.5.1 and 5.2, the two 3D models have been developed by SAP2000. Model 1 (Figure 3.8a) uses shell elements, and Model 2 (Figure 3.8b) is made of a planar grid of longitudinal (main T-section beams parallel to roadway) and transverse members (perpendicular to roadway). The former model is considered to be a more accurate representation of the structure, while the latter is more efficient. Effort has been made to correlate both the models with each other and the detailed explanation is found in Section 3.5.1. The advantage of using frame elements in the model (Model 2) is that the plastic hinge properties could be assigned to this kind of element; therefore, one is able to calculate the hinge properties (Figure 2.6) and assign them as the user-defined hinge properties in the program for each plastic hinge. To estimate the reliability index of the bridge superstructure, the calibrated

model (Model 2) based on the grillage analogy has been used for the rest of simulations since it is more simplified and deals with less number of parameters as compared to the shell-based model. The simplified model is closely correlated with the full model (shell-based) in order to capture the effect of all the details and damages in the bridge. The magnitudes of truck loads shown in Figure 3.8b are increased incrementally to reach the ultimate system capacity.

5.3.2 Estimating the Reliability Index for the Case Study Bridges

By using the generated random values for each of the structural parameters, a set of data including various cross sectional properties and corresponding moment-curvature diagrams for different T-section longitudinal beams have been established and applied into the Finite Element model of the bridge. Two side-by-side trucks are placed in the longitudinal direction to generate the maximum bending moment. The longitudinal critical location of trucks has been found based on the influence line calculations. The bridge resistance is defined in terms of GVW of two side-by-side trucks which causes failure. The incremental loading pushover method is adopted here to determine such loads. The resistance of the system R_{System} is calculated as the expected value of the GVWs estimated for different transverse positions (in this thesis seven transverse positions have been considered). For each set of generated random structural parameter, the ultimate system capacity is estimated, based on which the best fit probability density function is determined for the capacity (Box No. 5 , Figure 3.1). Simulations are continued until the calculated reliability index β at the system level stabilizes, with no significant change in successive iterations. Here, for each time instance, the minimum number of Finite Element model runs is 700.

Oracle Crystal Ball software has been used here to find the best fit GVW distributions. According to the live load model explained in Section 2.5.2, the maximum 75-year gross truck weight (live load including the dynamic effect) follows a normal distribution where the mean and standard deviation values are estimated as 415.59 KN and 61.5 KN for 17.5 m span, and 425.41 KN and 62.96 KN for 12 m span, respectively. The equivalent normal mean (μ_X^e) and the equivalent normal standard deviation (σ_X^e) of lognormal resistance distributions have been estimated according to the method explained in Section 2.4.2, and the reliability indices have been calculated through Rackwitz-Fiessler Iterative Method as discussed earlier. The System reliability index for each bridge, just before opening to the traffic, is considerably greater than that of the element-level target reliability index of 3.5 used for calibrating the LRFD bridge code in the USA (Nowak 1995). This is in accordance with the results of a study conducted on newly constructed composite steel girder bridges (Czarnecki and Nowak 2007) and the simulation results obtained in this study are consistent with it. The main reason for such substantial difference could be the interaction between structural elements, load redistribution, and ductility of the structure which is not considered at the single element-level assessment.

Table 5.1 Best fit distributions for the ultimate capacity and reliability index for the Case Study Bridges (just after construction)

Span length	Best fit ultimate resistance GVW distribution	Mean resistance GVW (KN)	Standard deviation of resistance GVW (KN)	System reliability index β
17.5 m	Lognormal	1566.11	214	7.43
12 m	Lognormal	1694.56	205	8.44

Chapter 6: Reliability-Based Deterioration Models for Bridge Decks

6.1 Introduction

The existing bridge management systems are based on the assumption that the probability of an element being in a particular state at any time depends only on its condition state in the previous inspection period (Frangopol and Neves 2004). In this process, the impact of the history of deterioration on the reliability of a structure is disregarded which may lead to inappropriate conclusions. To overcome these limitations, researchers have proposed deterioration models based on the structural safety in terms of the continuous reliability profile (Thoft-Christensen 1998, Kong and Frangopol 2003), while these models could not be updated based on the results of visual inspections (Frangopol and Neves 2004). As mentioned in Section 2.9, in order to improve the degradation models in a way to be updatable, researchers have proposed different mathematical functions to model the deterioration prediction curves, such as multi-linear function, biquadratic convex curve, and Weibull cumulative probability distribution function. The problem with predicting the deterioration pattern using these functions is that they represent the element-level deterioration; therefore, the interaction between different elements in relation to the structural integrity is ignored. These models are obtained based on expert judgment or historical evidences (Myamoto et al. 2001); consequently, they may not consider the specific functional and structural aspects of a structure. There is a need for a rational criterion to verify the correctness of such models from the structural integrity perspective. A Bridge Management System (BMS) applies the Bridge Condition Index (BCI) or the Bridge Health Index (BHI) obtained based on the element level condition indices as determined from the visual inspection results. Instead of applying the Bridge Condition

Index or the Bridge Health Index to indicate the condition of a bridge, the system reliability-based condition indicator can be introduced in the BMS to indicate the system level condition, or it can be added to the BMS as an additional parameter. A System reliability-based deterioration prediction model helps decision makers to predict the time for major potential interventions in a more precise and rational manner.

The aim of this chapter is to evaluate the system reliability of bridges at different time intervals using a rational and numerical technique where uncertainty of structural parameters, correlation between structural elements, load redistribution, and redundancy of the structure are considered. The effectiveness of developing the degradation profile for the whole structure is demonstrated here. The reliability index can be applied as a benchmark to indicate the performance of a system. By estimating the reliability index for different time intervals, one would be able to find the best fit deterioration function for a particular bridge structure. The reliability theory to establish a deterioration model based on the failure mechanisms of bridges is adopted here.

In case of conventional Steel-Reinforced Concrete Decks, the developed method has been applied to the case study bridges discussed in Section 5.3.2. Non-linear Finite Element models of the superstructures have been developed and the system reliability indices have been determined for different time intervals. In due course, the degradation profile of the bridge superstructure has been established and updated. For innovative Steel-Free Deck Systems, the Crowchild bridge in Calgary, Alberta is considered as the case study. Finally the deterioration patterns obtained from the two cases (i.e., steel-free deck and conventional deck bridges) have been compared.

6.2 A Deterioration Model for Conventional Steel-Reinforced Deck through System Reliability Analysis

The corrosion of steel reinforcement is the main cause of deck degradation due to the application of salt-based de-icing substances. Damage of any reinforced concrete bridge deck exposed to chlorides could be divided into the following main phases: early-age cracking of concrete, corrosion initiation of steel reinforcement, cracking of the concrete cover, and delamination or spalling. As discussed in Section 2.8.2, the following five variable parameters which mainly affect the prediction of service life of a steel reinforced concrete deck are: surface chloride content of concrete, C_s ; effective chloride diffusion coefficient of concrete, D_c ; chloride threshold of the reinforcement, C_{th} ; corrosion rate of steel reinforcement, λ ; and the concrete cover of steel reinforcement. In this thesis, in order to build up a primary deterioration model, the relevant mean values of the field data are selected from the literature for the New York state which is close to the environmental condition in Canada where considerable amount of deicing salt is used during the long and cold winters as discussed in Section 2.8.2 in detail.

Based on the degradation scenario explained in Section 3.3 and using the generated random values for each of the structural parameters (Section 2.10 and Section 5.2), a set of data including various cross-sectional properties and corresponding moment-curvature diagrams, as shown in Figure 2.6, for different T-section longitudinal beams have been established and applied in the non-linear Finite Element model of the bridge. In order to generate a system level deterioration model, the system reliability index β is estimated for different time intervals according to the procedure discussed in Section 5.3.2. This process is applied for the following instances of time during the life cycle of the bridge: (a) the first year after opening the bridge to the traffic, (b) the time

when reinforcing bars corrosion begins (onset of corrosion), (c) the time to longitudinal cracking of concrete (d) the time-to-spall and delamination of concrete cover, (e) the 50th year after construction, and (f) the 75th year after construction. Here, all these time periods have been estimated based on the nominal concrete cover of 60 mm as considered in the design specifications. It is important to note that to estimate the resistance distribution and reliability index β the random variable defining the concrete cover is assumed to have normal distribution as discussed in Section 2.10.

The best fit distributions for the ultimate capacity of the system for the bridge with 17.5 m span (as explained in Chapter 5) based on the truck GVW, and the corresponding statistical parameters are presented in Table 6.1. Oracle Crystal Ball software is used here to find the best fit GVW distributions. Considering the effect of the dynamic load, the maximum 75-year gross truck weight (live load including the dynamic effect) follows a normal distribution where the mean and standard deviation are estimated to be 415.59 KN and 61.5 KN, respectively. The equivalent normal mean (μ_X^e) and the equivalent normal standard deviation (σ_X^e) of the lognormal distribution are estimated according to the method explained in Section 2.4.2 and reliability indices are calculated using Rackwitz-Fiessler Iterative Method as discussed earlier.

Condition and reliability indices are interrelated as they both define the health of a structure, have the maximum values when structure is newly constructed, and decrease over time as the structure deteriorates. A degradation curve might be developed based on the condition index or the reliability index (Grussing *et al.* 2006).

Table 6.1 Best Fit Distributions for the Ultimate Capacity of the System for the Bridge with 17.5 m Span

Deterioration State	Time based on nominal cover (year)	Best fit ultimate resistance (GVW) distribution	Mean resistance GVW (KN)	Standard deviation of resistance GVW (KN)	System reliability index β
Just after construction	0	Lognormal	1566.11	214	7.43
Onset of corrosion	7.34	Lognormal	1553.38	213	7.36
Onset of longitudinal cracking	15.27	Lognormal	1513.53	210	7.14
Onset of spall	21.69	Lognormal	1443.17	246	5.92
50 th year	50	Lognormal	1150.48	191	4.87
75th year	75	Lognormal	1051.62	192	4.11

For the 17.5 m span case study bridge, the deterioration curve has been developed based on the system reliability indices mentioned in Table 6.1. The deterioration curves that are fit to reliability indices of Table 6.1 are compared based on the mathematical functions available in the literature (See Figure 6.1a). These functions are mainly developed based on expert judgment. Updating the curves with the theoretical estimate of the time-to-spall indicates that various deterioration curves such as the biquadratic convex curve (Myamoto *et al.* 2001), Weibull cumulative probability distribution function (Grussing *et al.* 2006), and the multi linear function (Frangopol and Neves 2004), follow similar patterns of deterioration in the system. By looking at the

deterioration history presented as the multi-linear pattern as a whole (Figure 6.1b), the Weibull and Multi-linear models calibrated up to the time of spall underestimate the performance of the bridge after spall up to the 75th year. This illustrates the fact that how important the continuous updating and calibrating the deterioration curve is in avoiding misjudgment regarding intervention.

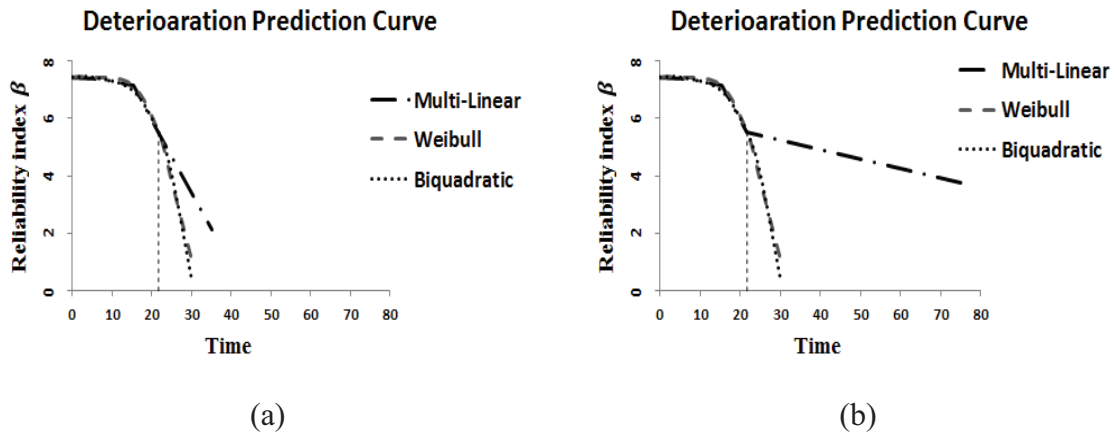


Figure 6.1 Deterioration Prediction Curves Based on Different Models: (a) up to the time to spall; and (b) covering the entire design service life

In this thesis, the maximum reasonable span for such bridge deck is considered to be 17 m. For longer spans other structural systems as well as prestressed precast concrete beams could be recommended. The minimum span where the super-structure of a bridge could be considered as a Slab-on-Girder bridge is 12 m (Priestley *et al.* 1996); otherwise a solid slab with no beam would be sufficient to carry the design truck loads. For this reason another bridge with 12m span (Figure 5.2) is considered and reliability indices for such systems also have been estimated for different time intervals as mentioned in Table 6.2. The deterioration curves for different time intervals and for different spans based on

the calculated reliability indices are illustrated in Figure 6.2. This is the last step of the methodology developed in this thesis as explained in Figure 3.1 (Box No. 10).

Table 6.2 Best Fit Distributions for the Ultimate Capacity of the System (12m span)

Deterioration State	Time based on nominal cover (year)	Best fit ultimate resistance (GVW) distribution	Mean resistance GVW (KN)	Standard deviation of resistance GVW (KN)	System reliability index β
Just after construction	0	Lognormal	1694.56	205	8.44
Onset of corrosion	7.34	Lognormal	1677.6	206	8.22
Onset of longitudinal cracking	16.8	Lognormal	1626.77	203	8.00
Onset of spall	26.15	Lognormal	1524.02	236	6.52
50th year	50	Lognormal	1122.17	152	5.32
75th year	75	Lognormal	928.77	118.22	4.37

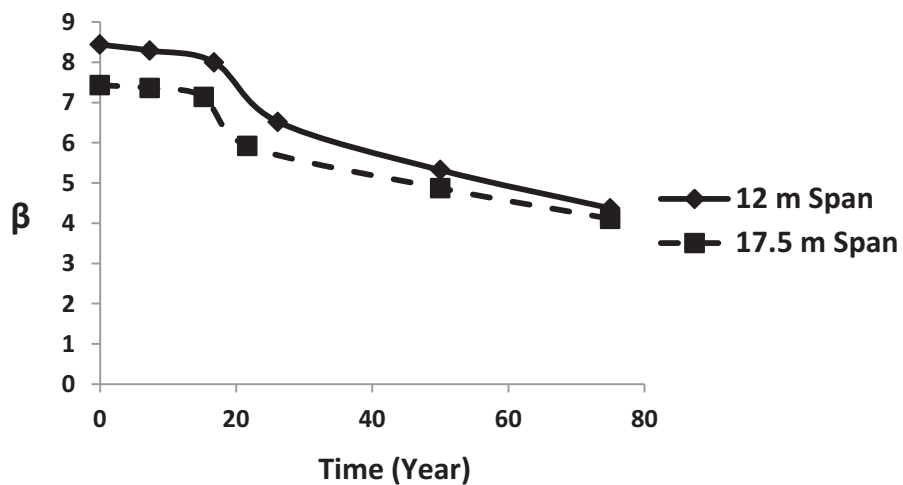


Figure 6.2 Deterioration Prediction Curves Based on Reliability Indices

Based on the generated deterioration models, decision makers are able to predict the appropriate time for the major interventions. The acceptable level of reliability depends on the budget and the strategy of the owner of the asset. As mentioned in the Section 2.2, structural safety could be defined through Bridge Condition Index (CI) with the range from 0 to 100. The CI may be categorized into five groups: 0-19, 20-39, 40-59, 60-79, and 80-100 which represent dangerous, slightly dangerous, moderate, fairly safe and safe levels respectively. In this thesis, the generated reliability-based deterioration curves in Figure 6.2 are normalized to yield the condition index (CI) of 100 at the time of opening the bridge to traffic for the first year. Figure 6.3 shows the normalized index based on system reliability (CI)-based deterioration curves.

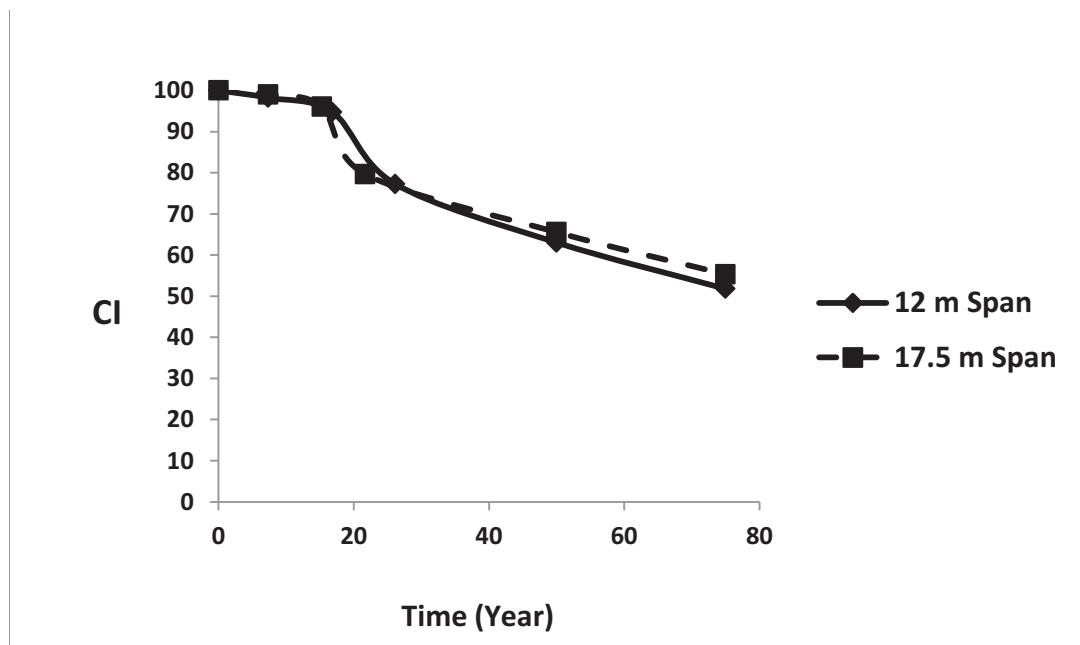


Figure 6.3 Normalized Deterioration Prediction Curves Based on the Bridge Condition Index

The resulting deterioration models are generated based on the assumptions already mentioned in this chapter. These curves should be updated based on the results of the inspections obtained and reported during the life cycle of the bridge in order to be applicable in the real structural and environmental situation. As illustrated in Figure 6.1, the degradation curves when calibrated up to the time of spall underestimate the performance of the bridge after spall up to the 75th year; therefore, the deterioration history should be presented in two different stages, before and after spall. Here; as a conservative approach, the best fit biquadratic convex curve (equation 2.36) is fit to the CI values estimated for the bridge with 17.5 m span and for the time period up to spall as given by the equation 6.1 (see Figure 6.3). After the time to spall, t_S , up to the 75th year, the best fit to the data obtained from two bridges is a linear function expressed in the equation 6.2. The best fit degradation curve for a newly constructed bridge is shown in Figure 6.4. In this case the time to spall is estimated to be $t_S = 21.69$ years.

$$CI = 100 - 9.18 \times 10^{-5} t^4, \quad 0 < t < t_S \quad (6.1)$$

$$CI = -0.488 t + 89.67, \quad t_S < t < 75 \quad (6.2)$$

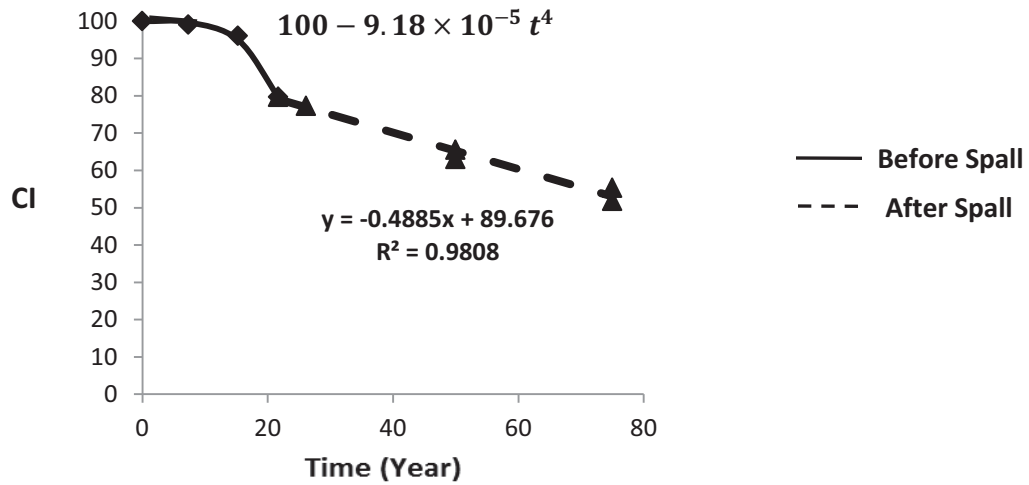


Fig 6.4 The Best Fit Deterioration Curve for a Newly Constructed Conventional Bridge

As mentioned in sections 2.9.2-3, biquadratic or Weibull deterioration curves could be updated based on one time inspection data only. As shown in Figures 6.5, modeling the deterioration process by using the estimated condition index for the 75th year entails unreasonable and detrimental decisions regarding the deck intervention.

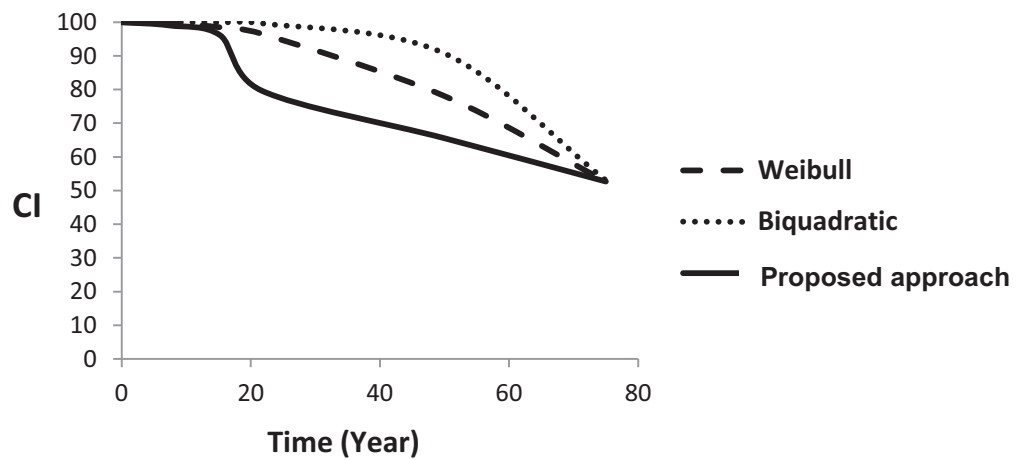


Fig 6.5 Deterioration Curves based on the estimated condition index for the 75th year

6.2.1 *Adoption of the developed model to an existing super structure as a case study*

As a case study, to show the application of such developed deterioration curve, the developed model is adopted to an old superstructure in Montreal as the case study. On May 10, 2000 the city of Montreal asked SNC Lavalin Inc. for an emergency visual inspection of the Monk Bridge (Zaki 2000). The superstructure of the bridge was a conventional steel-reinforced slab on concrete beams. The plan view and cross section of the bridge superstructure is shown in Figure 6.6. The results of the visual inspection revealed signs of severe deterioration on the concrete slab and beams. The destructive core test was also performed on the concrete slab. Cores were taken on site using core cutting machine and the laboratory results showed that cores were in severely deteriorated condition. The content of chloride ions passed the threshold of 240 ppm in about 50% of the concrete sample cores taken from the slab. Inspection of the concrete beams together with the laboratory results indicated that generally the concrete of the beams was in a much degraded condition. Spall and corrosion of steel reinforcements are evident in Figures 6.7-8.

According to the drawings, the bridge was designed in 1925. Assuming that the construction of the bridge was finished in the same year, at the time of inspection (year 2000) the bridge super structure was about 75 years old. Lack of the historical data regarding any other inspection or interventions during the life cycle of the bridge makes it difficult to model its in-service degradation profile. Assuming that no major rehabilitation was implemented on the deck and concrete beams, the effort was made to compare the predicted condition of the bridge using the model developed in this study.

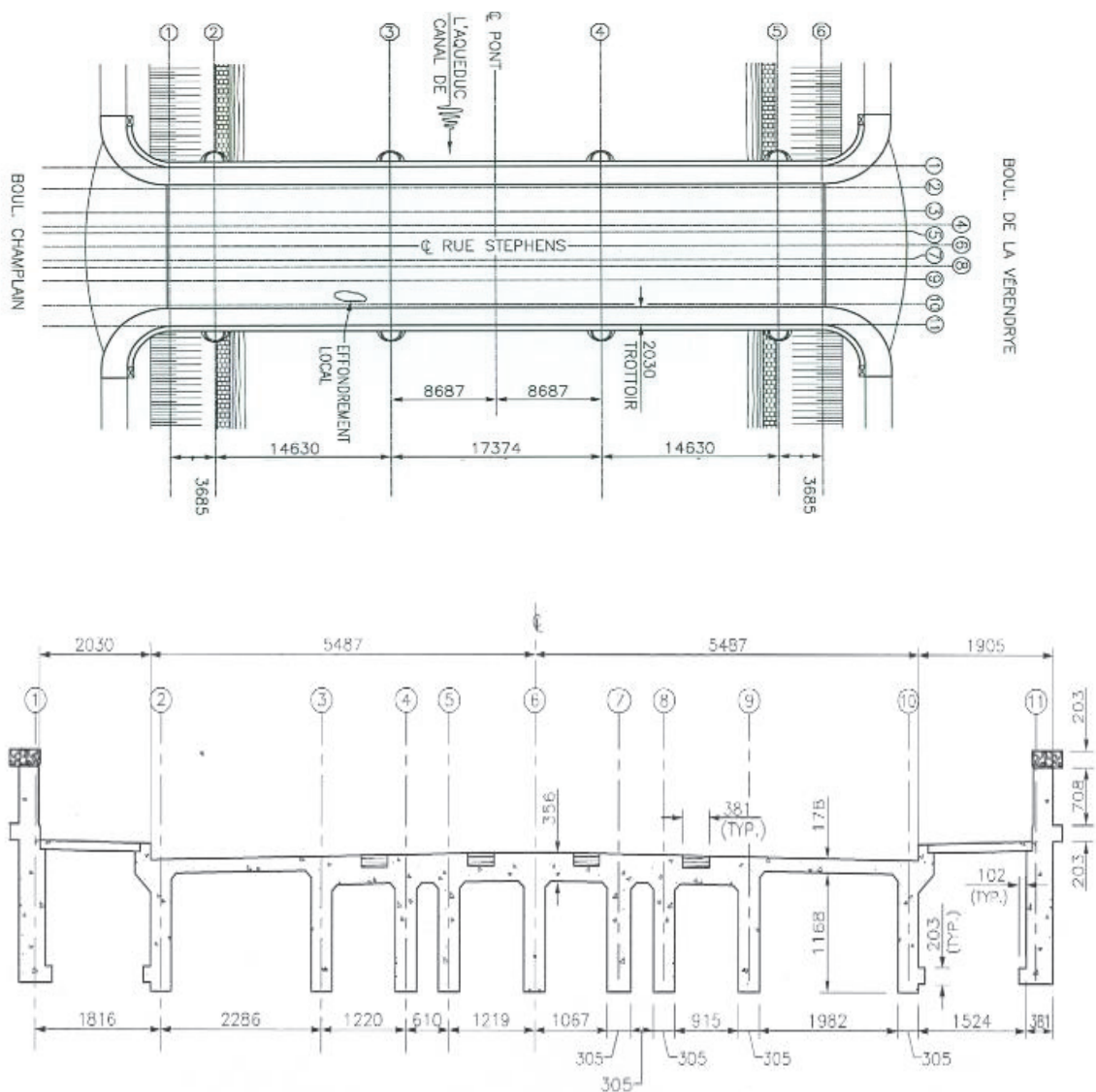


Figure 6.6 Plan View and Cross Section of the Monk Bridge, Montreal (Zaki 2000, with permission).

The results of inspections and calculations according to chapter 14 of the Canadian code (CHBDC-S6) showed that the slab was no longer able to carry the current level of design loads. Likewise, the analysis of the deteriorated concrete beams showed that the beams could not carry the code design loads. The core samples showed that the beams were severely degraded through de-icing salt and corrosion was evident on the

majority of beam surfaces. At the end, the bridge evaluators recommended that the traffic would be restricted for the trucks lighter than 10 tons for the time being. Engineers suggested a comparison be made between the following two alternatives: major rehabilitation of the superstructure or demolishing and reconstruction (Zaki 2000).



Figure 6.7 Spall and Deterioration on the Deteriorated Concrete Beam (Monk bridge Montreal), (Zaki 2000, with permission)



Figure 6.8 Spall and Deterioration Under the Deteriorated Concrete Slab (Monk bridge Montreal), (Zaki 2000, with permission)

As mentioned in Section 2.2, a bridge is categorized as ‘dangerous’ and ‘slightly dangerous’ conditions when the condition index CI is in the range of 0-19 and 20-39, respectively. Dangerous condition is when the bridge should be removed from the service, the deck or any other severely deteriorated component should be demolished and replaced with a new system immediately, while slightly dangerous condition indicates immediate major repair (Miyamoto 2001). Considering the engineer’s evaluation report for this bridge, the superstructure might be categorized as slightly dangerous. It is obvious that since such a bridge was designed long time ago, evaluating the bridge capacity with the current design loads, the value of the bridge condition index should be less than 100 even at the time when bridge was opened to traffic. Consulting the expert bridge engineers, the value of CI for such an old bridge could be in the range of 50-60 at

the time of construction (A.R. Zaki). The reason for such a drastic decrease in the condition index could be the poor construction and material quality controls as compared to the recent construction methods and technologies, and lower design loads at the time of such design as compared to the new design code loading. Further research is recommended to establish more rational criteria to prove this concept. The generated reliability-based deterioration curves shown in Figure 6.2 are normalized to yield the condition index of 60 at the time of opening the bridge to traffic for the first year, 1925. The deterioration curves in terms of the CI and the elapsed time (in years) are given by Equations 6.3-4 and are shown in Figure 6.9 where the time to spall is estimated to be $t_s = 21.69$ years.

$$CI = 60 - 5.509 \times 10^{-5}t^4, \quad 0 < t < t_s \quad (6.3)$$

$$CI = -0.293 t + 53.807, \quad t_s < t < 75 \quad (6.4)$$

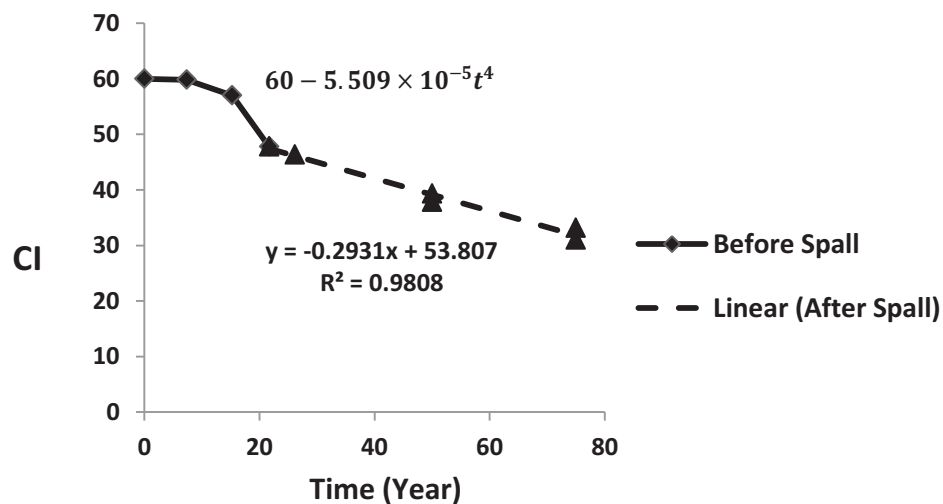


Figure 6.9 The Best Fit Deterioration Curves for the Old Bridge

The condition index at the end of the bridge life cycle (75th year) is estimated as 31.8 and the bridge could still be categorized in a slightly dangerous condition. This finding is in accordance with the results obtained from the bridge engineer's evaluation. Since in the system reliability-based deterioration model the correlation between structural elements and load redistribution is included, the higher reliability and condition indices are obtained as compared to the single element level evaluations. This is important to mention that this sample is mentioned here to illustrate how such developed deterioration model could be adopted in an existing old bridge structure to estimate the best time for repair primarily though there exist some drawbacks as follows:

- There is a lack of information regarding the history of the visual inspections and probable interventions for this case study bridge. In case where enough information exists, the deterioration model should be updated to obtain more accurate results on CI
- To develop the deterioration model, all the time periods are estimated based on the nominal concrete cover of 60 mm. However, for the Monk bridge, the real cover depth is unknown. In case where the real concrete cover is documented in the specifications or it could be measured on site, a more accurate deterioration curve could be obtained
- The developed deterioration curve is obtained based on the degradation scenario assumed for overpass bridge decks in Section 3.3. However, the Monk bridge is built on a river, and as a result it may not get the salt splashing from underneath as is the case in overpass bridges; while the under-side of the bridge deck may be exposed to heavy moisture because of the river under it. In addition, the under-

side of the deck may be contaminated as the result of salty water overflow due to drain blockage

- The old existing bridges such as the Monk Bridge may not correspond to the loading specifications of the current design codes; therefore, a criterion needs to be established for a reasonable estimation of the condition index of such a bridge representing its undamaged condition which should be less than 100. An alternative to this approach is to start the deterioration curve with a CI of 100% since the bridge was deemed adequate at the time of construction based on the 1925 code. Then, over the years, the CI should be calculated based on the given code corresponding to the time at which the CI is calculated. However, this would require the knowledge of the changes in the bridge design code and the detailed history of bridge inspection over time.

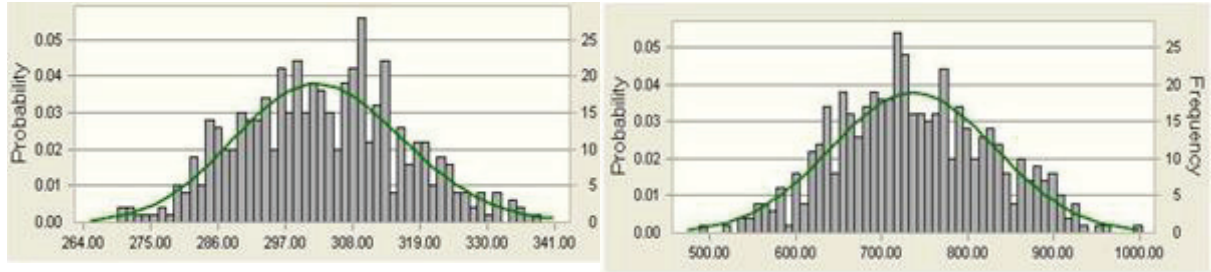
6.3 Reliability Based Deterioration Model for the Steel-Free Deck System Bridge

Since there is no established deterioration model available for the innovative systems (e.g. steel-free deck or FRP-reinforced concrete deck), it is difficult to predict the reliability of such systems at different time intervals. The developed methodology illustrated in Figures 3.1-2 has been applied to the Crowchild bridge which has an innovative structure with a Steel-Free Deck System, as a case study. The available methods for predicting the structural condition of a bridge as developed for conventional bridges do not apply to this system; therefore, the development of a deterioration model for such a system would be of interest.

As explained in Section 2.8.1, corrosion loss for steel members follows the following function $C = At^B$, where for locations with harsh corrosive environment and in

case weathering steel is used (as for the Crowchild bridge), $A = 40.2$ and $B = 0.56$ (Kayser and Nowak 1989). The degradation scenario illustrated in Figure 3.4 has been applied in the Finite element model of the steel structure (Figure 4.4). The top surface of the bottom flange and $\frac{1}{4}$ of the web height of the supporting steel girders (Kayser and Nowak 1989), and the surface of the steel straps are affected by corrosion where the corroded thickness of the corresponding elements have been calculated after 75 years of service. Here, the procedure explained in Section 4.3.1 is applied in calculating the best fit distributions for the lateral stiffness and the capacity of the corroded superstructure. Figure 6.10 shows the best fit distributions for the 75 year old bridge. By using Oracle Crystal ball software, the best fit distribution for the lateral stiffness of the system is found to be lognormal with a mean value of $\mu=302.97$ and the standard deviation of $\sigma =13.71$ in terms of N/mm/mm. The capacity of the system is found to be normally distributed with a mean value of $\mu=736.4$ KN and the standard deviation $\sigma =95.27$ KN.

The best fit to the Limit State Function is normally distributed in this case since the cumulative probability plotted on the normal probability chart is almost a straight line. The best line to fit the curves is plotted through a spreadsheet tool (Microsoft Excel). By extrapolating the cumulative distribution curve to intersect the vertical axis passing the origin $g(R,Q)=0$, as shown in Figure 6.11, for the first year, the reliability index is found to be 6.27 (as mentioned in Section 4.3.1), and for the 75th year β is estimated to be 6.17. The negligible difference indicates that no considerable deterioration for this system is expected over time.



Lateral stiffness model for the 75th year ,
Lognormal distribution ($\mu=302.97, \sigma =13.71$)
N/mm/mm

Deck capacity model for the 75th year
Normal distribution ($\mu=736.4, \sigma =95.27$) KN

Figure 6.10 BestFit Distributions for the Lateral Stiffness and the Capacity of the Steel-Free Deck for the 75th Year After Construction.

The reliability index β has been calculated for the 75th year by adopting the iterative method as explained in Section 2.4.2. The best fit distribution for the wheel load is lognormal with a mean value of $\mu_Q=97.86$ KN, and a standard deviation of $\sigma_Q=24.46$ KN. According to Equations (2.21) and (2.22), the equivalent normal mean value of $Q^*[1 - \ln Q^* + 4.55]$ and a corresponding equivalent normal standard deviation of $0.246Q^*$ are calculated for the load distribution. For each iteration, the reliability index (β) and the design point load value (Q^*) are estimated. Iterations are continued until a stable value of Q^* is attained. The results showed that the reliability index for the last iteration with $Q^*=186$ KN is estimated to be $\beta= 6.37$ which is quite close (3.1% difference) to the reliability index calculated by simulation ($\beta = 6.17$). This finding enhances the confidence in the simulation results.

The innovative system is found to be almost corrosion free, where the degradation of stiffness and strength is relatively low. There is a much lower probability of failure for

such a system in the next 75 years of its service life, as compared to a conventional steel-reinforced bridge superstructure.

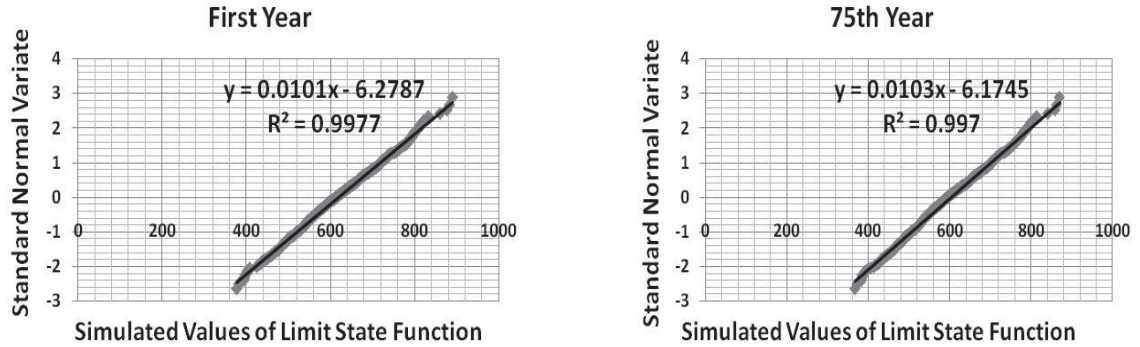


Figure 6.11 Plotted Limit State Function Simulated Values and Reliability Indices

6.3.1 Discussion on Innovative GFRP Bridge Decks

The developed model could be applied in any structural system as well as conventional Steel Reinforced bridge deck and innovative structural systems. One of the innovative non-conventional bridge systems is the FRP reinforced non-corroding deck. According to the recent tests conducted on the degradation of Glass-FRP (GFRP) bars embedded in concrete (Davalos *et al.* 2012), the dominant deterioration mechanism for such system is fiber/matrix interface de-bonding in an absolute laboratory environment which does not correspond to the real field situation regarding alkaline exposure. It has been found that the tensile strength of FRP fibers does not change substantially over time.

Val *et al.* (1998) have found that reduction of bond entails a negligible effect on bridge reliability in case of steel reinforcement and for typical corrosion rates. That is the reason why bond reduction could be ignored in reliability assessments (Vu and Stewart 2000). Since the absolute alkaline exposure, as exists in the laboratory environments, is not present in the field, it is predicted here that the non-corrosive GFRP reinforcement in

concrete will not experience considerable damage during the life cycle of a bridge deck. This is in accordance with the results of monitoring several in-service FRP structures mentioned by Mufti *et al.* (2007). It is concluded here that FRP bridge decks experience a similar deterioration pattern (marginal deterioration over the life cycle) as in the Steel-Free deck system, although Further research is recommended to prove this conclusion.

6.4 Comparison Between the Developed Deterioration Patterns for Conventional and Innovative Systems

A comparison is made between the deterioration profiles developed in this thesis for the conventional Steel-Reinforced and Steel-Free Deck system (see Figure 6.12). It is determined that both types of bridge deck systems are in a good condition during the initial stages of their service life. However, the condition of the conventional steel-reinforced concrete slab-on-girder bridges degrades faster than that of the steel-free deck bridge once corrosion begins in steel reinforcements and the concrete spalling occurs. In case of Steel-Free Deck, there is a low probability of failure for such a system during the 75 year life span of the bridge, while the same is much higher for a conventional bridge. As a result, the monitoring and inspection cost for conventional bridge systems is expected to be higher as compared to the innovative structures such as Steel-free Decks where steel reinforcements is absent and thus no considerable deterioration is observed during the life cycle of such bridges.

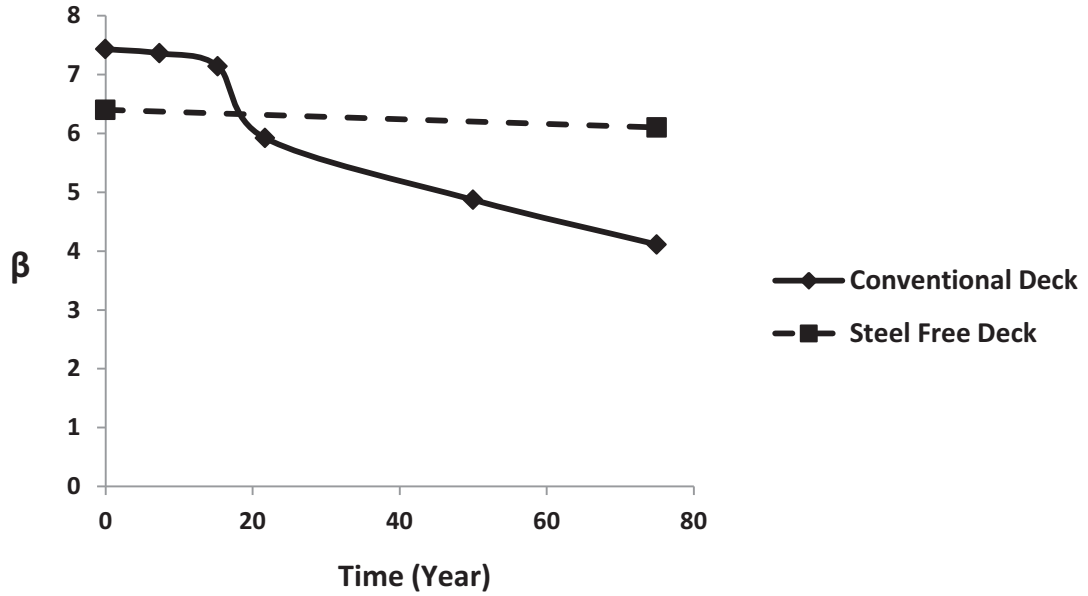


Figure 6.12 System Deterioration Curves for a Conventional and Steel-Free Deck

It is important to mention that this proposed approach may not be used to calculate the total service life of the bridge by extrapolating to the time at which the system reliability falls under a certain value. Since after the 75th years other modes of failure as well as fatigue criterion may come into consideration. The design life span of a bridge is 75 years according to the current codes (e.g., CHBDC-S6).

Chapter 7: Conclusions and Recommendations

7.1 Summary and Conclusions

7.1.1 Summary

In existing bridge management systems, the deterioration is modeled based on the visual inspections where corresponding condition states are assigned to individual elements and limited attention is given to the correlation between bridge elements from structural perspective. In this process, the impact of the deterioration history on the reliability of a structure is disregarded which may lead to inappropriate conclusions. An improved reliability-based estimate of service life of a bridge deck may help decision makers enhance the intervention plans and optimize life cycle costs. The degradation curve obtained through reliability-based estimates could be calibrated and updated based on the outcomes of the visual inspections. In case of corrosion-free and innovative structural systems, the cracking of concrete caused by regular live loads or other natural phenomena does not influence the failure modes of the system. Consequently, the current assessment techniques used in bridge management systems are not applicable and there is no established deterioration model available for these systems. Therefore, predicting the reliability of such systems at different time intervals is difficult.

In this thesis, a method has been developed in order to establish a deterioration model for bridge superstructures by applying the reliability theory and based on the bridge failure mechanisms. This method has been applied to conventional simply supported concrete bridge superstructures designed in accordance with the Canadian Highway Bridge Design Code (CHBDC-S6). The predicted element-level structural conditions are imposed on the non-linear Finite Element model of a bridge structure and

the system reliability indices are estimated for different time intervals. Also, the developed method has been applied to an innovative structure with a Steel-Free Deck System. The performance curves for the above mentioned structural systems are drawn and compared in order to evaluate the performance of different structural systems during the life cycle of bridges. In a case study on conventional reinforced concrete superstructure, the developed deterioration curve has been applied to an old bridge deck in Montreal. The obtained performance curves of Steel-Free Deck system were also applied to an innovative structure, namely the Crowchild Bridge, in Calgary, Canada. The results have are in accordance with inspections conducted by bridge engineers in both cases.

7.1.2 Conclusions

In this thesis, the performance of two conventional steel reinforced concrete decks designed based on the current Canadian code have been evaluated using a detailed Finite Element model and the reliability method. The performance of an innovative Steel-Free Deck System has been also evaluated through a detailed Finite Element model and the reliability method. By comparing the reliability indices for different time intervals, the methodology of drawing a deterioration curve based on a rational system reliability index is presented here. Several conclusions can be drawn as follows:

- The outcome here indicates that the conventional steel-reinforced bridge designed based on the simplified method of CHBDC-S6 is in an acceptable condition from the reliability point of view. Based on the reliability estimates, the conventional bridge decks are found to be in a good condition during the initial stages of their

service life. Their condition degrades faster once corrosion in steel reinforcements begins and the concrete spalling occurs

- While conducting the simulations in the this thesis, the observations indicate that for a newly constructed steel-reinforced concrete bridge girder, the ultimate state is governed by the crushing of concrete in compression; however, for a severely corroded girder at the end of service life of a bridge, the collapse is normally governed by the failure of the reinforcing steel in tension
- It is found that the element-level assessment of a concrete deck is a conservative approach since the interaction between the structural elements results in considerably higher reliability index and lower probability of failure. This finding is in accordance with the outcomes of a research conducted on another structural system
- By comparing different existing deterioration prediction models available in the literature, it is found that all major models considered here yield similar patterns up to the time of spall; however, the performance of the bridge after spall up to the 75th year is underestimated through the existing models calibrated up to the time of spall. It is essential to update and calibrate the deterioration model for misjudgement avoidance regarding intervention decisions. The frequent routine inspections are important for such conventional systems
- The study indicates that the modification of the deck behaviour from flexural to arching action provides a great improvement in the structural performance. According to the deterioration model developed in this thesis, Steel-Free Deck

structural system is found to be very robust and reliable for the whole service life of the bridge

- By comparing the reliability indices for different time intervals, no considerable deterioration is observed in Steel-Free Deck system over time. The reason for this may be the use of weathering corrosion-resistant steel for the steel girders and straps and not using internal steel reinforcements in the concrete bridge deck
- Compared to conventional bridge decks where corrosion of steel reinforcements is a significant problem, the innovative structures such as the Steel-Free Deck System are expected to be relatively corrosion free with a low rate of deterioration. The observation from the present study is consistent with the above expectation and the results of the field tests conducted in the early ages of service of the case study structure
- The frequent routine inspections may not be necessary for Steel-Free Deck system except for some key elements like construction joints, the drainage system (to prevent deck leakage), bearings, and the general condition of the steel structure, especially the steel straps. As a result, the maintenance cost and, in general, the life cycle cost of such a system is lower than that of conventional bridge systems

7.2 Research Contributions

This thesis demonstrates how the proposed system reliability-based evaluation method can be applied for determining the structural condition of a bridge which represents an important step forward in bridge management systems. The condition index for a bridge at a given time is usually determined through the element level condition indices based on the bridge inspection data and often by the bridge inspectors. The condition index as

determined above does not consider the interaction of the structural elements directly which in turn may not reflect the integrity of the structure. The system level condition index represented by the system reliability index considers the conditions of the individual elements in a bridge and the interaction of structural elements to determine the structural integrity of the whole system. The reliability index of a bridge can be calculated based on the condition information from visual inspection, non-destructive evaluation, past statistics and/or the structural health monitoring systems, if available. This newly developed method can be easily integrated in the existing BMS by replacing the existing condition index by the reliability index or adding it as an additional regulatory parameter. The system reliability-based evaluation model presents important contributions in the field of bridge management because:

- The performance of different structural systems as well as conventional and innovative corrosion free system bridges is assessed through it
- A rational deterioration model for conventional bridges considering interaction between structural elements is developed by it
- A rational performance curve for innovative corrosion-free structural systems is developed by it. The current assessment techniques adopted in bridge management systems are not applicable to the innovative structures and there is no established deterioration model available for these systems
- It helps the decision makers in predicting the appropriate time for major interventions from structural reliability point of view

- It helps the bridge authorities in predicting and comparing the performance and life cycle cost of different conventional and innovative decks over the bridge life span and selecting the most appropriate structural system.

7.3 Research Limitations

The developed System reliability-based evaluation and deterioration models have the following assumptions and limitations:

- There is a lack of information regarding the history of the visual inspections and probable interventions for the conventional case study bridge. In case where enough information exists, the deterioration model should be updated to obtain more accurate results on CI
- To develop the deterioration model for conventional bridges, all the time periods are estimated based on the nominal concrete cover of 60 mm. However, for the existing old bridges, the real cover depth might differ from the assumed value. In case where the real concrete cover is documented in the specifications or it could be measured on site, a more accurate deterioration curve could be obtained
- The following parameters mainly affect the prediction of service life of a steel reinforced concrete deck: surface chloride content of concrete, C_s , effective chloride diffusion coefficient of concrete, D_c , chloride threshold of the reinforcement, C_{th} , corrosion rate of steel reinforcement, λ , and the concrete cover of steel reinforcement. These parameters are highly variable, uncertain, and not easy to monitor. Therefore, the deterioration prediction models need to be updated and calibrated based on the results of visual inspections and instrumental observation, if available. In this thesis, the relevant field data are selected from the

literature of locations with similar environmental situation as in Canada where considerable amount of de-icing salt is consumed during the long and cold winter periods.

7.4 Potential Future Research

The potential future research would be here divided in two categories (i) current research enhancement, and (ii) future research extension.

7.4.1 *Current Research Enhancement*

The current research could be enhanced through the following approaches:

- More random variables might be considered to calculate the reliability of the bridge decks and different structural systems. This will enhance the model by applying more probability distributions of structural parameters affect the capacity of different systems. By applying more stochastic data input in Mont-Carlo simulation, more precise capacity distribution may be obtained
- More refined FE models might be applied to estimate the capacity of bridge decks. Here, in case of conventional bridge decks the simplified models are closely correlated with the more complex models. However, using more detailed Finite Element models, more accurate capacity estimations may be achieved
- The procedure presented here is time consuming, by automation the modeling process could be simplified
- In the developed deterioration model for conventional bridge deck system, for simplicity, the time intervals are estimated based on the mean values of the parameters that mainly affect the prediction of service life of a steel reinforced

concrete deck. A simulation process could be added to the current study considering the variation of such parameters. This will enhance the model by using probability distributions for different time intervals instead of merely using the mean values

- The proposed approach can be adopted to develop sets of pre-calculated deterioration curves of the system reliability index over time that can be computed for a number of combinations of key deterioration parameters for different structural types of bridges and for different span lengths. The key parameters may include: chloride diffusion coefficient based on concrete strength; surface chloride content based on severity of corrosive environment; corrosion rate based on type of steel reinforcing bars; concrete cover thickness based on required protection and element type; and presence and quality of waterproofing membrane and wearing surface. Such pre-calculated curves can be easily used in practice to estimate the reliability of a new or existing bridge.

7.4.2 *Future Research Extension*

The future extension areas are as follows:

- The developed methodology is applicable in different conventional bridge deck systems. This methodology could potentially be applied in other non-conventional bridge systems, as well as in FRP reinforced non-corroding deck systems and in bridges retrofitted with non-corrosive materials. Further research is recommended to prove this concept.
- Further work is required to correlate the reliability-based condition index with the traditional bridge condition index or health index so that the traditional

indices could be reinterpreted, updated and easily applied by the transportation authorities.

- The old existing bridges may not satisfy the loading specifications of the current design codes; therefore, a rational criterion needs to be established or a reasonable estimate of the condition index of such a bridge representing its undamaged condition be developed that could be rated less than 100.

References:

- American Association of State Highway and Transportation Officials(2004).“AASHTO LRFD bridge design specifications”, AASHTO, Washington.
- Bagchi, A. (2005). “Updating the mathematical model of a structure using vibration data.”*J. Vibration and Control*, 11 (12), 1469-86.
- Bakht, B., and Mufti, A.(1998).“Five Steel-Free Bridge Deck slabs in Canada”.*J. Structural Eng. International*, 8 (3), 196-200.
- Bennett, R. M., and NajemC. (1987). “Reliability of bolted steel tension members”, *J. structural Eng.*, 113(8), 1865-1872.
- Bisby, L.A. (2006). “An introduction to life cycle Engineering & Costing for innovative infrastructure”,*(ISIS) Canada Research Network*,Department of Civil Engineering, Queen’s University.
- Canadian Standards Association (2004).“Design of Concrete Structures, (CSA, A23.3-04)”, Ontario, Canada.
- Canadian Standards Association (2006).“Canadian Highway Bridge Design Code (CHBCD), (CAN/CSA-S6-06)”, Toronto, Ontario, Canada.
- Canadian Standards Association (2003).“Welded Steel Construction Code (Metal Arc Welding), (CAN/CSA-W59-03)”, Ontario, Canada.
- Cusson, D., Lounis, Z., and Daigle L. (2011).“Durability monitoring for improved service life predictions of concrete bridge decks in corrosive environments”, *J. Computer-Aided Civil and Infrastructure Engineering*, 26(7),524-541.
- Czarnecki, A.A., and Nowak A.S. (2007).“Reliability-based evaluation of steel girder bridges”.*Proc., Institution of Civil Engineers, Bridge Engineering*, 160(1), 9-15.
- Davalos, J. F., Chen, Y., and Ray, I.(2012).“Long-term durability prediction models for GFRP bars in concrete environment”.*J. composite materials*, 46 (16), 1899-1914.
- Dieter, G. E.(1986). “*Mechanical metallurgy, 3rd ed*”. New Yourk: McGraw-Hill.
- Dubey, B. (2008). “Integration of Structural Health Monitoring information to reliability based condition assessment and life cycle costing of bridges”, MSc. thesis,Concordia University, Montreal, Canada.
- Dunn, M. *et al*, (2005).“Tama County’s steel free bridge deck.”*Proc., Mid-Continent Transportation Research Symposium*, Ames, Iowa.

- Ellis, R. M., Thompson, P. D., Guy, R. (2008).“Design and implementation of a new bridge management system for the Ministry of Transport of Québec”, *Proc., 4th International Conference on Bridge Maintenance, Safety and Management*, 159-160.
- Frangopol, D.M., and Neves, L. C. (2004).“Probabilistic Life-Cycle Analysis of Deteriorating Structures Under Multiple Performance Constraints”. *Proc. of the 2004 Structures Congress - Building on the Past: Securing the Future*, 85-92.
- Frangopol, D. M., Kong, J. S., and Gharaibeh, E. S., (2001).“Reliability-based life-cycle management of highway bridges”, *J. Computing in Civil Engineering*, 15(1), 27-34.
- Gattulli, V. (2005). “Condition assessment by visual inspection for a bridge management system”, *J. Computer- Aided Civil and Infrastructure Engineering*, 20(2), 95-107.
- Glagola (1992). “The development of a bridge performance prediction model as a rational basis for a structures maintenance management systems” M.S.Thesis,School of Engineering and Applied Science, University of Virginia.
- Golabi, K., and Shephard, R., (1997).“Pontis: a system for maintenance optimization and improvement of US bridge networks”, *J. Interfaces*, 27(1), 71-88.
- Grussing, M.N., Uzarski, D.R. and Marrano, L.R.(2006).“Condition and reliability prediction models using the weibull probability distribution”, *Proc. Ninth International Conference on Applications of Advanced Technology in Transportation*, 19-24.
- Hammad,A., Yan,J., and Mostofi, B. (2007).“Recent Development of Bridge Management Systems in Canada”, *Proc. Annual Conference of the Transportation Association of Canada Saskatoon*, Saskatchewan, Canada.
- Johnson, M.B. and Shepard, R.W. (1999).“California Bridge Health Index.”*Proc. 8th International Bridge Management Conference*, TRB, National Research Council, Washington, D.C.
- Kayser, J. R. and Nowak, A S. (1989).“Reliability of corroded steel girder bridges”,*J. Structural Safety*, 6(1), 53-63.
- Kong, J.S., and Frangopol, D.M. (2003).“Life-cycle reliability-based maintenance cost optimization of deteriorating structures with emphasis on bridges”. *J. Structural Engineering*, 129(6), 818-828.
- Liu, Y., and Weyers R.E. (1998).“Modeling the time-to-corrosion cracking in Chloride contaminated reinforced concrete structures”*J. ACI Materials*, 95(6), 675-681.
- McDaniel, M, Celaya, M. and Nazarian, M. (2010).“Concrete Bridge Deck Quality Mapping with Seismic Methods: Case study in Texas”,*J. Transportation Research Board*, 2202, 53-60.

- Mirza, S.A., and MacGregor J.G. (1979a).“Variability of Mechanical Properties of Reinforcing Bars” *J. ASCE Journal of the Structural Division*,105(5):921-937.
- Mirza, S.A., and MacGregor J. G. (1979b). “Variations in Dimensions of Reinforced Concrete Members”,*J. ASCE Journal of the Structural Division*, 105(4):751-766.
- Miyamoto, A., Kawamura, K.; and Nakamura, H. (2000).“Bridge management system and maintenance optimization for existing bridges”,*J. Computer-Aided Civil and Infrastructure Engineering*, 15(1):45-55.
- Morcous,G. (2006).“Performance prediction of bridge deck systems using markov chains.”*J. Performance of Constructed Facilities*, 20(2):146-155.
- Morcous, G., and Lounis, Z. (2005).“Prediction of onset of corrosion in concrete bridge decks using neural networks and case-based reasoning”,*J. Computer-Aided Civil and Infrastructure Engineering*, 20(2):108-17.
- Mufti, A.A.,Onofrei, M. , and Benmokrane,B.(2007).“Field Study of Glass-Fiber-Reinforced-Polymer Durability in Concrete”, *Canadian J.of Civil Engineering*, 34(3):355-366.
- Myamoto, A., Kawamura, K. and Nakamura, H. (2001).“Development of a bridge management system for existing bridges”,*J. Advances in Engineering Software*, 32(10-11):821-833.
- Newhook, J. P. (1997).“The behaviour of steel-free concrete bridge deck slabs under static loading conditions”, PhD. thesis, DalTech - Dalhousie University,Canada.
- Nowak, A. S., and Eamon, C. D. (2008).“Reliability analysis of plank decks”, *J. Bridge Engineering*, 13(5):540-546.
- Nowak, A. S. (2004).“System reliability models for bridge structures”, *Bulletin of the Polish Academy of Sciences , Technical Sciences*, 52(4):321-8.
- Nowak, A. S. and Collins, K. R. (2000).“Reliability of structures”, McGraw-Hill.
- Nowak, A.S. (1999).“Calibration of LRFD Bridge Design Code.” NCHRP Rep. No. 368,Transportation Research Board , Washington, D.C.
- Nowak, A. S. (1995).“Calibration of LRFD Bridge Code.”*J. structural engineering*, 121(8):1245-1251.
- Nowak, A. S., Kim, S.J., and Laman, J. A. (1994a).“Effect of truck loads on bridges.”Rep. No.UMCE 94-26, Dept. of Civil Engineering Univ. of Michigan, Ann Arbor, Mich.

- Nowak, A. S., Kim, S.-J., and Laman, J. A. (1994b). "Truck loads on selected bridges in the Detroit area", Rep. No.UMCE 94-34, Dept. of Civil Engineering, Univ. of Michigan, Ann Arbor, Mich.
- Nowak, A. S. (1993). "Live Load Model for Highway Bridges." *J. Structural Safety*, 13(1-2):53-66.
- Ontario Ministry of Transportation (2008). "Ontario Structure Inspection Manual (OSIM)", Ontario, Canada.
- Oracle Inc. (2008), "Oracle Crystal Ball User's Manual.11.1.1 ed.", Denver, USA.
- Park, R., and Paulay T. (1975), "Reinforced Concrete Structures", John Wiley & Sons.
- Phares, B.M., and Washer, G.A. (2004). "Routine highway bridge inspection condition documentation accuracy and reliability", *J. Bridge Engineering*, 9(4):403-413.
- Prakash, V., Powell, G. H., and Campbell, S. (1993). "Drain-2DX Base Program Description and User Guide Version 1.10", Structural Engineering Mechanics and Materials Report No. UCB/SEMM-93-18. Berkeley : University of California.
- Priestley, M. J. N., Seible, F., and Calvi, G.M. (1996). "Seismic Design and Retrofit of Bridges.", John Wiley and Sons.
- Rens, K.L., and Nogueira, C. L. (2005). "Bridge management and nondestructive evaluation", *J. Performance of Constructed Facilities*, 19(1):3-16.
- Computers and Structures, Inc (2003), "SAP2000 User's Manual", Berkeley, Calif.
- Stallings, J.M., and Yoo, C. H. (1992). "Analysis of slab-on-girder bridges" *J. Computers and Structures*, 45(5-6):875-880.
- Stewart, M.G., and Rosowsky D.V. (1998). "Structural safety and serviceability of concrete bridges subject to corrosion." *J. Infrastructure Systems*, 4(4):146- 155.
- Tabsh, S.W., and Aswad, A. (1997). "Statistics of High-Strength Concrete Cylinders Members." *J. ACI Materials*, 94(5):361-364.
- Thoft-Christensen, P. (1998). "Assessment of the reliability profiles for concrete bridges", *J. Engineering Structures*, 20(11):1004-1009.
- Thompson P., Small E., Johnson M., and Marshall A. (1998). "The Pontis Bridge Management System", *J. Structural Engineering International*, 8(4):303-308.

- Thorburn, J., and Mufti, A.A. (2001).“Design recommendations for externally restrained highway bridge decks.”*J. Bridge Engineering*, 6(4):243-249.
- Val, D., Stewart,M.G. and Melchers, R.E. (1998).“Effect of reinforcement corrosion on reliability of highway bridges.”,*J. Engineering Structures*, 20(11):1010-1019.
- VanZwol, T.R., Cheng, J.J.R. and Tadros, G. (2008).“Long-Term Structural Health Monitoring of The Crowchild Trail Bridge.”,*J. Canadian Journal of Civil Engineering*, 35(2):179-89.
- Vu, K.T., Stewart, M.G., and Mullard, J. (2005).“Corrosion-induced cracking: experimental data and predictive models.” *J. ACI Structural Journal*, 102(5):2005719-726.
- Vu, K.T., and Stewart, M.G. (2000). “Structural reliability of concrete bridges including improved chloride- induced corrosion models”,*J. Structural Safety*, 22(4):313-333.
- Wacker, J.P., and Groenier, J.S. (2010). “Comparative Analysis of Design Codes for Timber Bridges in Canada, the United States, and Europe.”*J. Transportation Research Board*, 2200:163-168.
- Weyers, R.E. (1998), “Service Life Model for Concrete Structures in Chloride Laden Environments”,*J. ACI Materials*, 95(4):445-453.
- Xue,H., Hao, Q., and Shen,W. (2008). “Monitoring and Assessment of Built Structures.”, QNRC-CNRC Report RR-259.

Appendix A

Design Procedure of Conventional Steel Reinforced Concrete Superstructure

Part I - General Information

As case studies, two simply supported conventional concrete bridge superstructures are designed according to the simplified method of Canadian Highway Bridge Design Code (CHBDC-S6). The design procedure for the two lane bridge superstructure with 17.5 m span (Centre-to-Centre of bearings) is explained here. Figure 5.1 shows the geometry of the bridge together with the cross section of the T-section main beams. Four simply supported concrete beams (Roller support for one side and hinge support for the other), which are 2.3 m apart support the 0.2 m thick concrete slab. In order to meet the requirements of the code and for simplicity, the nominal concrete cover is assumed to be 60 mm on all surfaces. Four concrete diaphragms are designed and installed in the transverse direction at two ends and quarters of the span on each side. All the symbols and abbreviations mentioned in this calculation report are in accordance with CSA, A23.3-04 and CHBDC-S6.

Part II- Loading

Two main load cases are considered here, the Dead load and Live load. The Dead load; *DL*, is the weight of cast in place concrete and the weight of the wearing surface with 100 mm thickness. The nominal values for specific weight of concrete and wearing surface are assumed to be 24 KN/m³ and 23.5 KN/m³, respectively. Live load is the CL-625 loading of CHBDC-S6.

i: Dead Load

To determine the dimensions of the T-section beams the following requirements are satisfied.

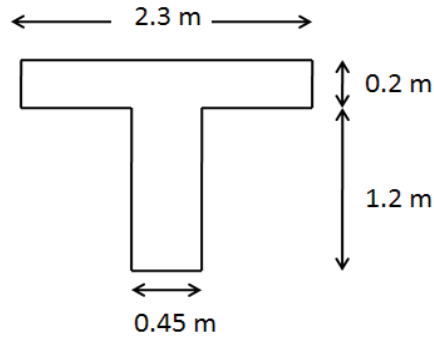


Figure A.1 T-section Concrete Beam Designed for the Bridge Superstructure with 17.5 m Span

$$\text{CAN/CSA-A23.3-04: } b_T = \min\left(\frac{17.5}{5}, 12 \times 0.2, \frac{(2.3-0.45)}{2}\right) = 0.925$$

$$\text{Width of flange: } b_f = 2 \times b_T + 0.45 = 2.3 \text{ m}$$

$$\text{CAN/CSA-A23.3-04, Table 9.2: } h \cong \frac{1}{16} \times 17.5 = 1.1 \text{ m} < 1.4 \text{ m}$$

$$\text{AASHTO: } h_{min} = \frac{1.1 \times (17.5 + 3)}{18} = 1.25 \text{ m} < 1.4 \text{ m}$$

$$w = 24 \times (1.2 \times 0.45 + 2.3 \times 0.2) + 23.5 \times (2.3 \times 0.1) = 29.05 \text{ KN/m}$$

Governing Dead load moment and shear force for the simply supported beam with 17.5 m span:

$$\text{Shear Force: } V_{max,DL} = \frac{29.05 \times 17.5}{2} = 258 \text{ KN}$$

$$\text{Moment : } M_{max,DL} = \frac{29.05 \times 17.5^2}{8} = 1112 \text{ KN.m}$$

ii: Live Load

The live load considered here is the CL-625 loading of Canadian Highway Bridge Design Code (CHBDC-S6). CL-625 truck is a five-axle truck as shown in Figure A.2. The corresponding lane load consists of a truck load with each axle reduced to 80% of the values shown in Figure A.2 and a uniformly distributed load of 9 KN/m. The lane load is illustrated in Figure A.3.

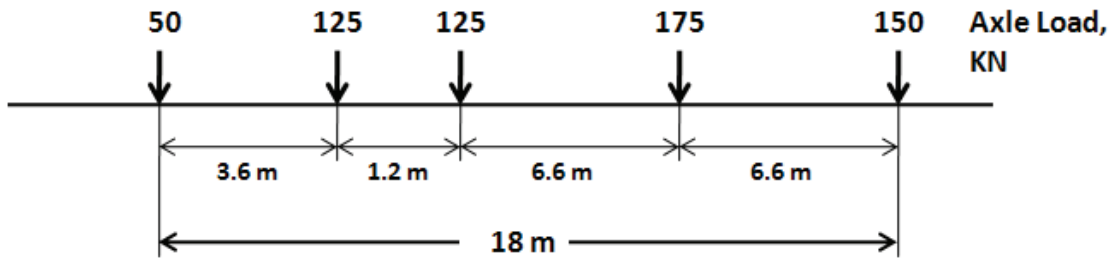


Figure A.2 CL-625 Truck (adapted from CHBDC-S6)

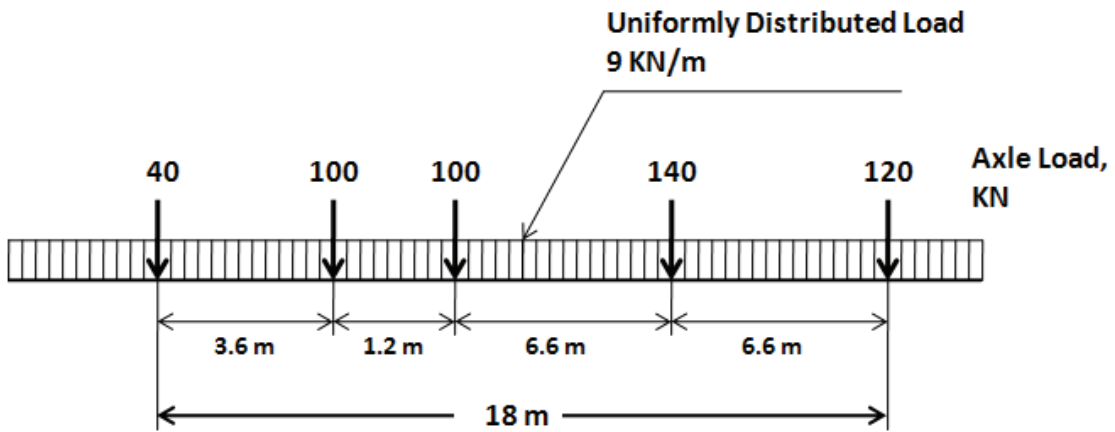


Figure A.3 CL-625 Lane Load (adapted from CHBDC-S6)

The critical longitudinal location of truck has been found based on the influence line calculations. Four alternatives have been considered here to estimate the design shear force and bending moment as shown in Figure A.4. The dynamic load allowance, DLA, is estimated according to the clause 3.8.4.5.3 of CHBDC-S6 and for each load case, if applicable.

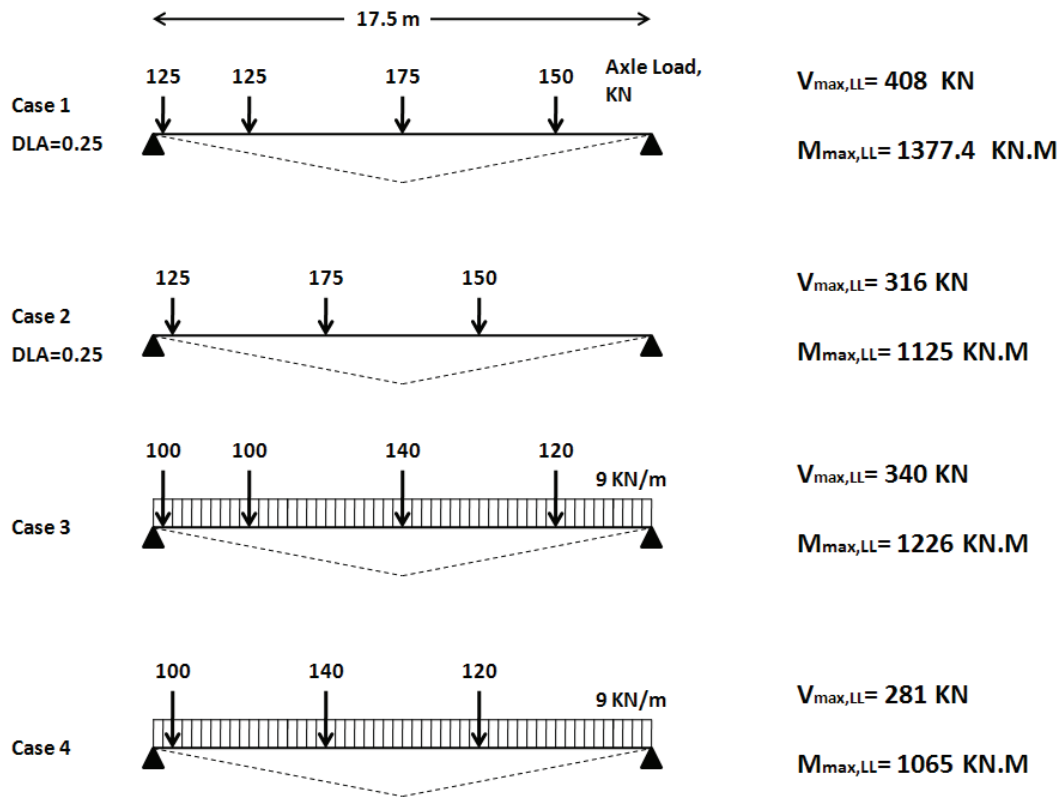


Figure A.4 Four alternatives to estimate the design shear force and bending moment

In the current study, the simplified method of CHBDC-S6 is used to estimate the governing live load moment and shear in the internal and external concrete beams. The summary of calculation process is mentioned here as follows.

Table 5.3, CHBDC-S6:

$$F_{Internal} = 7.2 - \frac{14}{17.5} = 6.4$$

$$F_{External} = 6.8 - \frac{3}{17.5} = 6.62$$

$$C_{f,internal} = C_{f,external} = 10 - \frac{25}{17.5} = 8.57$$

$$\text{Lane width} = W_e = \frac{W_c}{2} = \frac{9 - 2 \times 0.9}{2} = 3.6 \text{ m}$$

$$\mu = \frac{W_e - 3.3}{0.6} = 0.5 < 1.0$$

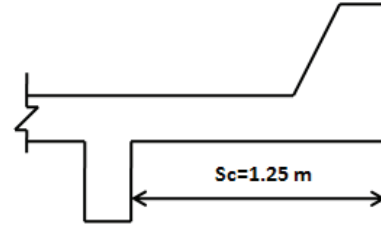
$$S_c > 0.5 S \rightarrow 1.25 > 0.5 \times 2.3$$

For external beams $\rightarrow F_{m,External} = F_m \times 1.05$

$$F_m = \frac{S \times N}{F \left[1 + \frac{\mu \times C_f}{100} \right]}$$

$$F_{m,Internal} = \frac{2.3 \times 4}{6.4 \left[1 + \frac{0.5 \times 8.57}{100} \right]} = 1.38$$

$$F_{m,External} = \frac{2.3 \times 4}{6.62 \left[1 + \frac{0.5 \times 8.57}{100} \right]} \times 1.05 = 1.4$$



Clause 3.8.4.2, CHBDC-S6:

Modification factor for multi-lane loading = $R_L = 0.9$

Governing live load moment in the internal and external concrete beams:

$$M_g = F_m \times n \times M_T \times R_L / N$$

$$M_{g,Internal} = 1.38 \times 2 \times 1377.4 \times \frac{0.9}{4} = 862 \text{ KN.m}$$

$$M_{g,External} = 1.4 \times 2 \times 1377.4 \times \frac{0.9}{4} = 875 \text{ KN.m}$$

Table 5.7, CHBDC-S6 $\rightarrow S > 2m \rightarrow F = 6.1$

$$F_V = \frac{S \times N}{F} = \frac{2.3 \times 4}{6.1} = 1.51$$

$$V_g = F_V \times V_{g,ave} = F_V \times \frac{n \times V_T \times R_L}{N} = 1.51 \times \frac{2 \times 408 \times 0.9}{4} = 277.24 \text{ KN}$$

Governing Live load moment and shear force

Shear Force: $V_{max,LL} = 278 \text{ KN}$

$$\text{Moment : } M_{max,LL} = \frac{29.05 \times 17.5^2}{8} = 875 \text{ KN.m}$$

Part III- Design of Steel Reinforcement for the T-Section Concrete Beam

As shown in Figure 5.1, two layers of reinforcement used in the concrete slab, and the skin reinforcement as designed based on clause 8.12.4 of CHBDC-S6 is included in strength calculations.

According to CHBDC-S6, the main load combination considered here is as follows:

$$1.2 DL + 1.7 LL$$

$$M_f = 1.2 \times 1112 + 1.7 \times 875 = 2822 \text{ KN.m}$$

The resisting moment of the section shown in Figure 5.1 is calculated in as follows:

$$\sum F = 0 \rightarrow \alpha_1 \phi_c f'_c \beta_1 C b_f - \phi_s \times \sum A_s f_s = 0 \rightarrow C = 80.93 \text{ mm}$$

where C is the depth of the neutral axis from the outermost compression fibre.

$$\text{CHBDS-S6} \rightarrow \phi_s = 0.9, \phi_c = 0.75$$

$$f'_c = 40 \text{ MPa}, f_y = 400 \text{ Mpa}$$

$$\alpha_1 = 0.85 - 0.0015 \times f'_c = 0.85 - 0.0015 \times 40 = 0.79$$

$$\beta_1 = 0.97 - 0.0025 \times f'_c = 0.97 - 0.0025 \times 40 = 0.87$$

$$d = 1400 - \left(60 + 10 + 35 + 1.4 \times \frac{35}{2} \right) = 1270.5 \text{ mm}$$

$$M_u = \alpha_1 \phi_c f'_c \beta_1 C b_f \times \left(d - \frac{\beta_1 C}{2} \right) - \phi_s \times \sum A_s f_s \times (d - d'_i) = 3126 \text{ KN.m} > M_f$$

$$S_{min} = \max(1.4d_b, 1.4a_{max}, 30) = 49 \text{ mm}$$

$$b_{min} = 3 \times 35 + 2 \times 49 + 2 \times 10 + 2 \times 60 = 343 \text{ mm} < 450 \text{ mm}$$

$$\rho_b = \frac{\alpha_1 \beta_1 \phi_c f'_c}{\phi_s f_y} \times \frac{700}{700 + f_y} = 0.024$$

$$\rho = \frac{A_s}{bd} = 0.0017 < \rho_b$$

$$M_{cr} = 609 \text{ KN.m} \rightarrow M_r > 1.2M_{cr}$$

$$A_e = 450 \times 2 \times 129.5 = 1165 \text{ mm}^2$$

$$Z = f_s \times \sqrt[3]{d_c \times A} = 6343 < 25000$$

Use 5-35M rebar

Part IV- Shear Design According to CHBDC-S6

According to CHBDC-S6 both the general method (Clause 8.9.3.7) and the simplified method has been adopted in Shear design as explained in the following:

$$\text{Clause 8.4.1.8.1} \rightarrow f_{cr} = 0.4\sqrt{f'_c} = 0.4\sqrt{40} = 2.53 < 3.2 \text{ (Clause 8.9.3.4)}$$

$$\text{Clause 8.9.3.4} \rightarrow V_c = 2.5\beta\phi_c f_{cr} b_v d_v = 445.7 \text{ KN, where } \beta = 0.18 \text{ (Clause 8.9.3.6)}$$

$$\text{where } d_v = \max(0.9d, 0.72h) = 1160 \text{ mm, } b_v = 450 \text{ mm}$$

$$V_f = 1.2 V_{DL} + 1.7 V_{LL} = 1.2 \times 258 + 1.7 \times 278 = 782 \text{ KN, Conservatively from the edge of the beam.}$$

$$V_s = V_f - V_c = 782 - 445 = 337 \text{ KN}$$

$$\text{Clause 8.9.3.5} \rightarrow V_s = \frac{\phi_s f_y A_v d_v \cot \theta}{s} \rightarrow T r y S = 300 \text{ mm}$$

$$\text{Clause 8.9.3.3} \rightarrow 0.25\phi_c f'_c b_v d_v = 5433 > V_f$$

$$\text{Clause 8.9.1.3} \rightarrow A_{v,min} = 0.15f_{cr} \left(\frac{b_v \times s}{f_y} \right) = 150 \text{ mm}^2 < A_v = 200 \text{ mm}^2$$

Use 10M@300 c/c

Part V- Deflection Control According to CHBDC-S6

The maximum mid-span deflection of the bridge superstructure has been estimated based on different longitudinal locations of the CL-625 design truck. The critical location is shown in Figure A.5. This maximum deflection is calculated based on deflection influence line as shown in Figure A.5.

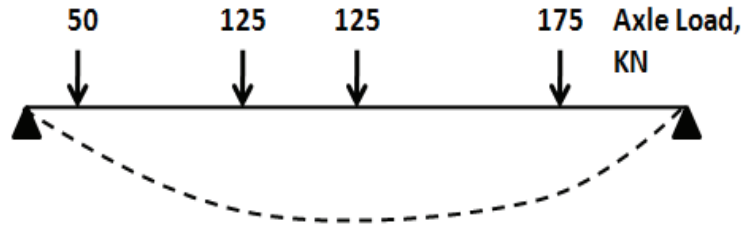


Figure A.5 The critical location of CL-625 design truck to estimate the deflection

$$d_{ZX} = \frac{Z(L - X)}{6EI L} (2LX - X^2 - Z^2), \quad Z < X$$

where, Z is the location in which the deflection is estimated and X is the location of the unit load. Therefore, for the truck location illustrated in Figure A.5, the maximum mid-span deflection is $\Delta = 9 \text{ mm}$.

$$\text{CHBDS-S6, Table 5.4, Type C, two lane bridge} \rightarrow F_{tab} = 4.6 - \frac{6}{L} = 4.257$$

$$F = F_{tab} \left[1.0 + (0.29S - 0.35) \left(\frac{L - 10}{40} \right) \right] = 1.059 F_{tab} = 4.508$$

$$\mu = \frac{W_e - 3.3}{0.6} = 0.5$$

$$C_f = 5 - \frac{15}{L} = 4.143$$

$$F_m = \frac{S \times N}{F \left[1 + \frac{\mu \times C_f}{100} \right]} = 1.99$$

$$DLA = 0.25 \rightarrow \Delta_{beam} = \Delta \times \frac{F_m}{N} \times (1 + DLA) \times 0.9 = 5.04 \text{ mm}$$

$$\text{Weight per unit length of the superstructure } m = 135 \frac{\text{KN}}{\text{m}}$$

$$\text{Gross moment of inertia: } I_g = 1.0645 \text{ m}^4$$

$$\text{The first flexural frequency } f_b = \frac{\pi}{2L^2} \sqrt{\frac{EI}{m}} = 6.76 \text{ HZ}$$

$$\text{CHBDC-S6, Figure 3.1} \rightarrow \Delta_{allowable} = 10 \text{ mm} > 5.04 \text{ mm}$$